NASA · CR · 72019
WCAP · 2972

IRRADIATION OF REFRACTORY FUEL COMPOUNDS, UO_2 AND UC, AT HIGH SPECIFIC POWER TO HIGH BURNUPS

POST IRRADIATION EXAMINATION OF CAPSULE 1

by

RICHARD E. SCHREIBER

prepared for

NATIONAL AERONAUTICS AND SPACE ADMINISTRATION
CONTRACT NAS 3-3392 PB

WESTINGHOUSE ELECTRIC CORPORATION
ATOMIC POWER DIVISIONS

Requests for copies of this report should be referred to

National Aeronautics and Space Administration
Office of Scientific and Technical Information
Attention: AFSS-A
Washington, D.C. 20546

WCAP-2972

NASA-CR-72019
WCAP-2972

First Interim Report

IRRADIATION OF REFRACTORY FUEL COMPOUNDS, UO_2 AND UC, AT HIGH SPECIFIC POWER TO HIGH BURNUPS - POST-IRRADIATION EXAMINATION OF CAPSULE 1

by

Richard E. Schreiber

Prepared for

National Aeronautics and Space Administration
August 1, 1966
Contract NAS-3-3392-PB
Technical Management
NASA Lewis Research Center
Cleveland, Ohio
Technical Liaison Office
Dominic C. DiIanni

Westinghouse Electric Corporation
Atomic Power Division
P. O. Box 355
Pittsburgh, Pennsylvania 15230

NASA Distribution List

NASA-Lewis Research Center
21000 Brookpark Road
Cleveland, Ohio 44135

R. M. Caves	MS 105-1
D. C. DiIanni (3)	49-2
P. L. Donoughe	49-2
L. V. Humble	49-2
S. J. Kaufman	49-2
A. F. Lietzke	49-2
Dr. B. Lubarsky	500-201
J. F. Mondt	500-309
F. E. Rom	49-2
E. W. Sams	49-2
N. D. Sanders	302-1
W. R. Thielke	54-2
Report Control	5-5
Library (2)	60-3

NASA-Lewis Research Center
Plum Brook Station
Sandusky, Ohio 44871

R. F. Barrows
R. J. Koch
Library (2)

AEC-NASA Space Nuc. Prop. Office
U. S. Atomic Energy Commission
Washington, D. C. 20545

F. C. Schwenk
J. J. Lynch

NASA Scientific and Technical
Information Facility (6)
Box 5700
Bethesda, Maryland

U. S. AEC Technical Information Service (3)
P. O. Box 65
Oak Ridge, Tennessee

U. S. Atomic Energy Commission (3)
Technical Report Library
Washington, D. C. 20545

Irradiation of Refractory Fuel Compounds, UO_2 and UC, at High Specific Powers to High Burnups

Post-Irradiation Examination of Capsule 1

by

Richard E. Schreiber

35219

ABSTRACT

The first of thirteen capsules, each containing four fuel pins, has been irradiated and examined. Three of the pins are UO_2 and the fourth is UC. Mean power levels of 33 kw/ft and burnups of 2.26×10^{20} fission/cc were achieved in each of the 0.3000 inch diameter, 4.0 inch long fuel pellet columns. The AISI 348 stainless steel clad was 10, 20, or 30 mils thick on the UO_2 pins and 20 mils on the UC. All pins were gas bonded, surrounded by NaK, and operated at approximately 760°C fuel surface temperature. Fission gas release, density changes, melting behavior and dimensional changes agreed well with predictions. The 20 mil clad UO_2 pin failed, evidently by local NaK deprivation.

Table of Contents

List of Tables

List of Figures

List of Figures (cont'd)

Irradiation of Refractory Fuel Compounds, UO_2 and UC, at High Specific Power to High Burnups

Post-Irradiation Examination of Capsule 1

SUMMARY

A joint Westinghouse (APD)-NASA program has been undertaken for the irradiation of refractory fuel compounds, both UC and UO_2, at high specific power to high burnups in the NASA Plumbrook Reactor Facility (PBRF).

WAPD has designed and fabricated fuel bearing capsules, twelve containing three UO_2 fuel pins and one UC fuel pin and one containing one UO_2 pin and three UC pins. The power levels expected in each capsule have been calculated from flux perturbation measurements made in NASA's Mockup Reactor (MUR) at the Plumbrook site. Scheduling the irradiation sequences to give desired burnup and power levels is being done in cooperation with NASA and according to available reactor space based on program priority.

Design and safeguards and operating procedures manuals have been prepared. The majority of post-irradiation examination is being conducted at PBRF. In addition to disassembly, this includes photography, dimensioning, fission gas collection, sectioning of fuel pins, preliminary mounting of metallographic specimens, density measurement of fuel samples and burnup analysis by Cs-137 radiochemistry and U and Pu isotopic distribution by mass spectrograph. Final preparation and photography of metallographic specimens and analysis of fission gas are being done by WAPD in its own hot cells. In addition to the fuel pins, a number of tensile wires representing a variety of potential cladding materials are built into the capsules. These will be tested by WAPD.

Nominally, four power levels will be investigated between 25 and 50 kw/ft, each at three burnups, ranging from 10,000 to 80,000 MWD/MTU. In order to achieve power level control in the available fluxes, a set of neutron absorber sleeves has been prepared to surround the fuel capsules. The sleeves are made of either

aluminum, stainless steel, or boronated stainless steel. As depletion of U-235 occurs, and thus power drops in the capsules, the absorber sleeve is exchanged for one which depresses the flux less. As the power drops off again, the capsule position in the reactor is changed to provide a higher flux. The effect of this stepwise adjustment of power is to simulate operation of the fuel in a normally cycled core.

At present, WAPD and NASA personnel are evaluating the nuclear requirements and reactor space availability to achieve the program goal in the shortest time possible.

Each fuel pin is composed of a 4 inch long column of 0.300 inch diameter, half inch long, undished pellets. The UC is arc cast, hyperstoichiometric (excess C). The UO_2 is of nominal composition, 96% of theoretical density. In each pin there is a suitable diametral gap to accommodate thermal expansion of fuel operating at a nominal power of 25 (Capsules 1-3), 30 (Capsules 4-6), 40 (Capsules 7-9, 13), or 50 (Capsules 10-12) kw/ft. The pins are clad with annealed AISI 348 stainless steel. In each capsule the clad on the UO_2 pins is 10, 20, and 30 mils thick and the clad on the UC pin is 20 mils thick. Each pin is surrounded by either NaK (Capsules 1-6) or Na (Capsules 7-13) contained in stainless steel cans. Three tensile wires are fitted into the NaK or Na annulus of each can and four tensile wires are trapped in each of the four flow dividers in the capsule for a total of 28 wires. In addition to the fuel in each pin, there is a tubular spacer above the fuel to provide a plenum for fission gas, as well as to restrict the free aixal expansion of the short fuel column, thus making the pin equivalent to a much longer fuel rod. There is a deformable expansion marker below the fuel which records the maximum relative axial motion of clad and fuel.

INTRODUCTION

Uranium monocarbide and uranium dioxide are two currently available fuel materials of high uranium density. Both fuels have the potential of being utilized at high specific power levels to high burnups in a variety of reactor types. However, additional irradiation data on both carbides and oxides will be required to establish with confidence the performance limit of these fuels.

Uranium monocarbide has proved to be a very promising fuel for use in liquid metal cooled reactors with high specific power density cores. The metallic thermal conductivity and high uranium density[1] of UC enables it to be used as the fuel in small, high power density reactors. UC, however, has a temperature and burnup limit due to fuel volume changes[2,3] and reaction with fuel rod cladding materials at high temperatures. Carburization of the cladding is a serious problem in high temperature reactors particularly if a liquid metal is used as a heat transfer media between hyperstoichiometric UC and cladding.[4]

UO_2 has been developed to an advanced stage primarily for use in central station power reactors. Although UO_2 fuel is inert to reactor coolants, refractory, dimensionally stable under irradiation and easy to fabricate, it has not been considered for use in reactors requiring high specific power cores because of its very low thermal conductivity[5] in the solid state. This limit may be overcome if the fuel is allowed to operate partially molten. As power levels are allowed to exceed the limit for center melting, a question arises about the long term stability of the fuel rod. Extensive melting releases large amounts of fission gas, affects overall swelling of the fuel, and can redistribute the fuel axially in the central void that develops. It is also possible that the molten core of the fuel, if large enough, may come in contact with the clad, causing it to rupture.

In order to demonstrate the ability of UO_2 to be used as a high specific power fuel when irradiated to high burnups, and to establish operating limits for

both UO_2 and UC, an irradiation test program has been designed. The independent variables are: a) fuel rod power level, b) fuel burnup, and c) degree of restraint offered by the clad.

Table I shows the combinations of nominal power and burnup planned for each capsule. Table II gives the fuel, enrichment and clad thickness (AISI Type 348, annealed) for each fuel pin.

Description of Irradiation Test Assembly

The capsules are irradiated in tandem pairs in a holder. The holders are designed to fit the "L" holes in the primary beryllium reflector. This assembly is shown in Figure 1. The individual capsule is shown in Figure 2. The cans positioned in Capsule 1 - the subject of this report - are illustrated in data sheet Figures 3, 4, 5, 6. The tensile wire identifications and liquid metal loadings are listed, in addition to the dimensions. The fuel pins contained in their respective cans are shown in data sheet Figures 7, 8, 9, 10. The pellet densities listed in Figures 7, 8, 9, 10 were computed from the weights and dimensions given. Data sheet Figure 11 identifies the tensile wires located in the capsule flow dividers and the positions of the fuel cans in the capsule.

Presentation of Data

Characterization of Materials

Fuel

The UO_2 was supplied by United Nuclear Corporation and was fabricated by conventional cold pressing and hydrogen sintering. The UO_2 pellets had densities ranging around 96% of theoretical. The ratio of oxygen to uranium atoms ranged from 1.992 to 1.995. The analysis of impurities is given in Tables III and IV. All pellets were centerless ground to a diameter of 0.2995 ± 0.0005 inches with a surface finish of 32

microinches RMS or better. The cylindrical pellets are 0.450 to 0.500 inch long; the ends are flat.

The UC was supplied by Atomics International and was made by arc melting and casting. The composition varies from stoichiometric up to 1.13 wt. % excess C. No impurity analysis is available. The pellets were centerless ground to the same tolerances as the UO_2. The length is approximately the same; the pellet ends are also flat.

Clad

The analysis of the weldrawn, annealed AISI 348 stainless steel is given in Table V. The end plugs are type 304 stainless steel which gives a tough, ductile weld to the type 348. The minimum mechanical properties were determined from axial tension tests on the tubing:

Yield Strength	=	39,800 psi
Ultimate Strength	=	87,000 psi
Elongation in 2 in.	=	40 %

The 304 stainless steel end plug material is stronger and more ductile than 348 stainless steel, so the weld zones are stronger and more ductile than the clad. All clad tubing was 100% eddy current tested for defects.

Tensile Wires

None of the wires from the capsules were tested, but have been stored until the wires from several capsules are available for test. The preirradiation characterization of the wires will appear in a later report when the irradiated wires have been tensile tested.

Fuel Pin Assembly Procedure

To insure the integrity of the fuel pin cladding, a sequence of nondestructive tests were performed during the fabrication of the pins.

In the following procedure, the parentheses, (), represent an assembly operation, and a square [ ], refers to an inspection step:

(1) Bottom 304 SST end plug is TIG welded to 348 SST tubing.

[2] Bottom weld is radiographed.*

[3] Bottom weld is helium leak tested.**

(4) Fuel pellets, previously identified in separate containers, are loaded into the tubes. UC fuel handling is all done in a helium atmosphere glove box.

(5) Upper 304 SST end plug is TIG welded in a helium atmosphere. Both UO_2 and UC pins now contain helium at one atmosphere pressure.

[6] Upper weld is radiographed.*

[7] Entire rod is helium leak tested.**

(8) Overall length and diameter measurements are taken prior to loading pin in outer can.

* Radiography Technique

Two radiographs are taken of each weld 90° apart using SST correction forms. The sensitivity of the process is better than 2% revealing any defect or lack of weld penetration.

** Helium Leak Test

All welds are first examined at 45X for gross defects such as holes or under cutting prior to leak testing. The fuel pins are then placed in a chamber which is evacuated and backfilled with helium to 45 psi. This pressure is maintained for 30 minutes. The pins are removed from the chamber, and after 15 minutes, placed in a vacuum retort connected to a helium mass spectrometer. The retort is evacuated through the spectrometer to detect helium loss from the pins. The sensitivity of this test is better than 1×10^{-6} cc/sec.

Design Calculations

Heat Transfer - Temperature Distributions

Capsule equivalent diameter, De = 0.198 in.

Coolant velocity, V = 27.2 fps

Coolant flow, F = 60 gpm

Coolant inlet Temperature, T_{in} = 52°C

Coolant temperature rise, ΔT_{rise} = $\frac{3.78P}{F}$, °C

where $P = P_L \times \frac{4\text{" fuel length}}{12\text{"/'}} \times \frac{4 \text{ pins}}{\text{cap.}}$, kw.

P_L = kw/ft, each pin.

Coolant outlet temperature, T_{out} = $T_{in} + \Delta T_{rise}$, °C

Mean coolant temperature, T_{mean} = $\frac{T_{in} + T_{out}}{2}$, °C

Coolant film temperature, T_f = $\frac{T_{mean} + T_{surf}}{2}$, °C

Surface temperature of can, T_{surf} = $T_{mean} + \frac{(Q/A)_{can}}{h}$, °C

Can surface heat flux, $\left(\frac{Q}{A}\right)_{can}$ = $P_L \times \frac{4\text{"}}{12\text{"/'}} \times \frac{3415}{\pi D/12}, \frac{BTU}{hr\text{-}ft^2}$

Can outside diameter, D = 0.625 in.

Heat transfer coefficient, h = $N(T_f) \frac{V^{.8}}{De^{.2}} \times \frac{10^4}{5.67} \times 1.8, \frac{BTU}{hr\text{-}ft°C}$

V and De are in the units given above and $N(T_f)$ is a water properties function of film temperature only.

Maximum fuel pin power, P_L = 49.6 kw/ft

Mean fuel pin power, P_L = 33.19 kw/ft

Then: ΔT_{rise} = 2.79 C°, (based on mean P_L)

$\left(\frac{Q}{A}\right)_{can}$ = 0.3451 x 10^6 Btu/hr-ft^2 (Based on max P_L)

Assume T_f = 62.8°C, then $N(T_f)$ = 0.215 and h = 17,930 Btu/hr-ft^2-C°

$$T_{mean} = 52 + \frac{2.79}{2} = 53.4°C$$

$$T_{surf} = 53.4 + \frac{.3451 \times 10^6}{.01793 \times 10^6} = 72.7°C$$

Checking $T_f = \frac{53.4 + 72.7}{2} = 63.0\ °C \simeq 62.8$, O.K.

The temperature drop across the successive annulii - can, NaK, clad - are approximately expressed by:

$$\Delta T_{ann.} = \frac{P_L}{2\pi k} \ln\left(\frac{OD}{ID}\right), \ °C$$

P_L = max linear power, 49.6 kw/ft

k = thermal conductivity

Region	k, kw/ft-°C	OD, in.	ID, in.	$\Delta T_{ann.}$, °C
can (304 SST)	0.00501	0.625	0.525	267.9
NaK (78% K)	0.00791	0.525	.324 pin 1	481.5
			.344 pin 2	422.1
			.364 pin 3	365.3
			.342 pin 4	422.1
clad (348 SST)	0.00685	.324	.304 pin 1	73.4
		.344	.304 pin 2	142.4
		.364	.304 pin 3	207.4
		.342	.302 pin 4	142.4

The annular temperature differences for a mean P_L = 33.19 kw/ft are pro-

portionally less. The can surface temperature for the mean P_L is about 66°C.

The fuel surface temperature depends on the heat flux and gas gap conductance. The latter can vary - depending on interfacial pressure and surface roughness of clad and fuel - over the range 500 to 4000 Btu/hr-ft-°F. We initially select a value of 2000 for estimating fuel temperatures. The heat flux at the gap is about the same for all pins:

$$\left(\frac{Q}{A}\right)_{gap} = \left(\frac{Q}{A}\right)_{can} \times \frac{.625}{.300}$$

$$= 0.719 \times 10^6 \text{ Btu/hr-ft}^2 \text{ for } P_L \text{ max.}$$

$$= 0.481 \times 10^6 \text{ Btu/hr-ft}^2 \text{ for } P_L \text{ mean}$$

The temperature drop across the gas gap in each pin,

$$\Delta T \text{ gap} = \frac{0.719 \times 10^6}{2000 \times 1.8} = 200 \text{ C° for } P_L \text{ max.}$$

$$\Delta T \text{ gap} = 134 \text{ C° for } P_L \text{ mean}$$

The central temperature of the fuel pins may be characterized by the sum of two integrals:

$$\int_o^{T_{center}} k \, d\theta = \int_o^{T_{surface}} k \, d\theta + \int_{T_s}^{T_c} k \, d\theta$$

where the fuel thermal conductivity, $k = k(\theta)$

The method of Robertson[16] may be used to evaluate the terms in the expression and to determine the fuel center temperature (if all solid) or the radius of melting. At a power level of 49.6 kw/ft, the fuel surface temperature is about 1100°C. The value of the first integral, $\int_o^{T_s} k \, d\theta \simeq 50$ w/cm.*

The value of the second integral depends on the flux depression factor, f, as well as the power level. At 8.5% enrichment and 0.3000 inch diameter, f = 0.8825.*

*WAPD UO_2 thermal conductivity and flux depression data are used rather than Robertson's.

$$\int_{T_s}^{T_c} k\, d\theta = 0.8825 \times \frac{49.6 \text{ kw/ft}}{4\pi} \times \frac{10^3 \text{ w}}{\text{kw}} \times \frac{1 \text{ ft}}{30.5 \text{ cm}}$$

$$= 114.2 \text{ w/cm}$$

If the sum of these integral, $\int_{o}^{T_c} k\, d\theta > 97$ w/cm, there is center melting. This is clearly the case for the UO_2 fuel pins.

For f = 0.8825, a dimensionless neutron diffusion parameter, Ka ≈ 1.5. The fuel radius, a = 0.381 cm. The integral to the radius of the molten zone, r_m,

$$\int_{T_s}^{2800°C} k\, d\theta = \frac{49.6 \times 10^3 \, f(r_m)}{4\pi \times 30.5} = 97-50 = 47 \frac{W}{cm}$$

where 97 is the value from 0 to 2800°C

50 is the value from 0 to T_s

and $f(r_m)$ is the flux depression into r_m

Solving, $f(r_m) = 0.363$, for which the dimensionless radius of melting,

$\frac{r_m}{a} = 0.8$, for Ka = 1.5

The radius of melting, r_m = .303 cm is nearly the same for all three UO_2 pins.

The center temperature of the UC is simpler to calculate since k_{UC} does not vary strongly with temperature and there is no melting. In the temperature range above 300°C, $k_{UC} \approx 0.2249 \frac{w}{cm - °C}$.

The melting point of UC is about 2450°C.

$$\int_{T_s}^{T_c} k_{UC}\, d\theta \approx k_{UC}\, \Delta T = .2249 (T_c - 1105) = 114.2 \frac{W}{cm}$$

Solving, T_c = 1613°C (<2450°C) for P_L = 49.6 kw/ft. The same procedure is followed for P_L = 33.19 kw/ft. The temperature distributions are given in Tables VI and VII. The temperature profile is used to estimate the fission gas release and dimensional changes of the pins.

Fission Gas Release and Clad Expansion

The U-235 burnup is an effective full power time of 3.24×10^6 seconds is 0.2264×10^{21} fissions/cc fuel. The fission gas yield (Kr and Xe), including decay, is 0.295. At STP (0°C and 1 atm), one cc of (monatomic) fission gas is composed of 2.69×10^{19} atoms. The volume of gas generated in each of the pins per unit volume of fuel,

$$V = \frac{0.2264 \times 10^{21} \text{ fissions/cc fuel} \times 0.295 \text{ atoms of Kr and Xe per fission}}{2.69 \times 10^{19} \text{ atoms/cc gas at STP}}$$

$$V = \frac{2.48 \text{ cc gas at STP}}{\text{cc fuel}}$$

The fuel volume in each pin is 4.268 cc. Therefore, the volume of gas generated in each pin is $2.48 \times 4.268 = 10.58$ cc.

The fraction of gas release is estimated by the method of Booth[7]. The activation energy for fission gas diffusion in UO_2 is taken as 82 Kcal/mole and the diffusion constant at 1400°C,

$$D' \ (1400°C) = 2 \times 10^{13} \text{ sec}^{-1}$$

This gives

$$D' \ (2800°C) = 1.5645 \times 10^{-8} \text{ sec}^{-1}$$

and in general,

$$D' \ (T) = 2 \times 10^{13} \exp \left[-4.13 \left(\frac{10^4}{T + 273} - 5.98 \right) \right]$$

where T = °C

The parameter, $\frac{1}{\pi^2 D' \ (2800)} = 6.476 \times 10^6$ sec

which is greater than the effective full power time, 3.24×10^6 sec. In this case, the fraction of gas released may be approximated by,

$$F = 4\sqrt{D' t/\pi} - 3D' t/2$$

for 2800°C, $F = .432$

D' for $T \leq$ 1100°C is 9.2×10^{-16} sec^{-1}.

For temperature this low, $f \simeq o$.

The mean temperature in the solid fuel annulus, $T_m \simeq \frac{T_s + 2800}{2}$

At $P_L = 49.6$ kw/ft, $T_s \approx$ 1100°C

to give $T_m = 1948$°C. Then

$$D'_{(1948°C)} = 9 \times 10^{-11} \text{ sec}^{-1}$$

and $F_{(1948°C)} = .0381$

For the whole solid portion, ignoring axial temperature gradient,

$$F_{solid} = 1/6 \left[F_{2800} + 4F_{1948}\right] = 0.0974$$

The volume of solid UO_2, weighted for flux depression, is $f_{(rm)} = .363$. The fraction of gas released from the molten fuel is 1.0. The total for the whole pin,

$$F = 1 - .363 + .0974 \times .363 = .672$$

The volume of gas released,

$$V_{gas} = .672 \times 10.58 = 7.11 \text{ cc, STP.}$$

A method analogous to this for UC is not available, but it is believed that a negligible quantity of gas would be released.

At mean $P_L = 33.19$ kw/ft, the fuel is partially molten, though not to the extent calculated for $P_L = 49.6$ kw/ft. At the mean power, $f_{(rm)} = .6525$ and $T_s \approx 757$°C. The surface is less than 1100°F, so diffusion processes are negligible in that part of the solid which is less than 1100°C, but recoil processes, which are independent of temperature, release fission gasses from the solid as though it were at a uniform temperature of 1100°C. Thus, Booth's method will underestimate the fission gas release from fuel with less than 1100°C surface temperature.

This is partly compensated, however, by using the initial mean power rather than the mean power over the exposure, 31.24 kw/ft.

$$T_m = \frac{2800 + 757}{2} = 1779°C$$

$$D'_{(1779°C)} = 1.96 \times 10^{-11} \text{ sec}^{-1}$$

$$D't = 6.35 \times 10^{-5}$$

$$F_{(1779)} = 0.0179$$

$$F_{Total,solid} = 0.0839$$

$$F_{pin} = 0.402$$

The 40.2% fission gas release corresponds to 4.25 cc (STP).

Retained fission products contribute to fuel swelling. If the temperatures are less than 1100°C, the contribution of bubble expansion to fuel swelling is negligible. The atomic volume effect, however, is operative and amounts to about 1.3 volume per cent for the 2.264×10^{20} fission/cc experienced in the capsule 1 fuel. This is the maximum swelling possible in the solid part of the fuel. The correction for fission gas lost from the solid part is negligible.

The volume change of UO_2 upon melting is 10.6%; the thermal expansion of liquid UO_2 is uncertain and will be ignored. The fractional volume of melted UO_2 at P_L = 49.6 kw/ft is 64%; the molten part @ P_L = 33.19 kw/ft is 30.25%. The initial void (porosity) is 5% or less; this serves to absorb part of the expansion.

The thermal expansion of the UO_2 fuel relative to the clad is more than offset by the 0.040 inch initial axial gap and 0.004" diametral gap.

$$\left(\frac{\Delta D}{D}\right)_{UO_2, \text{ solid}} = 2.9 \times 10^{-9} (T)^2 + 6.8 \times 10^{-6} T + 1.72 \times 10^{-4}$$

T = °C

$$\frac{\Delta D}{D}\Big/_{clad} \simeq 19.8 \times 10^{-6} \text{ (T-25)}$$

T = °C

At P_L = 49.6 kw/ft, T_{UO_2}, solid = 1948°C,

$T_{clad} \simeq$ 834°C

ΔD_{UO_2}, solid = $0.300 \times 24.42 \times 10^{-3}$ = 0.00733 inch

ΔL_{UO_2}, solid = $3.7 \times 24.42 \times 10^{-3}$ = 0.0904 inch

$\Delta D_{clad\ ID}$ = $0.304 \times 16.02 \times 10^{-3}$ = 0.00487 inch

$\Delta L_{UO_2,\ solid}$ - ΔL clad - axial gap = .0904 - .0593 - .040 = -.009 inch

No interference.

At P_L = 33.19 kw/ft, $T_{UO_2\ solid}$ = 1779°C, $T_{clad} \simeq$ 576°C.

@ P_L = 33.19 kw/ft:

- $\Delta D_{UO_2, solid}$ = $0.3000 \times 21.45 \times 10^{-3}$ = 0.0064 inch
- $\Delta D_{clad\ ID}$ = $0.304 \times 10.91 \times 10^{-3}$ = 0.0033 inch.

To translate the volumetric terms into diametral ones, the expansion is assumed isotropic:

@ P_L = 49.6 kw/ft:

$\Delta D_{\text{molten } UO_2 \text{ part of pellet}} = .64 \times \frac{.106}{3} \times .300 = .0068$ inch

$\Delta D_{\text{fission products (in solid } UO_2)} = (1-.64) \times \frac{.013}{3} \times .300 = .0005$ inch

ΔD_{UO_2} (minus porosity) = .0096 inch

ΔD_{clad} (including initial gap) = .0089 inch

diametral hot interference = .0007 inch @ P_L = 49.6 kw/ft

@ P_L = 33.19 kw/ft:

$\Delta D)_{\text{molten } UO_2} = .3025 \times \frac{.106}{3} \times .300 = .00325$ inch

$\Delta D)_{\text{f.p.'s}} = (1-.3025) \times \frac{.013}{3} \times .300 = .00091$ inch

$\Sigma\Delta D_{UO_2}$ (less porosity) = .0055 inch

$\Sigma\Delta D$ clad (+ cold gap) = $\underline{.0073}$ inch

diametral hot gap= .0018 inch

$\Delta L_{UO_2 \text{ solid}} - \Delta L \text{ clad} - \text{axial gap} = 3.7 (21.45 - 10.91) \times 10^{-3} - .040 = -.001$

No interference.

No net change in clad diameter or length is expected since the initial void is larger than the permanent UO_2 expansion.

The total expansion of UC is described by $\frac{\Delta L}{Lo} = (3.487 + 1.143 \ln T)(T-20) \times 10^{-6}$

T = °C

T_{mean} (@ P_L = 49.6 kw/ft) = 1359°C

T_{mean} (@ P_L = 33.19 kw/ft) = 927°C

$\Delta D_{\text{f.p.'s}} = \frac{.013}{3} \times .3 = .0013$

Initial porosity = 0

ΔD Therm. = 0.0157 x .3 = $\underline{.0047}$

$\Sigma\Delta D_{UC} = .0060$ @ P_L = 49.6 kw/ft

Cold gap = 0.0020

ΔD therm., clad= 0.0049

$\Sigma\Delta$ clad = $\underline{.0069}$ @ P_L = 49.6 kw/ft

diametral hot gap = .0009 inch

$\Delta L_{UC} = \left(\frac{.013}{3}\right) \times 3.7 + .0157 \times 3.7 = 0.0741$ inch } axial hot gap

$\Delta L_{\text{clad}} + \text{axial gap (cold)} = .0593 + .042 = 0.1013$ } = 0.027 inch

@ P_L = 33.19 kw/ft

ΔD therm. UC = 0.01035 x .3 = 0.0031 inch

ΔD f.p.'s = 0.0013

$\Delta\Sigma D_{UC}$ = 0.0044 inch

ΔD therm, clad = .0033

cold gap = .0020

$\Sigma\Delta$ clad = 0.0053 inch

diametral hot gap = 0.0009

$\Delta L_{UC} = 0.01035 \times 3.7 + \frac{.013}{3} \times 3.7 = .0543$ inch

ΔL_{clad} + axial gap = $10.91 \times 10^{-3} \times 3.7 + .042 = 0.0824$

axial hot gap = 0.0281

If these hot gaps existed, the UC would probably increase in temperature until it touched the clad since only under the condition of clad-fuel contact can the high conductance postulated be achieved. The clad temperature would not change since this depends only on the heat flux through it.

The UO_2 would tend to expand for the same reason, but, having touched the clad, would exert little force because of the large central void and molten region which cannot support radial loads. The UC, however, is not molten, develops no central void, and thus is able to support radial loads. The higher temperature in the UC that is necessary for adequate thermal expansion to touch the clad raises it significantly above the 1100°C threshold for the formation of fission gas bubbles in the fuel. These exert pressure on the UC, causing it to creep and thus swell with time. The force exerted on the clad by the fuel may be sufficient to cause the clad to creep and thus have a permanent diametral increase when examined after irradiation. Under these circumstances, it is impossible to predict either

the operating temperature in the UC fuel or amount of clad swelling associated with it.

The expected fission gas release and estimated clad dimension changes computed in this section are presented in Tables VI and VII.

Exposure History

The exposure history for capsule 1 is given for each cycle in data sheet figures 12 through 18. The reactor power variation for the entire exposure is given in figure 19. The calculated* mean power variation in a typical fuel pin is also shown in figure 19.

Figures 12 through 18 are included in this report, but may be omitted in later reports. This group of figures illustrates the method of management employed to control an increasingly complex series of irradiation experiments. Considering the number of capsules to be irradiated, the variety of reactor positions available, and the variation in equipment used, this represents a convenient way to keep track of the tests.

Post-Irradiation Examination

Fission Gas Release

After removal of the four cans from Capsule 1 and cursory examination, the first destructive test was to puncture each can and extract the cover gas over the NaK to see if the pin had failed, releasing fission gas into the can. The activity of the gas samples was checked and, if negligible, was released.

The gas sample taken from can 1-2 had substantial activity. When the pin was removed from the can it was found to be ruptured. The other fuel pins were intact and were punctured to extract their fission gas after dimensions and photographs were taken.

---

*Scale in Figure 19 is based on initial U-235 content. Actual mean power (at 60 MW) drops about 2 kw/ft during exposure.

The amount of gas in the pin or can was determined from the pressures recorded in the sampling system before and after puncture, and the known volume of the various components. The basic expression is:

$$P_1V_1 = P_3 (V_1 + V_2) - P_2V_2$$

where

P_1 = gas pressure in pin or can prior to rupture, μ
V_1 = volume of gas in pin or can, cc
P_2 = pressure in system, including sample bulb, prior to puncture, μ
V_2 = volume of system and sample bulb = 2015 cc
P_3 = pressure in system after puncture, μ
V_3 = $V_1 + V_2$, cc

The amount of gas shipped to Westinghouse Atomic Power Division is given by:

$$P_BV_B = P_1V_1 - P_4V_4$$

where

P_B = pressure in bulb after sweeping gas from system into bulb, μ
V_B = sample bulb volume = 100 cc
P_4 = pressure in system after sweep, μ
V_4 = $V_3 - V_B$, cc

If the pressure in the can is desired, as in 1-2, the free volume in can and pin, V_1 = 6.189 cc. The free volume in each of the unruptured pins, V_1, varies slightly. The recorded and calculated quantities mentioned above for capsule 1 are given in Table VIII. All pressures are at room temperature .

After arrival of the gas samples at WAPD, the quantity of gas that had been present in each pin was again determined, this time by analysis. Mass spectrographic analysis revealed some air contamination of the gas samples. In addition to air and fission gas, there is considerable helium, most of which is the original cover gas in the pin (or pin and can), and some decomposition and reaction products of contaiminants originally present in the fuel, such as

water. The glass bulb containing the gas from can 1-2 was damaged in separating it from the sampling apparatus; the gas was lost. The analyses of the three remaining gas samples are reported in Tables IX and X.

The amount of gas and the pressure calculated from the analysis is in good agreement with the P_1V_1 calculated from the Plumbrook sampling data. The respective quantities are given in Tables IX and VIII.

Dimensional Changes and Appearance

In general appearance, pins 1-1, 1-3 and 1-4 were unchanged after irradiation. Pin 1-2 failed by melting of the clad along one side of the lower third of the enriched fuel column. Some of the fuel was extruded to form a crust. Chemical and physical analysis of the crust showed it to be a porous mass of UO_2, NaK residue, and beads of cladding. There was no material which could defintely be characterized as reaction product between clad and fuel. No gross swelling was associated with the rupture. No dimensions were taken, but the axial expansion marker was examined and found to be undeformed. Figure 20 presents several views of the rupture, with and without the crust.

The dimensions of pins 1-1, 1-3, 1-4 are given in Table XI. The maximum diametral increase in pin 1-1 was 1.424%. This was accompanied by an axial shrinkage of 0.06% and small diametral shrinkage at the top and base of the pin. The maximum diametral increase in pin 1-3 was 0.659%. This was accompanied by an axial shrinkage of 0.06% and small diametral changes at the top and base of the pin. The diametral measurements on pin 1-4 are apparently in error; they suggest a 2.2% shrinkage. Checks on metallographic specimens from pin 1-4 show clad diametral increases as large as 4.4%. The increase in diameter was also confirmed by fuel density measurements, reported fully in a later section. Pin 1-4 apparently increased in length 0.07%.

The volume change of the pins may be estimated from the expression.

$$\frac{\Delta V}{Vo} \simeq 2\frac{\Delta D}{Do} + \frac{\Delta L}{Lo}$$

where $\frac{\Delta D}{Do}$ is the mean diametral change

Fuel Pin	$\frac{\Delta D}{Do}$	$\frac{\Delta L}{Lo}$	$\frac{\Delta V}{Vo}$	Displacement Volume Change
1-1	+0.00031	-0.000596	∿0	+18%
1-3	+0.00165	-0.00062	0.00268	0
1-4	(+0.022)*	+0.00066	0.04466	+27%

*Half of maximum estimated from metallographic specimen.

It is evident that the displacment measurement is worthless; it has been dropped from the procedure.

Fuel Sectioning and Preliminary Examination

After fission gas samples and dimension were taken, the pins were sectioned at the enriched pellet interfaces. The top and bottom of each pellet were photographed while the section was held by manipulators. One pellet was crushed and some material lost from the others. A new method of supporting the sections for photographing is being developed. The photos of sectioned pins 1-1, 1-3, 1-4 are presented in Figures 21, 22, 23. The central void and columnar grain growth regions are clearly visible, but the photos are too crude for quantitative evaluation.

The sections of each pin were allocated as follows for further examination:

Pellet Number	Use
1,6	Burnup Analysis
2,5	Metallography
4,8	Density
3,7	Spare

Burnup Analysis

A radiochemical analysis for Cs-137 was performed on pellets 1 and 6 of each pin at Plumbrook, in addition to a mass spectrographic analysis for uranium isotopic distribution. The dissolved samples were shipped to WAPD where confirmatory Cs-137 measurements were made. Consensus values of fission density are presented in Table XII.

Calculations of the atom percent burnup, based on mass spectrographic results, are given in Table XIII.

Metallography

Pellets 2 and 5 from pins 1-1, 1-3, 1-4 were mounted at Plumbrook, and ground and polished at WAPD. Pin 1-2 was sent intact to WAPD for mounting, sectioning, grinding and polishing. None of the specimens were etched. Macrophotographs were prepared to show extent of melting, grain growth, swelling, and central void development. These are presented in figures 24 through 38.

The size of the central void in pellet 1-1-2 is difficult to estimate because of fuel loss during handling. Pellet 1-1-5 is also badly fractured but the cavity is about 25% of the fuel diameter. Pellets 1-3-2 and 1-3-5 are more intact, so some estimate may be made of fuel redistribution during operation. On volume basis, the void in 1-3-2 is 9.6% and the void in 1-3-5 is 0.61%. The average of these quantities is close to the initial porosity of 5%. If the closed initial porosity, as well as the fission gas, migrates to a central void which extends over the length of the fuel, the UO_2 density should slightly increase. In fact, it did: from 95% to 97%.

The difference in void size between pellets 1-3-2 and 1-3-5 is due to fuel slumping. Pellet 2 operated in a 12% lower flux (unperturbed) than pellet 5, but the fuel slumping reduced the perturbation sufficiently to cause the upper part of the fuel to operate at a higher rate of fission density. The fission density measurements confirm this. The actual linear power distribution is proportional to the product of fission density rate and fuel cross sectional area at each level. The linear power is responsible for the temperature distribution, which in turn affects the amount of fuel slumping to the base of the pin. The complexity of the situation makes it difficult to predict power and temperature distributions, or reactivity effects, in fuel columns which are largely molten. This is the reason molten UO_2 operation is usually avoided in commercial reactor operation. The possibility of clad rupture due to contact with molten UO_2 aggravates this problem.

The central void everywhere above the rupture zone in pin 1-2 is nearly uniform: 46% of the fuel diameter. Since some fuel was lost through the opening at the base of the enriched fuel column, it may be assumed that most of the molten portion above the rupture has left that region. Thus, the void diameter above the rupture in pin 1-2 is nearly as large as the region which operated in the molten state. The predicted molten zone, based on the mean linear power, was 55% of the fuel diameter. This number, however, did not consider loss of molten fuel from this region. The maximum void that can exist due to the 5% initial porosity is only 22.4% of the fuel diameter. The actual cavity of twice this amount clearly represents molten fuel loss.

Microphotographic surveys at 500X, after etching, were made of pellets 1-4-2 and 1-4-5 to see if a significant amount of bubbles had formed. A typical central region of 1-4-5 is shown in Figure 39. Point count analysis of several grain boundaries gave the estimate that the grain boundary bubbles alone accounted for as much as 2.8% of the volume in pellets 1-4-2 and 1-4-5. The mean value for all areas surveyed was 2%. Some bubbles are also evident in the matrix of the UC, but these were not counted.

Fuel Density

Pellet densities were determined by the CCl_4 displacement method at Plumbrook. The weights, dry and immersed, of the fuel plus clad and the clad alone were measured. The temperature of the CCl_4 was recorded and its density calculated according to the expression:

$$d_{CCl_4} = 1.63255 - 1.9110 \times 10^{-3}\, t - 0.690 \times 10^{-6}\, t^2 \pm 0.0002,\ g/cc,\ 0<t<40^{\circ}C$$

The fuel density was calculated from the expression:

$$d_{fuel} = \frac{(\text{fuel, dry weight}) \times (d_{CCl_4})}{(\text{fuel, dry weight}) - (\text{fuel, immersed weight})}$$

where

(fuel, dry weight) = (clad plus fuel, dry weight) - (clad, dry weight)

(Fuel, immersed weight) = (clad plus fuel, immersed weight) - (clad, immersed weight)

Two measurements were made of each quantity, so the probable error was taken as half the difference between them. The fuel density error was determined in the standard manner:

The formula for fuel density is of the form: $d_{fuel} = \frac{A \times B}{C}$

This leads to the density error expression:

$$e_{d\ fuel} = \sqrt{\left(\frac{B}{C}\right)^2 e_A^2 + \left(\frac{A}{C}\right)^2 e_B^2 + \left(\frac{AB}{C^2}\right)^2 e_C^2}$$

where e_A, e_B, e_C are the errors in A, B, C.

Table XIV gives the measured weights and calculated fuel densitities. A slight densification of the UO_2 is evident and the UC is significantly less dense than non-irradiated material. There is apparently some error in the density of pellet 1-3-8.

The UC densities, pre- and post-irradiation may be used to calculate the swelling:

$$\frac{\Delta V}{Vo} = \frac{\frac{1}{d_f} - \frac{1}{d_o}}{\frac{1}{d}} = \frac{d_o}{d_f} - 1$$

where subscripts o and f refer to initial and final densities.

Pellet	1-4-4	1-4-8
d_o, g/cc	13.3170	13.2982
d_f, g/cc	12.8086	12.8225
$\frac{\Delta V}{Vo}$	0.03969	0.03710

Data Interpretation

Despite the wide variations in air contamination of the fission gas samples, it

was possible to determine the amount of fission gas released and the pressure it exerted in the pin prior to puncture to a very acceptable degree of accuracy. This is attested to by the excellent agreement of P_1V_1 (and P_1) values for UO_2 pins 1-1 and 1-3 which operated under nearly identical conditions. Also, fair agreement between the P_1V_1 product calculated from the PBRF data (Table VIII) and the P_1V_1 product calculated from the gas analysis (Table IX) implies fair gas sampling technique in the PBRF hot cells.

The fraction of fission gas released from the UO_2 in pins 1-1 and 1-3 (Table X) is in good agreement with the predicted release based on mean pin power (Table VII), given the limitations of the diffusion model below 1100°C and the uncertainty in the gap conductance. The gas release from the UC pin 1-4 was low, as expected. The internal pressure, P_1, in the pins was in all cases too low to cause significant stress in the cladding.

The clad dimensional measurements were not entirely satisfactory. The apparent diametral shrinkage of the annealed stainless steel cald has no reasonable explanation. Certainly the diameter of UC pin, 1-4, did not shrink since the UC swelled noticeably during irradiation, as shown by density measurements and by examination of the mounted metallographic specimens. Greater care with the optical gage is recommended, such as interspersing the pin diametral measurements with checks on standard bars. It may be that the plunger is not hitting the top of the pin. The overall length changes were so small that no judgement regarding their accuracy can be made.

The nature of the failure of UO_2 pin 1-2 cannot be conclusively determined. Since the failure was unaccompanied by general swelling or chemical reaction, and was exposed to the same conditions as the other UO_2 pins, which showed no signs of incipient failure, it must be concluded that the failure was a freak. Two mechanisms of failure may be conjectured:

1. Molten UO_2 touching the clad via a random crack in the solid UO_2 annulus, may have so weakened the clad that the gas pres-

sure forced a small leak. At the next reactor shutdown, the gas pressure - now reversed - forced NaK into the pin. At startup, the boiling, churning mass of NaK and molten UO_2 was forced out of the pin by the NaK vapor pressure. As the mixture left the pin and flowed down the outside of the clad, the UO_2 froze, forming the crust observed. This crust deprived the clad locally of heat transfer medium, causing it to melt, further exposing the fuel. Successive power cycling caused more fuel to leave the pin until the structure we observed was established.

2. Movement in and out of the reactor of the holder containing the capsule, including the time it was sent to the hot cells for gamma scanning, provided an opportunity for a bubble of helium cover gas to be trapped underneath the pin. This is possible since the annulus is partly constricted by a support disc over the end plug, called a spider, which holds the tensile wires in place. If such a bubble later escapes - say, due to hydraulic vibration - while the pin is operating at substantial power, the clad is momentarily deprived of NaK heat transfer medium. The clad overheats, burns-out, and molten UO_2 fuel is released which freezes to form a crust.

The second of these conjectured mechanisms depends on the heat transfer medium being liquid at room temperature. Thus, if this is the failure mode, it should not occur in the Na capsules (7 through 13).

If the first mechanism is operative, i.e., failures occur in Na as well as NaK capsules, then failures is random, and suitable statistics cannot be established unless a great many high power tests are run.

The results of burnup analyses (Table XII) for UO_2 fission density are very close to the predicted value for the given exposure time (Table VII).

The axial variation of calculated UO_2 fission density based on Cs-137 is not meaningful due to the considerable axial redistribution of Cs-137. The UC, which saw the same axial (unperturbed) flux gradient - higher flux in pellet

6 than in pellet 1 - reflects this in the calculated fission density based on Cs-137. The axial fission density distribution in the UO_2, however, should not be identical to that in the UC, largely due to the molten UO_2 slumping and its effect on flux perturbation.

The metallographic examination confirmed the UO_2 fuel slumping, the UC swelling, the UO_2 densification, and the radius of UO_2 melting predicted on the basis of mean linear power and the assumed gap conductance. The central void size in the unruptured UO_2 pins was entirely accounted for in terms of the initial closed porosity. The axial variation in void size explained the difference between the fission density gradient and the unperturbed flux gradient. Measurement of the UC clad diameter in the metallographic mounts at WAPD and bubble counts at high magnification confirmed PBRF's density measurement and rejected their diametral measurement of the UC. The release of the UO_2 closed porosity to form a central void explained the measured increase in UO_2 density. The void size above the rupture in pin 1-2 was very nearly equal to that predicted for the radius of melting at mean linear power. Apparently the rupture allowed most of the molten UO_2 to flow out of the pin.

The fuel density measurements considered the whole pellet and thus represent a mean radial fuel density. The CCl_4 does not penetrate the closed porosity; this made it possible to estimate volumetric changes in the UC fuel due to fission gas bubbles. It also permitted an estimate of the UO_2 fuel densification due to loss of initial porosity. The 4% volume change of the UC was confirmed by metallographic examination.

CONCLUSIONS

In general, it was possible - despite some experimental difficulties - to confirm the predicted fuel pin behavior based on the mean linear power of 33.19 kw/ft. The fission gas release, radius of melting, and density change of the UO_2 were in good agreement with predicted values even though there was considerable axial redistribution of fuel. The irradiation behavior of the UC could not be predicted quantitatively, but the qualitative expectations were confirmed.

The nature of the failure of pin 1-2 remains the thorniest problem to be solved. Further study of that failure will be justified only if a pattern of failures develops as the entire experiment proceeds.

At this low burnup, even at this high power, it is not possible to develop an empirical model of the UO_2 fuel swelling, nor to determine the restraining effect of varying clad thickness. It seems safe to say that the threshold burnup for UO_2 fuel swelling has not been reached.

REFERENCES

1. Rough, F. A., and Chubb, W., "An Evaluation of Data on Nuclear Carbides," BMI-1441, May 1960.

2. Hare, A. W., and Rough, F. A., "Irradiation Effects on Massive Uranium Carbide," BMI-1452, July 1960.

3. Sinizer, D. I., Webb, B. A., and Berger, S., "Irradiation Behavior of Uranium Carbide Fuels," International Atomic Energy Symposium on Radiation Damage in Solids and Reactor Materials, Venice, Italy, May 1962.

4. Webb, B. A., "Carburization of Austenitic Stainless Steel by Uranium Carbides in Sodium Systems," NAA-SR-6242, February 1962.

5. Belle, J., ed., "Uranium Dioxide: Properties and Nuclear Applications," Naval Reactors, Division of Reactor Development, USAEC: p. 177-189, July 1961.

6. Robertson, J. A., "$\int k \, d\theta$ in Fuel Irradiations," CRFD-835, April 1959.

7. Booth, A. H., "A Method of Calculating Fission Gas Diffusion From UO_2 Fuel and its Application to the X-2-f Loop Test," CRDC-721, January 1960.

Table I

Nominal Power and Burnup for UO_2* Fuel Pins in Each Capsule

Burnup 10^3 MWD/MTU	Power Level, Each Pin kw/ft			
	25	30	40	50
10	Capsule 1	4	7	--
25	2	5	8	10
40	3	6	9	11
60	--	--	13	--
80	--	--	--	12

*The UC pins are designed to give the same power level as the UO_2 pins, but being denser in U, their enrichment must be less. This makes their burnup in terms of total uranium less than the UO_2.

Table II

Materials, Enrichment and Clad Thickness - Each Fuel Pin

Identification Capsule - Pin	Fuel	Enrichment U-235, %	348 Stainless Steel clad wall, 10^{-3} Inch
1-1	UO_2	8.5	10
1-2	↓	↓	20
1-3	↓	↓	30
1-4	UC	6.8	20
2-1	UO_2	8.5	10
2-2	↓	↓	20
2-3	↓	↓	30
2-4	UC	6.8	20
3-1	UO_2	8.5	10
3-2	↓	↓	20
3-3	↓	↓	30
3-4	UC	6.8	20
4-1	UO_2	12.5	10
4-2	↓	↓	20
4-3	↓	↓	30
4-4	UC	10	20
5-1	UO_2	12.5	10
5-2	↓	↓	20
5-3	↓	↓	30
5-4	UC	10	20
6-1	UO_2	12.5	10
6-2	↓	↓	20
6-3	↓	↓	30
6-4	UC	10	20
7-1	UO_2	17.5	10
7-2	↓	↓	20
7-3	↓	↓	30
7-4	UC	14	20
8-1	UO_2	17.5	10
8-2	↓	↓	20
8-3	↓	↓	30
8-4	UC	14	20
9-1	UO_2	17.5	10
9-2	↓	↓	20
9-3	↓	↓	30
9-4	UC	14	20
10-1A*	UO_2	12.5	10
10-2A	↓	↓	20
10-3A	↓	↓	30
10-4A	UC	10	20
11-1A	UO_2	12.5	10
11-2A	↓	↓	20
11-3A	↓	↓	30
11-4A	UC	10	20
12-1A	UO_2	12.5	10
12-2A	↓	↓	20
12-3A	↓	↓	30
12-4A	UC	10	20
13(10)-3**	UO_2	8.5	30
13(10)-4	UC	6.8	20
13(11)-4	↓	↓	20
13(12)-4	↓	↓	20

*The A stands for the alternate (higher) enrichment finally selected for the manufacture of these fuel pins.

**The number in parenthesis refers to the capsule originally designated for fuel of this enrichment.

Table III

Analysis of UO_2 Impurities

Four samples of pellet chips from each enrichment were spectrographically analyzed. The range of the results on all the samples are reported below in parts per million of UO_2.

Element	Amount, ppm	Element	Amount, ppm
Ag	<.4	Mn	2.9-7.6
Al	<10-23	Mo	3.1-25.0
Au	<2	Na	<1-2.8
B	<.2-.33	Ni	18-200
Ba	<10	P	<50
Be	<.02-.04	Pb	<1
Bi	<.4	Rb	<2
Ca	<.5-36	Sb	<2
Cd	<.4	Si	86-340
Co	1.0	Sn	<1-2.7
Cr	19-51	Sr	<20
Cs	<10	Ti	<1-3.6
Cu	7.3-75	Tl	<10
Fe	73-160	V	<2
In	<2	W	<20
K	<1	Zn	<20
Li	<.2	Zr	<20
Mg	3.7-18		

Table IV

Analysis of Rare Earth Content of UO_2

One sample was spectrographically analyzed from each enrichment. Results are in parts per million of UO_2. The results were the same for all three enrichments.

La	<.3
Ce	< 1
Pr	< 1
Nd	<.3
Sm	<.1
Eu	<.03
Gd	<.03
Tb	<.1
Dy	<.1
Ho	<.1
Er	<.03
Tm	<.3
Yb	<.01
Lu	<.3

Table V

Analysis of AISI 348 Stainless Steel

Used for Cladding all Fuel Pins

Element	Weight %
C	0.074
Mn	1.70
Si	0.77
S	0.012
P	0.022
Cr	18.39
Ni	10.39
Mo	0.08
Cu	0.06
Co	0.013
Cb + Ta	0.87
Ta	0.079
Fe	Balance

Table VI

Designed Behavior of Capsule 1

Based on Maximum (Initial) Power* = 49.6 kw/ft

	Fuel Pin			
	1-1	1-2	1-3	1-4
Fuel	UO_2	UO_2	UO_2	UC
Enrichment, %	8.5	8.5	8.5	6.8
Burnup, 10^{21} Fissions/cc (Calculated for actual time)	0.2264	0.2264	0.2264	0.2264
Effective fuel power time, 10^6 sec (Actual)	3.24	3.24	3.24	3.24
Temperature Profile				
Clad OD, °C	821.9	762.5	705.7	762.5
Clad ID, °C	895.3	904.9	913.1	904.9
Fuel Surface, °C	1095.2	1104.8	1113.0	1104.8
Fuel Center (solid), °C	---	---	---	1613
Relative radius of melting, rm/a	.8	.8	.8	--
Fission gas release				
%	67.2	67.2	67.2	0
STP cc	7.11	7.11	7.11	0
Clad diameter change, %	0	0	0	**

*Includes 1 kw/ft γ heat.

**Cannot be predicted

Table VII

Designed Behavior of Capsule 1

Based on Mean (Initial) Power* = 33.19 kw/ft

	Fuel Pin			
	1-1	1-2	1-3	1-4
Fuel	UO_2	UO_2	UO_2	UC
Enrichment %	8.5	8.5	8.5	6.8
Burnup, 10^{21} $\frac{\text{fission}}{\text{cc}}$ (Calculated for Actual Time)	.2264	.2264	.2264	.2264
Effective fuel power time, 10^6 sec (Actual)	3.24	3.24	3.24	3.24
Temperature Profile				
Clad OD, °C	567.5	527.7	489.7	527.7
Clad ID, °C	616.6	623.0	628.5	623.0
Fuel Surface, °C	750.6	757.0	762.5	757.0
Fuel Center (solid), °C	--	--	--	1096.7
Relative radius of melting, rm/a	.55	.55	.55	--
Fission gas release				
%	40.2	40.2	40.2	0
STP cc	4.25	4.25	4.25	0
Clad diameter change, %	0	0	0	**

*Includes 1 kw/ft γ heat.

**Cannot be predicted.

Table VIII

Fission Gas Samples Taken at Plumbrook Hot Cells

NOTE: All operations and pressure measurements made at room temperature.

	Fuel Pin or Can			
	1-1	1-2	1-3	1-4
System pressure before puncture, P_2, μ	12	4	7	7
Pin or can free volume, V_1, cc	2.065	6.189	2.024	1.993
System pressure after puncture, P_3, μ	3000	4500	2350	710
Total volume, V_3, cc	2017	2021.2	2017	2017
Pressure after sweep, P_4, μ	200	250	160	46
Volume after sweep, V_4, cc	1917	1921.2	1917	1917
Pressure in pin or can, P_1, atm	3.94	1.93	3.07	0.935
Amount of gas shipped, P_BV_B, atm-cc	7.44	11.322	5.8133	1.747
Amount of gas in pin (or can), P_1V_1, atm-cc	7.94	11.954	6.2168	1.863

Table IX

Analysis of Gas Samples, Mole %

	Fuel Pin		
	1-1	1-3	1-4
Species			
H_2	0.37	2.30	2.73
He	14.86	22.95	88.79
N_2	25.91	2.38	3.12
O_2	6.45	0.19	1.29
Ar	0.32	0.05	0.07
CH_4	0.16	0.18	0.30
Other Hydrocarbons	-	-	0.90
Kr	7.05	9.84	0.43
Xe	44.88	62.11	2.37
"Fission Gas" (Xe + Kr)	51.93	71.95	2.80
"Air" (N_2 + O_2 + Ar)	32.68	2.62	4.48
Calculated P_1V_1 (room temp.), atm-cc	6.4838	7.3999	2.1627
Calculated P_1 (room temp.), atm	3.14	3.66	1.085

Table X

Quantity of Individual Isotopes of Kr and Xe
Present in the Fuel Pins, atm-cc @ 0°C

	Fuel Pin		
	1-1	1-3	1-4
Kr-83	0.0902	.0934	1.07×10^{-3}
Kr-84	0.1793	.1850	2.77×10^{-3}
Kr-85	0.0478	.0494	0.75×10^{-3}
Kr-86	0.3420	.3526	4.26×10^{-3}
Xe-131	0.4266	.4353	4.80×10^{-3}
Xe-132	0.6590	.6774	7.68×10^{-3}
Xe-134	1.2508	1.3002	14.61×10^{-3}
Xe-136	1.8617	1.8821	21.75×10^{-3}
Total released	4.8574	4.9754	57.69×10^{-3}
Total generated	10.58	10.58	10.58
% Fission gas released	45.91	47.03	0.55

Table XI

Post-Irradiation Dimensions of Fuel Pins 1-1, 1-3, 1-4

		Fuel Pin 1-1	Fuel Pin 1-3	Fuel Pin 1-4
Length, in. (3 readings taken)		8.7143	8.7028	8.7079
		8.7138	8.7025	8.7079
		8.7134	8.7025	8.7072
	mean =	8.7138 ± 0.0005	8.7026 ± 0.0002	8.7077 ± 0.0005
Diameter, in. (mas and min)				
	top	0.32270	0.36280	0.33301
		0.31612	0.36249	0.33299
	mean =	0.3194 ± 0.0033	0.3626 ± 0.0002	0.3330 ± 0.0000
	Center	0.32758	0.36640	0.33361
		0.32728	0.36728	0.33348
	mean =	0.3274 ± 0.0002	0.3668 ± 0.0004	0.3335 ± 0.0001
	Base	0.32225	0.36544	0.33511
		0.32234	0.36570	0.33581
	mean =	0.3223 ± 0.0000	0.3656 ± 0.0001	0.3355 ± 0.0004
Displacement volume, cc		13	14	14

Table XII

Fission Densities from U-isotope and Cs-137 Measurements on Pellets 1 and 6 from Pins 1-1, 1-3, 1-4

		1-1-1	1-1-6	1-3-1	1-3-6	1-4-1	1-4-6
U-isotope	Fission density, f/cc	2.38×10^{20}	2.36×10^{20}	4.75×10^{20}	1.86×10^{20}	7.51×10^{20}	2.65×10^{20}
	Mean* fission density for pin f/cc	2.37×10^{20}		2.73×10^{20}		4.11×10^{20}	
Cs-137	Fission density, f/cc	3.20×10^{20}	2.00×10^{20}	3.17×10^{20}	1.77×10^{20}	2.28×10^{20}	2.57×10^{20}
	Mean* fission density for pin f/cc	2.36×10^{20}		2.19×10^{20}		2.48×10^{20}	

*Assuming linear axial gradient.

Table XIII

Atom Percent Burnup from Mass Spectrographic Measurements on Pellets 1 and 6 from Pins 1-1, 1-3, 1-4

Pellet	Atom Percent U Burnup	
	Spectrograph	Mean* for pin
1-1-1	1.16 ± 0.21	1.15
1-1-6	1.15 ± 0.20	
1-3-1	2.26 ± 0.14	1.31
1-3-6	0.90 ± 0.16	
1-4-1	2.29 ± 0.05	1.25
1-4-6	0.81 ± 0.07	

*Assuming linear axial gradient.

Table XIV

Density Measurements on Fuel Samples from Capsule 1

	Fuel Pellet					
	1-1-3	1-3-4	1-4-4	1-1-8	1-3-8	1-4-8
Fuel Material	UO_2	UO_2	UC	UO_2	UO_2	UC
Clad + fuel, dry weight (mean), grams	2.78670 ± 0	5.19855 ± 0.00005	7.16685 ± 0.00015	4.86865 ± 0.00005	9.34975 ± 0.00005	8.0061 ± 0.0001
Clad, dry weight (mean), grams	0.58904 ± 0.00005	1.4206 ± 0	1.10095 ± 0.00005	0.52725 ± 0.00005	2.43060 ± 0.0001	1.1848 ± 0
Clad + fuel, immersed weight (mean), grams	2.34065 ± 0.00005	4.34065 ± 0.00035	6.18975 ± 0.00015	4.10635 ± 0.00025	7.74925 ± 0.00025	6.9194 ± 0.0003
Clad, immersed weight (mean) grams	0.47065 ± 0.00015	1.13205 ± 0.00015	0.87825 ± 0.00005	0.41845 ± 0.00005	1.9400 ± 0	0.9461 ± 0.0001
CCl_4 temperature, °C	20.56	20.00	20.56	20.00	20.56	20.0
CCl_4 density, g/cc	1.59297 ± 0.00020	1.59405 ± 0.0002	1.59297 ± 0.0002	1.59405 ± 0.0002	1.59297 ± 0.0002	1.59405 ± 0.0002
Fuel density, g/cc	10.68454 ± 0.00558	10.5774 ± 0.00725	12.8086 ± 0.00414	10.5898 ± 0.00449	9.9306 ± 0.00275	12.8225 ± 0.00527
Percent of Theoretical Density	97.40	96.42	93.97	96.53	90.53	94.08

647J123

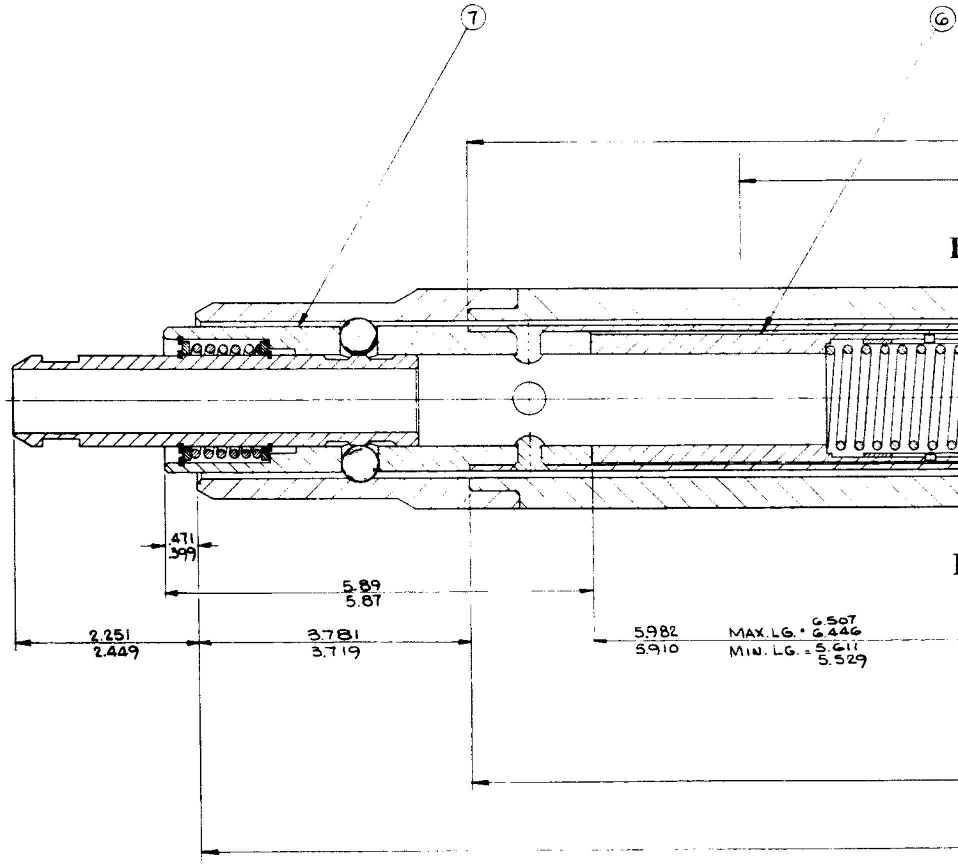

DGR 5001	1	
DGR 5001	2	ECN 1081
DGR	3	ECN

1-1

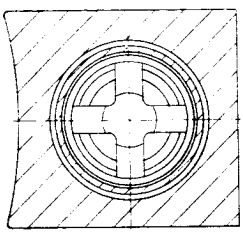

D-D

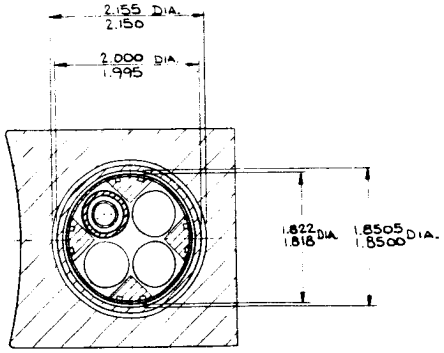

C-C

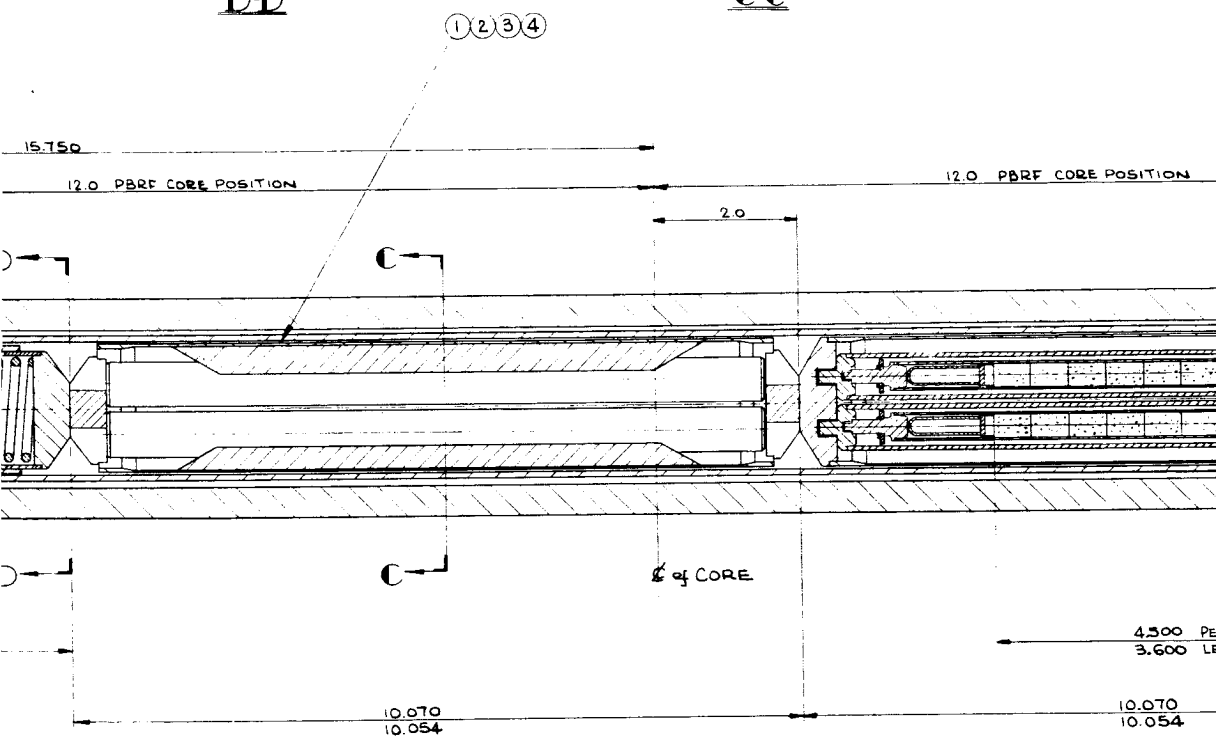

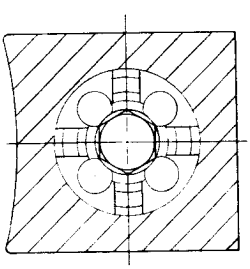

A-A

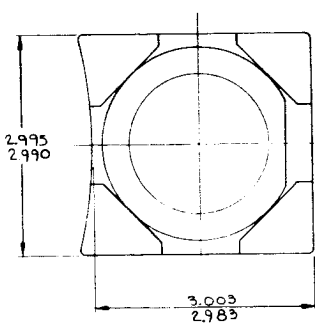

E-E

647J123
SUB 1 SEC 2 OF 2

1-2

BILL OF MATERIAL					NO. REQ.			
NOTE	ITEM	TITLE	DRAWING & GR. OR IT.	MATERIAL SPECIFICATION	PROPRIETARY SPECIFICATION FOR ONE ONLY	GR. 1	GR. 2	GR. 3	GR. 4
	1	CAPSULE	674C473-GR1			2	-	-	
	2	CAPSULE	674C473-GR2			-	2	-	
	3	CAPSULE	674C473-GR3			-	-	2	
	4	CAPSULE	674C473-GR4			-	-	-	2
	5	BASKET LATCH ASSY.	499B809-GR1			1	1	1	1
	6	SPRING PIN ASSEM.	674C472-GR1			1	1	1	1
	7	PLUNGER ASSEM.	674C463-GR1			1	1	1	1

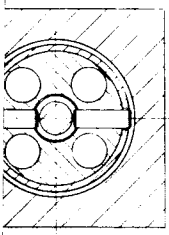

B-B

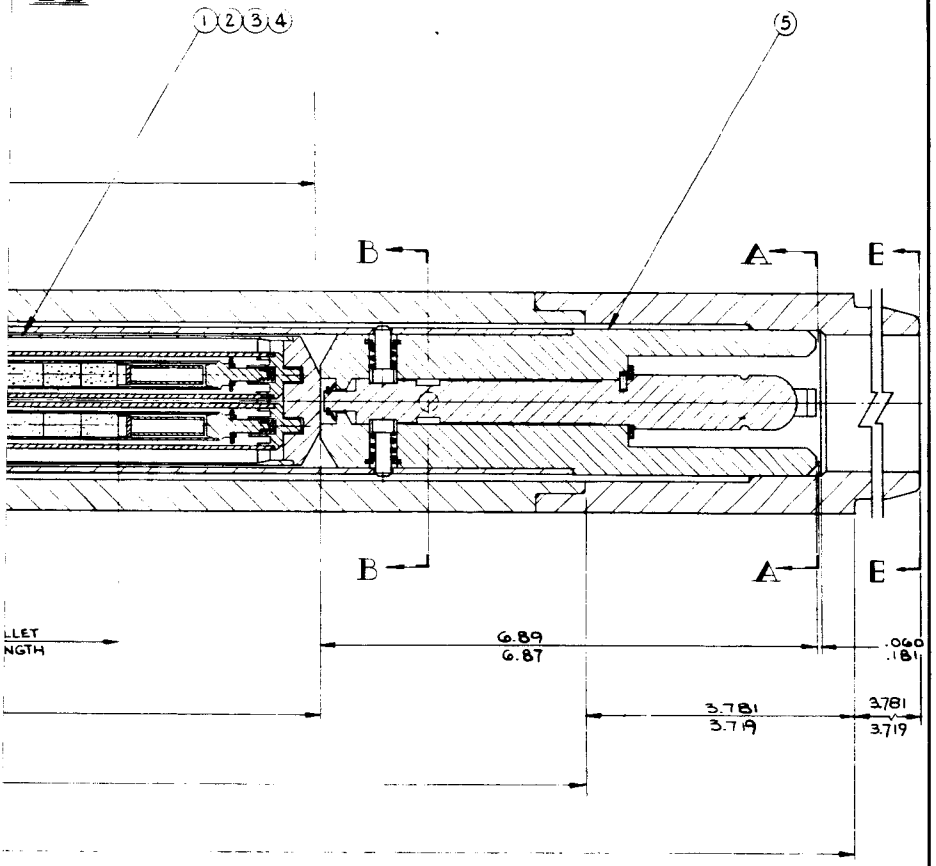

FIGURE 1

DFTM T B Wilson	1/10/63	WESTINGHOUSE ELECTRIC CORPORATION	
CHKR T B Wilson	2/6/63	ATOMIC POWER DIV. PITTSBURGH, PA. U.S.A.	
DES ENG	2/1/63	TITLE PLUM BROOK REACTOR FACILITY IN-PILE IRRADIATION EXPER. - GENERAL ASSEMBLY	
MFG ENG			
NTLS ENG			
APP	2/11/63	SCALE 1:1	647J123
APP		DIMENSIONS IN INCHES	
DFTG SUPV K Taylor	2-13-63	DO NOT SCALE	SUB # 23 SEC. 1 OF 2

NEXT ASSY

REF DWG

1-3

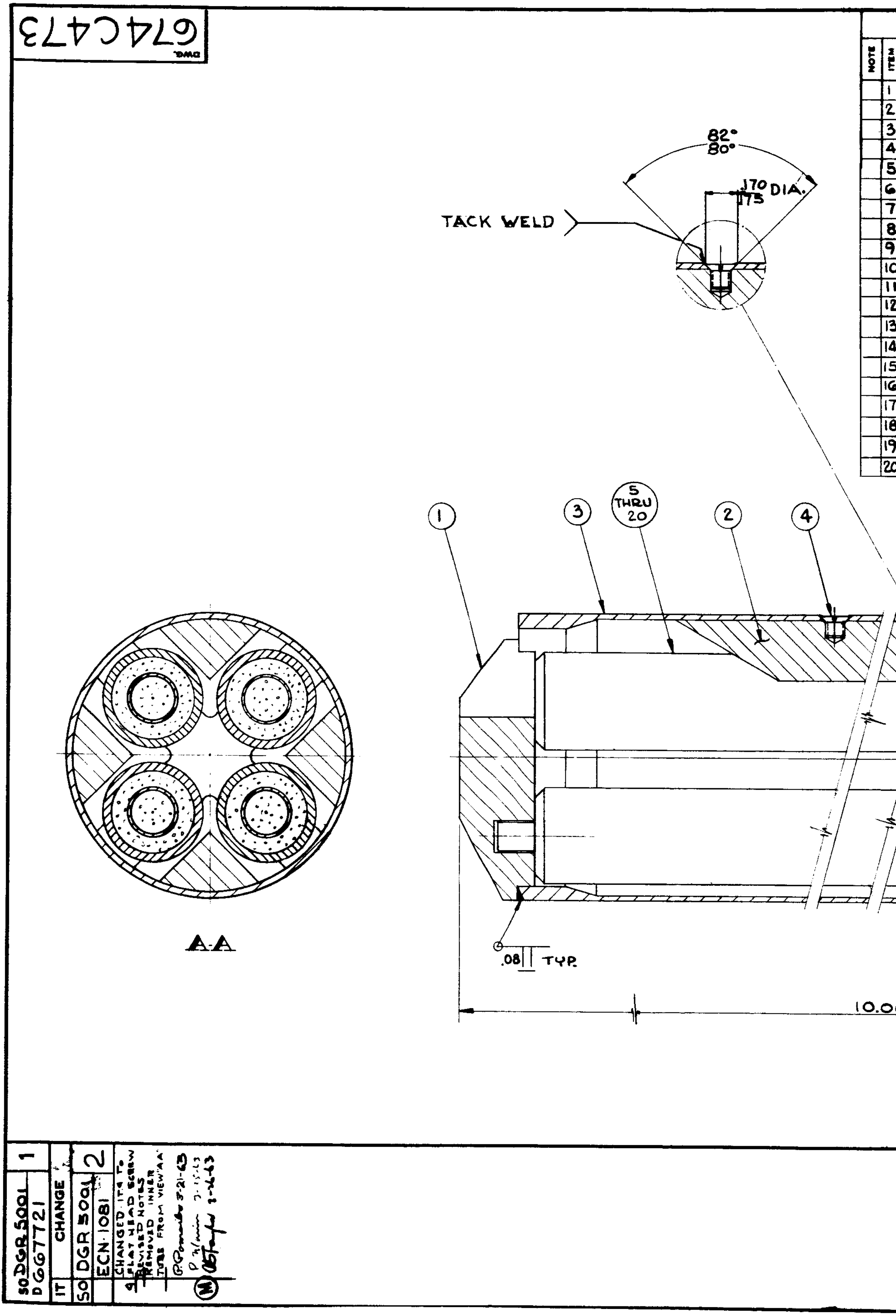

DWG. G74C473
82°
80°
.170
.175
DIA.
TACK WELD
1
3
5 THRU 20
2
4
A-A
.08 TYP.
10.0
SO DGR 5001 1
D GG7721
IT CHANGE
SO DGR 5001 2
ECN 1081
CHANGED IT 4 TO FLAT HEAD SCREW
REVISED NOTES
REMOVED INNER TUBE FROM VIEW 'AA'

BILL OF MATERIAL

TITLE	DRAWING & GR. OR IT.	MATERIAL SPEC.	EQUIV. SPEC.	NO. REQ. Gr.1	Gr.2	Gr.3	Gr.4
CAPSULE END PLUG	674C472-IT.1			2	2	2	2
FLOW BLOCKER	674C472-IT.2			4	4	4	4
CAPSULE TUBE	674C472-IT.3			1	1	1	1
SCREW	674C472-IT.4			12	12	12	12
FUEL ROD CAN ASSEM.	881D852-Gr.1			1			
↓	↓ -Gr.2			1			
	-Gr.3			1			
	-Gr.4			1			
	-Gr.5				1		
	-Gr.6				1		
	-Gr.7				1		
	-Gr.8				1		
	-Gr.9					1	
	-Gr.10					1	
	-Gr.11					1	
	-Gr.12					1	
	-Gr.13						1
	-Gr.14						1
↓	↓ -Gr.15						1
FUEL ROD CAN ASSEM.	881D852 Gr.16						1

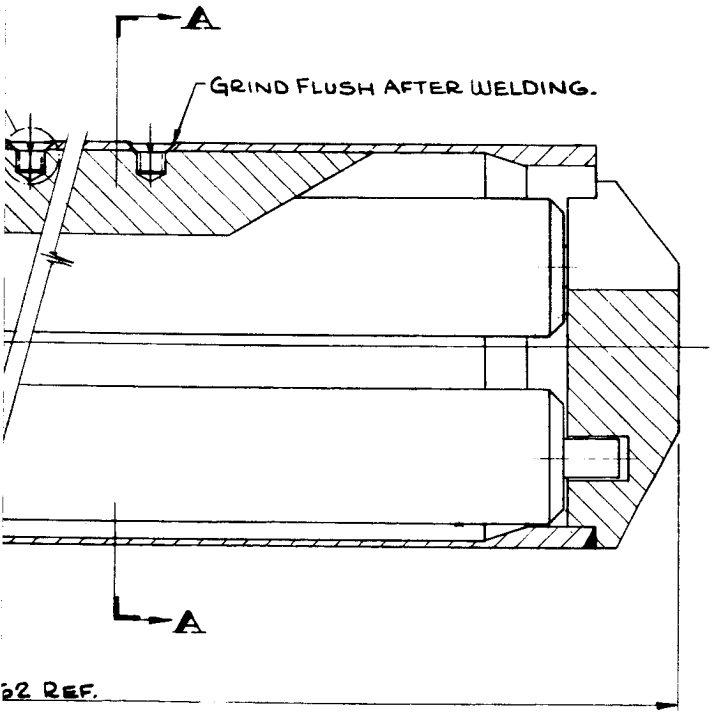

FIGURE 2

NEXT ASSY. 647J23	DFTM. T.D. Wiese	2/11/63	WESTINGHOUSE ELECTRIC CORPORATION
REF. DWGS.	CHKR. T.D. Wiese	2/11/63	ATOMIC POWER DIV.. PITTSBURGH, PA., U.S.A.
	DES. ENG. R. DUNCAN	2/11/63	TITLE: PLUM BROOK REACTOR FACILITY IN-PILE IRRADIATION EXPER: CAPSULE ASSEM.
	MFG. ENG.		
	MTLS. ENG.		
	APP. P Magnus	2/11/63	SCALE 2:1 — 674C473
	APP.		DIMENSIONS IN INCHES
	DEPTS. SUPV.	2-13-63	DO NOT SCALE — SUB ± 2

2-2

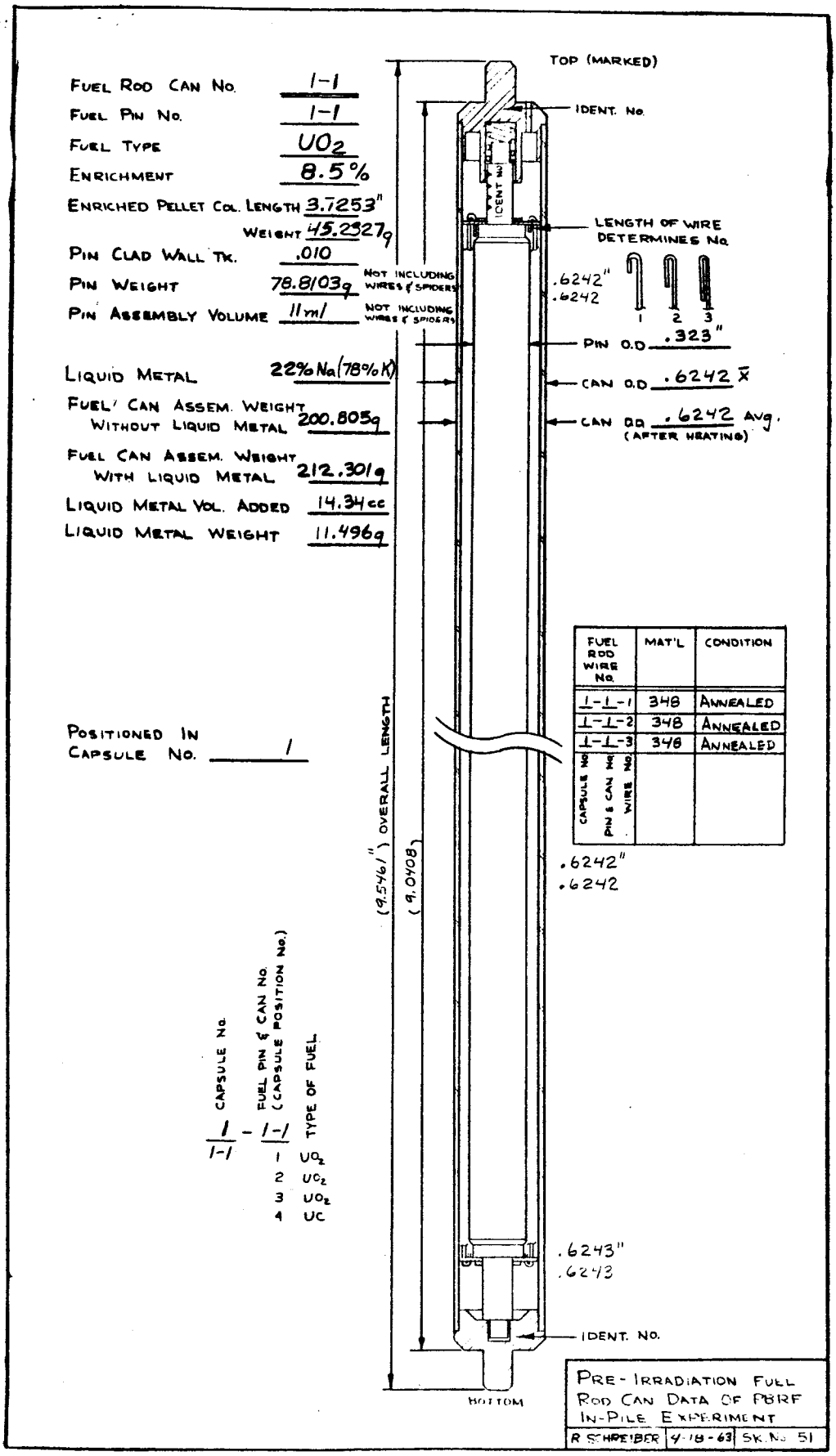
FUEL ROD CAN NO. 1-1
FUEL PIN NO. 1-1
FUEL TYPE UO2
ENRICHMENT 8.5%
ENRICHED PELLET COL. LENGTH 3.7253"
WEIGHT 45.2527g
PIN CLAD WALL TK. .010
PIN WEIGHT 78.8103g NOT INCLUDING WIRES & SPIDERS
PIN ASSEMBLY VOLUME 11ml NOT INCLUDING WIRES & SPIDERS
LIQUID METAL 22% Na (78% K)
FUEL CAN ASSEM. WEIGHT WITHOUT LIQUID METAL 200.805g
FUEL CAN ASSEM. WEIGHT WITH LIQUID METAL 212.301g
LIQUID METAL VOL. ADDED 14.34cc
LIQUID METAL WEIGHT 11.496g
POSITIONED IN CAPSULE NO. 1
TOP (MARKED)
IDENT. No.
LENGTH OF WIRE DETERMINES No.
1 2 3
.6242"
.6242
PIN O.D .323"
CAN O.D .6242 X̄
CAN OD .6242 Avg. (AFTER HEATING)
(9.5461") OVERALL LENGTH
(9.0408)
.6242"
.6242
.6243"
.6243
IDENT. No.
BOTTOM
FUEL ROD WIRE No. | MAT'L | CONDITION
1-1-1 | 348 | ANNEALED
1-1-2 | 348 | ANNEALED
1-1-3 | 348 | ANNEALED
CAPSULE NO. PIN & CAN NO. WIRE NO.
CAPSULE No. / FUEL PIN & CAN No. (CAPSULE POSITION No.) 1-1
TYPE OF FUEL
1 UO2
2 UC2
3 UO2
4 UC
PRE-IRRADIATION FUEL ROD CAN DATA OF PBRF IN-PILE EXPERIMENT
R SCHREIBER | 4-18-63 | SK. No. 51

Figure 3

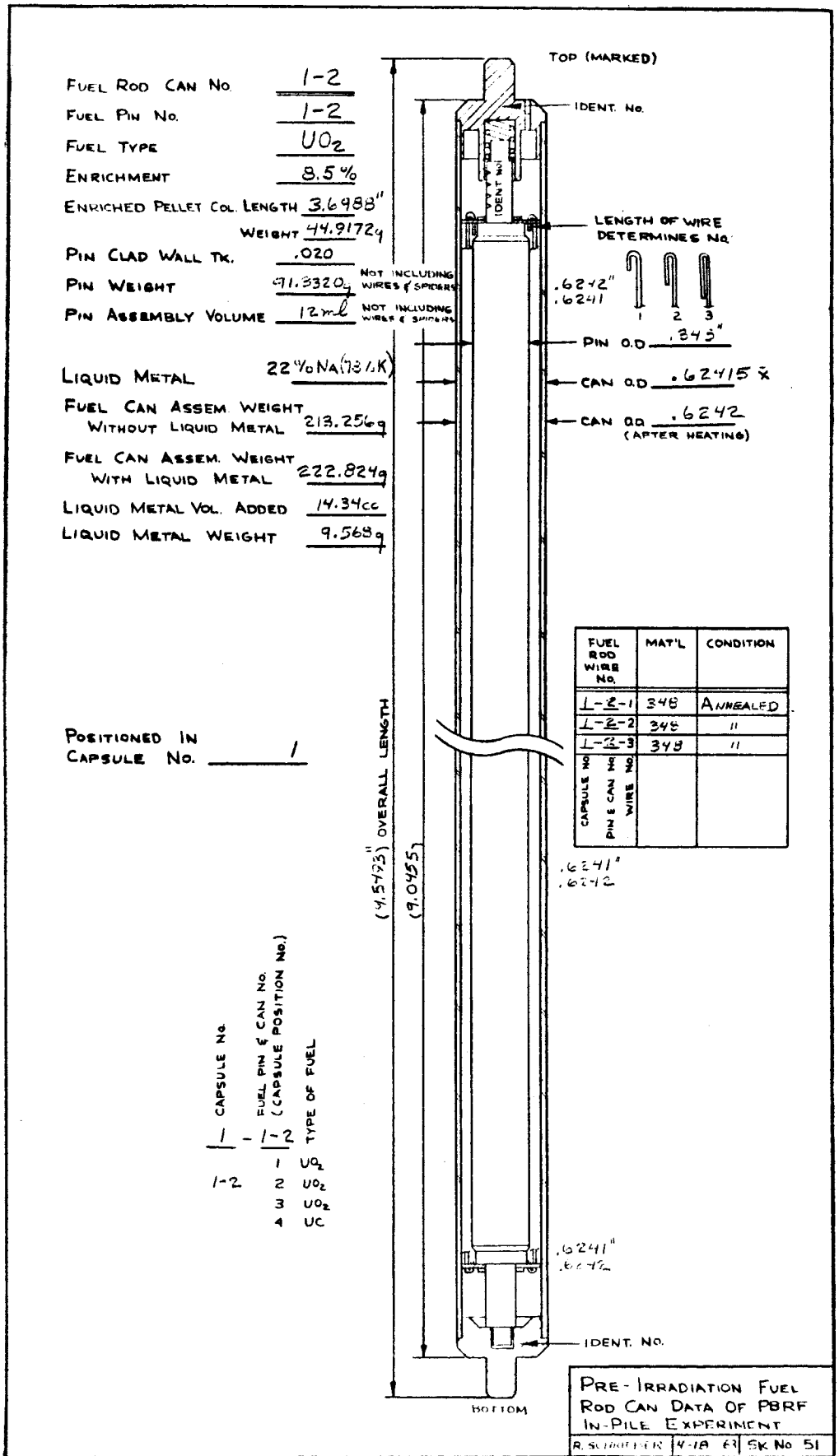
Fuel Rod Can No. 1-2
Fuel Pin No. 1-2
Fuel Type UO_2
Enrichment 8.5%
Enriched Pellet Col. Length 3.6988"
Weight 44.9172g
Pin Clad Wall Tk. .020
Pin Weight 91.3320g Not including wires & spacers
Pin Assembly Volume 12ml Not including wires & spacers
Liquid Metal 22%Na(78%K)
Fuel Can Assem. Weight Without Liquid Metal 213.256g
Fuel Can Assem. Weight With Liquid Metal 222.824g
Liquid Metal Vol. Added 14.34cc
Liquid Metal Weight 9.568g
Positioned In Capsule No. 1
Capsule No. 1 - Fuel Pin & Can No. 1-2 (Capsule Position No.)
Type of Fuel
1 UO_2
2 UO_2
3 UO_2
4 UC
Top (Marked)
Ident. No.
Length of Wire Determines No.
1 2 3
.6242"
.6241
Pin O.D .345"
Can O.D .62415"x
Can O.D .6242 (After Heating)
(4.5423") Overall Length
(9.0455)
.6241"
.6242
.6241"
.6242
Ident. No.
Bottom
Fuel Rod Wire No. | Mat'l | Condition
1-2-1 | 348 | Annealed
1-2-2 | 348 | "
1-2-3 | 348 | "
Capsule No. Pin & Can No. Wire No.
Pre-Irradiation Fuel Rod Can Data of PBRF In-Pile Experiment
R. Schaefer | 4-18-63 | SK No 51

Figure 4

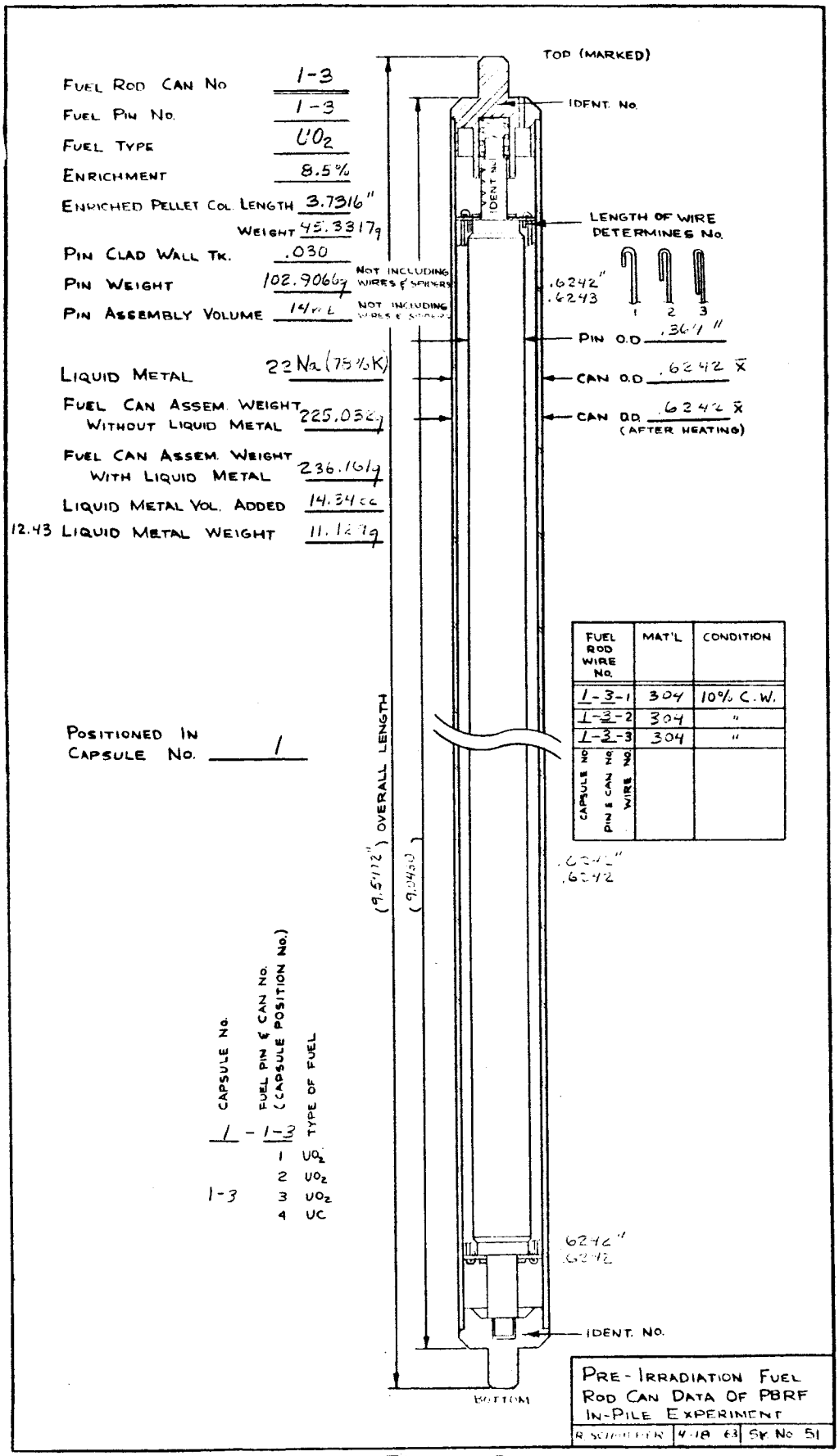
Fuel Rod Can No. 1-3
Fuel Pin No. 1-3
Fuel Type UO_2
Enrichment 8.5%
Enriched Pellet Col. Length 3.7316"
Weight 45.3317g
Pin Clad Wall Tk. .030
Pin Weight 102.9066g Not including wires & spacers
Pin Assembly Volume 14 ml Not including wires & spacers
Liquid Metal 22 Na (75% K)
Fuel Can Assem. Weight Without Liquid Metal 225.052g
Fuel Can Assem. Weight With Liquid Metal 236.161g
Liquid Metal Vol. Added 14.34 cc
12.43 Liquid Metal Weight 11.127g
Positioned In Capsule No. 1
Capsule No. 1 - Fuel Pin & Can No. (Capsule Position No.)
1-3
1 UO_2
2 UO_2
3 UO_2
4 UC
Type of Fuel
TOP (MARKED)
IDENT. No.
LENGTH OF WIRE DETERMINES No.
1 2 3
.6242"
.6243
Pin O.D .361"
Can O.D .6242 $\bar{x}$
Can O.D .6242 $\bar{x}$ (After Heating)
(9.5112") Overall Length
(9.2450)
.6242"
.6242
.6242"
.6242
IDENT. No.
BOTTOM
Fuel Rod Wire No. | Mat'l | Condition
1-3-1 | 304 | 10% C.W.
1-3-2 | 304 | "
1-3-3 | 304 | "
Capsule No. Pin & Can No. Wire No.
Pre-Irradiation Fuel Rod Can Data of PBRF In-Pile Experiment
R. Schneider | 4-18-63 | Sk. No. 51

Figure 5

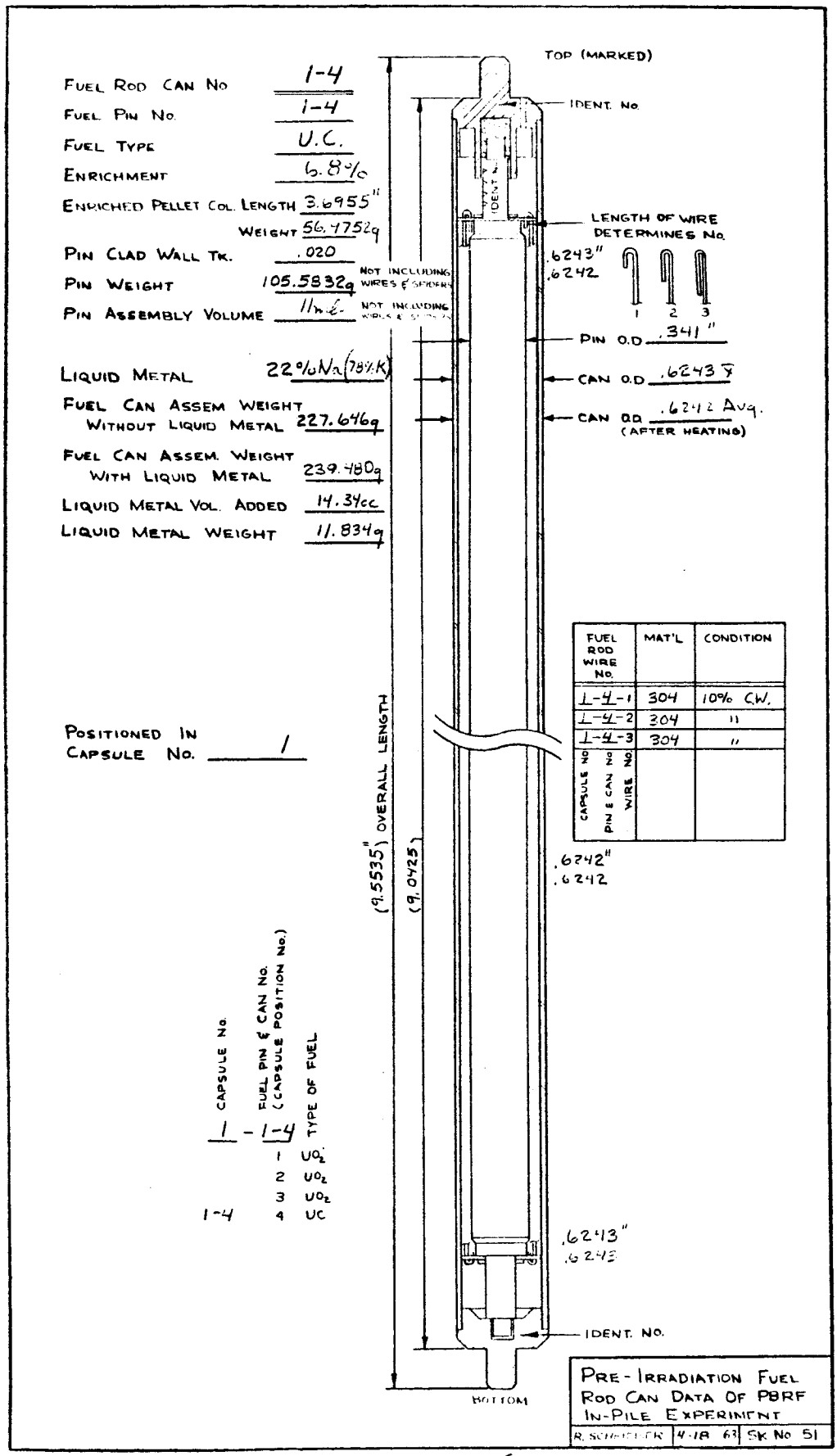
Fuel Rod Can No. 1-4
Fuel Pin No. 1-4
Fuel Type U.C.
Enrichment 6.8%
Enriched Pellet Col. Length 3.6955"
Weight 56.4752g
Pin Clad Wall Tk. .020
Pin Weight 105.5832g Not including wires & spiders
Pin Assembly Volume N.E. Not including wires & spiders
Liquid Metal 22%Na (78%K)
Fuel Can Assem Weight Without Liquid Metal 227.646g
Fuel Can Assem. Weight With Liquid Metal 239.480g
Liquid Metal Vol. Added 14.34cc
Liquid Metal Weight 11.834g
Positioned In Capsule No. 1
TOP (MARKED)
IDENT. No.
LENGTH OF WIRE DETERMINES No.
.6243"
.6242
1 2 3
Pin O.D .341"
Can O.D .6243 Max.
Can O.D .6242 Avg. (After Heating)
(9.5535") OVERALL LENGTH
(9.0425)
FUEL ROD WIRE No. | MAT'L | CONDITION
1-4-1 | 304 | 10% C.W.
1-4-2 | 304 | "
1-4-3 | 304 | "
CAPSULE No. PIN & CAN No. WIRE No.
.6242"
.6242
.6243"
.6243
IDENT. No.
BOTTOM
CAPSULE No. 1 - FUEL PIN & CAN No. 1-4 (CAPSULE POSITION No.)
TYPE OF FUEL
1 UO2
2 UO2
3 UO2
1-4 4 UC
PRE-IRRADIATION FUEL ROD CAN DATA OF PBRF IN-PILE EXPERIMENT
R. SCHAEFER 4-18 63 SK No 51

Figure 6

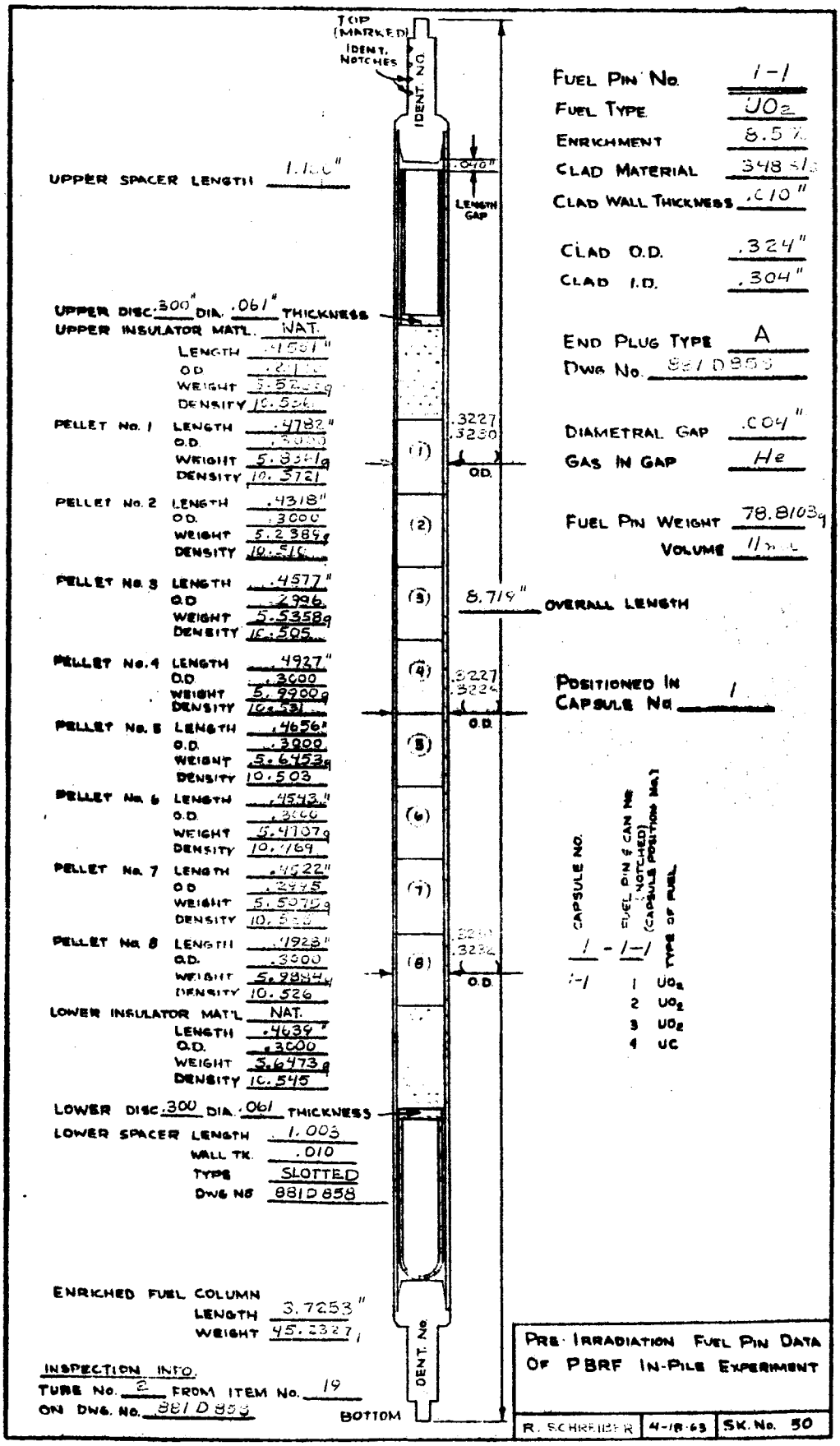
TOP (MARKED)
IDENT. NOTCHES
IDENT. NO.
.046"
LENGTH GAP
UPPER SPACER LENGTH 1.100"
UPPER DISC. .300" DIA. .061" THICKNESS
UPPER INSULATOR MAT'L. NAT.
LENGTH .4581"
O.D. .2110
WEIGHT 5.5259g
DENSITY 10.526
PELLET No. 1 LENGTH .4782"
O.D. .3000
WEIGHT 5.8341g
DENSITY 10.3721
PELLET No. 2 LENGTH .4318"
O.D. .3000
WEIGHT 5.2389g
DENSITY 10.515
PELLET No. 3 LENGTH .4577"
O.D. .2996
WEIGHT 5.5358g
DENSITY 10.505
PELLET No. 4 LENGTH .4927"
O.D. .3000
WEIGHT 5.9900g
DENSITY 10.331
PELLET No. 5 LENGTH .4656"
O.D. .3000
WEIGHT 5.6453g
DENSITY 10.503
PELLET No. 6 LENGTH .4543"
O.D. .3000
WEIGHT 5.4707g
DENSITY 10.769
PELLET No. 7 LENGTH .4522"
O.D. .2975
WEIGHT 5.5070g
DENSITY 10.528
PELLET No. 8 LENGTH .1928"
O.D. .3000
WEIGHT 5.9884g
DENSITY 10.526
LOWER INSULATOR MAT'L NAT.
LENGTH .4639"
O.D. .3000
WEIGHT 5.6473g
DENSITY 10.545
LOWER DISC. .300 DIA. .061 THICKNESS
LOWER SPACER LENGTH 1.003
WALL TK. .010
TYPE SLOTTED
DWG NO 881D858
ENRICHED FUEL COLUMN
LENGTH 3.7253"
WEIGHT 45.2327g
INSPECTION INFO.
TUBE No. 2 FROM ITEM No. 19
ON DWG. No. 881D853
BOTTOM
DENT. No.
(1)
(2)
(3)
(4)
(5)
(6)
(7)
(8)
.3227
.3230
O.D.
8.719" OVERALL LENGTH
.3227
.3224
O.D.
.3230
.3234
O.D.
FUEL PIN No. 1-1
FUEL TYPE UO2
ENRICHMENT 8.5 %
CLAD MATERIAL 348 S/S
CLAD WALL THICKNESS .010"
CLAD O.D. .324"
CLAD I.D. .304"
END PLUG TYPE A
DWG No. 881D859
DIAMETRAL GAP .004"
GAS IN GAP He
FUEL PIN WEIGHT 78.8103g
VOLUME 11 cc
POSITIONED IN CAPSULE No. 1
CAPSULE NO.
FUEL PIN & CAN NO (NOTCHED)
(CAPSULE POSITION No.)
TYPE OF FUEL
1 - 1-1
1-1
1 UO2
2 UO2
3 UO2
4 UC
PRE-IRRADIATION FUEL PIN DATA OF PBRF IN-PILE EXPERIMENT
R. SCHREIBER
4-18-63
SK. No. 50

Figure 7

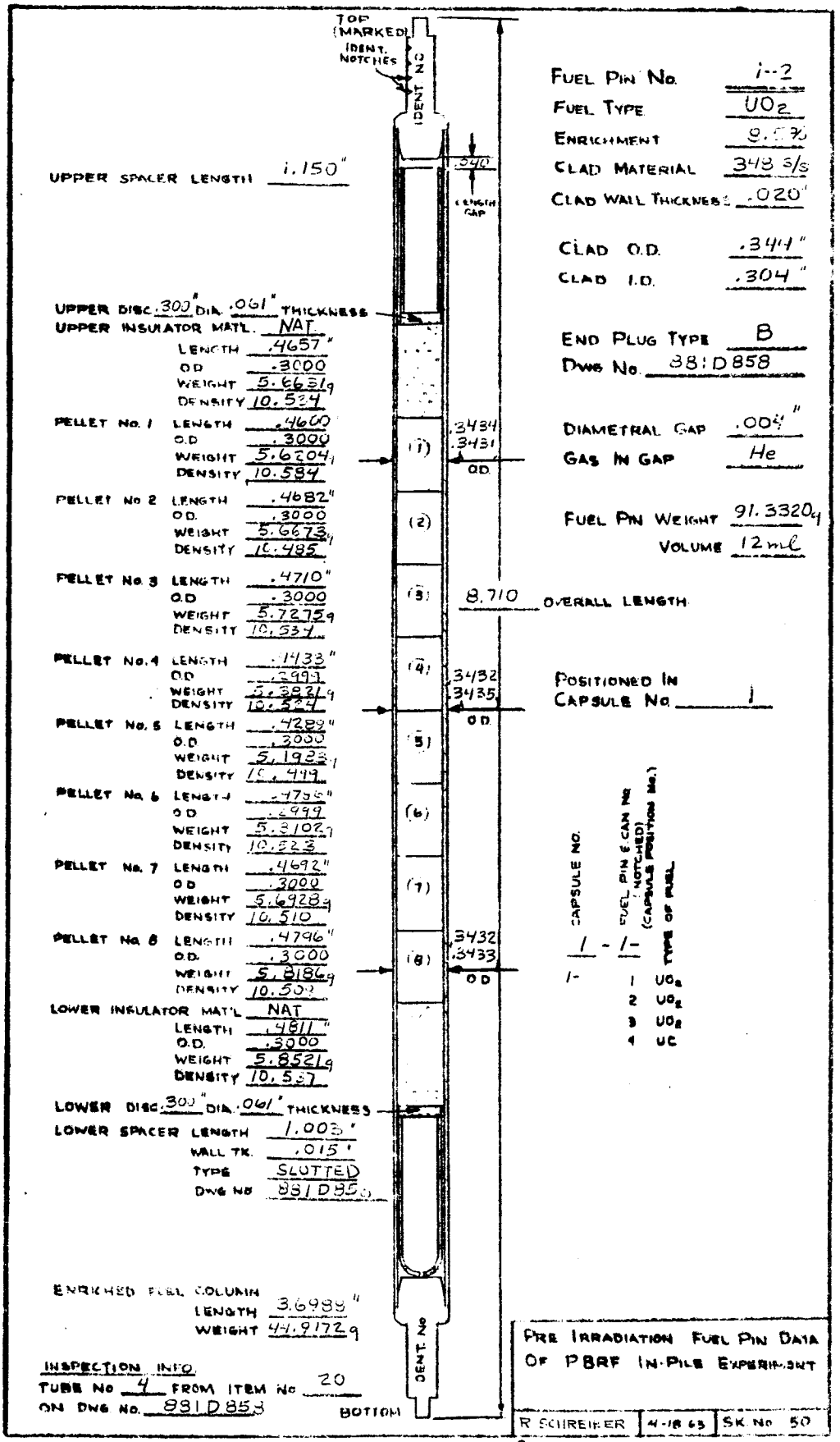
TOP (MARKED) IDENT. NOTCHES
IDENT. NO.
UPPER SPACER LENGTH 1.150"
.340
LENGTH GAP
UPPER DISC .300" DIA. .061" THICKNESS
UPPER INSULATOR MATL. NAT
LENGTH .4657"
O.D .3000
WEIGHT 5.6631g
DENSITY 10.534
PELLET No. 1 LENGTH .4600
O.D .3000
WEIGHT 5.6204g
DENSITY 10.584
PELLET No 2 LENGTH .4682"
O.D. .3000
WEIGHT 5.6673g
DENSITY 10.485
PELLET No 3 LENGTH .4710"
O.D .3000
WEIGHT 5.7275g
DENSITY 10.534
PELLET No. 4 LENGTH .1433"
O.D .2993
WEIGHT 1.7382g
DENSITY 10.524
PELLET No. 5 LENGTH .4289"
O.D .3000
WEIGHT 5.1923g
DENSITY 10.499
PELLET No. 6 LENGTH .4756"
O.D .2999
WEIGHT 5.7102g
DENSITY 10.523
PELLET No. 7 LENGTH .4692"
O.D .3000
WEIGHT 5.6928g
DENSITY 10.510
PELLET No. 8 LENGTH .4796"
O.D. .3000
WEIGHT 5.8186g
DENSITY 10.509
LOWER INSULATOR MAT'L NAT
LENGTH .4811"
O.D. .3000
WEIGHT 5.8521g
DENSITY 10.537
LOWER DISC .300" DIA. .061" THICKNESS
LOWER SPACER LENGTH 1.003"
WALL TK. .015"
TYPE SLOTTED
DWG NO 881D855
ENRICHED FUEL COLUMN
LENGTH 3.6989"
WEIGHT 44.9172g
INSPECTION INFO.
TUBE No 4 FROM ITEM No 20
ON DWG No. 881D853
BOTTOM
(1)
(2)
(3)
(4)
(5)
(6)
(7)
(8)
.3434
.3431
OD
.3432
.3435
OD
.3432
.3433
OD
8.710 OVERALL LENGTH
FUEL PIN No. 1-2
FUEL TYPE UO2
ENRICHMENT 9.7%
CLAD MATERIAL 348 S/S
CLAD WALL THICKNESS .020"
CLAD O.D. .344"
CLAD I.D. .304"
END PLUG TYPE B
Dwg No. 881D858
DIAMETRAL GAP .004"
GAS IN GAP He
FUEL PIN WEIGHT 91.3320g
VOLUME 12 mℓ
POSITIONED IN CAPSULE No. 1
CAPSULE NO.
FUEL PIN & CAN NO. (CAPSULE POSITION No.)
TYPE OF FUEL
1 - 1-
1- 1 UO2
2 UO2
3 UO2
4 UC
PRE IRRADIATION FUEL PIN DATA OF PBRF IN-PILE EXPERIMENT
R SCHREIBER | 4-18-63 | SK No 50

Figure 8

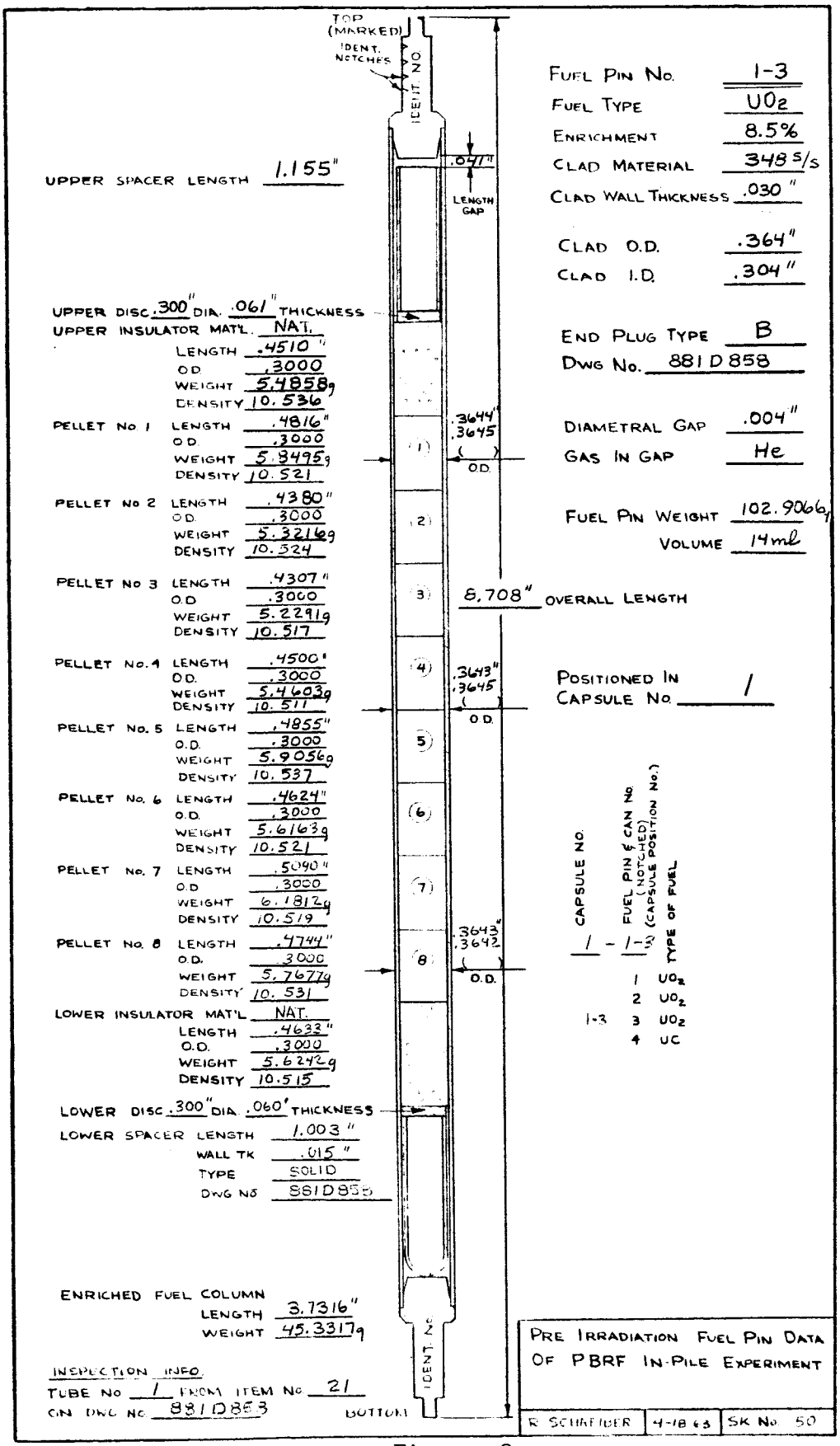
TOP (MARKED)
IDENT. NOTCHES
IDENT NO
.641"
LENGTH GAP
UPPER SPACER LENGTH 1.155"
UPPER DISC .300" DIA .061" THICKNESS
UPPER INSULATOR MAT'L NAT.
LENGTH .4510"
O.D .3000
WEIGHT 5.4858g
DENSITY 10.536
PELLET No 1 LENGTH .4816"
O.D. .3000
WEIGHT 5.8495g
DENSITY 10.521
PELLET No 2 LENGTH .4380"
O.D. .3000
WEIGHT 5.3216g
DENSITY 10.524
PELLET No 3 LENGTH .4307"
O.D .3000
WEIGHT 5.2291g
DENSITY 10.517
PELLET No. 4 LENGTH .4500"
O.D. .3000
WEIGHT 5.4603g
DENSITY 10.511
PELLET No. 5 LENGTH .4855"
O.D. .3000
WEIGHT 5.9056g
DENSITY 10.537
PELLET No. 6 LENGTH .4624"
O.D. .3000
WEIGHT 5.6163g
DENSITY 10.521
PELLET No. 7 LENGTH .5090"
O.D .3000
WEIGHT 6.1812g
DENSITY 10.519
PELLET No. 8 LENGTH .4744"
O.D. .3000
WEIGHT 5.7677g
DENSITY 10.531
LOWER INSULATOR MAT'L NAT.
LENGTH .4633"
O.D. .3000
WEIGHT 5.6242g
DENSITY 10.515
LOWER DISC .300" DIA .060" THICKNESS
LOWER SPACER LENGTH 1.003"
WALL TK .015"
TYPE SOLID
DWG No 881D859
ENRICHED FUEL COLUMN
LENGTH 3.7316"
WEIGHT 45.3317g
INSPECTION INFO
TUBE No 1 FROM ITEM No 21
CIN DWG No 881D853
BOTTOM
IDENT No
1
2
3
4
5
6
7
8
.3644" .3645" O.D.
.3643" .3645" O.D.
.3643" .3642" O.D.
8.708" OVERALL LENGTH
FUEL PIN No. 1-3
FUEL TYPE UO2
ENRICHMENT 8.5%
CLAD MATERIAL 348 S/S
CLAD WALL THICKNESS .030"
CLAD O.D. .364"
CLAD I.D. .304"
END PLUG TYPE B
DWG No. 881D858
DIAMETRAL GAP .004"
GAS IN GAP He
FUEL PIN WEIGHT 102.9066g
VOLUME 14ml
POSITIONED IN CAPSULE No. 1
CAPSULE NO. 1 - 1-3
FUEL PIN & CAN No. (NOTCHED) (CAPSULE POSITION No.)
TYPE OF FUEL
1 UO2
2 UO2
1-3 3 UO2
4 UC
PRE IRRADIATION FUEL PIN DATA OF PBRF IN-PILE EXPERIMENT
R SCHNEIDER
4-18-63
SK No 50

Figure 9

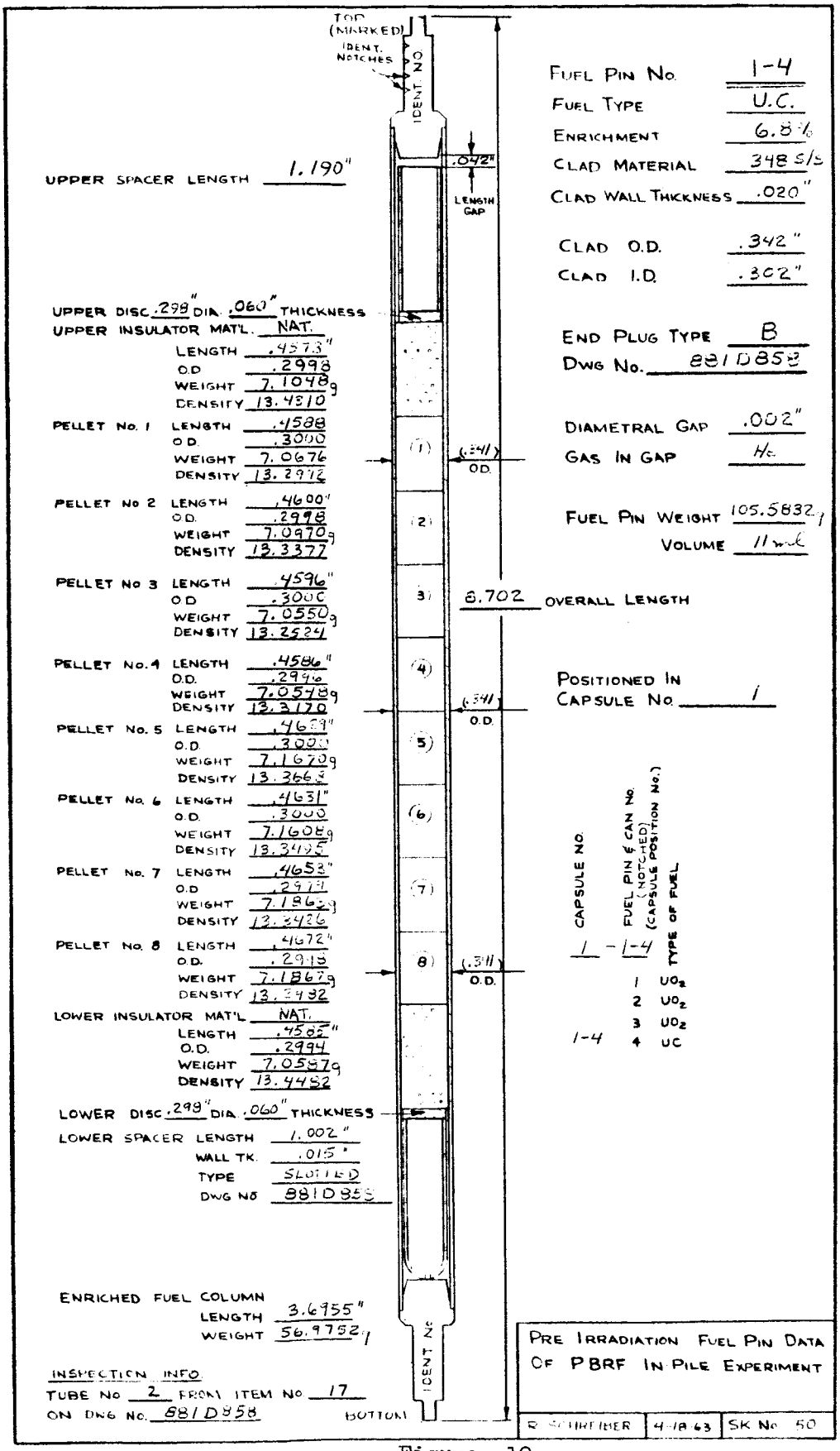
TOP (MARKED)
IDENT. NOTCHES
IDENT. NO
.042"
LENGTH GAP
UPPER SPACER LENGTH 1.190"
UPPER DISC .298" DIA .060" THICKNESS
UPPER INSULATOR MAT'L. NAT.
LENGTH .4573"
O.D. .2998
WEIGHT 7.1048g
DENSITY 13.4310
PELLET No. 1 LENGTH .4588
O.D. .3000
WEIGHT 7.0676
DENSITY 13.2972
PELLET No 2 LENGTH .4600"
O.D. .2998
WEIGHT 7.0970g
DENSITY 13.3377
PELLET No 3 LENGTH .4596"
O.D .3000
WEIGHT 7.0550g
DENSITY 13.2524
PELLET No.4 LENGTH .4586"
O.D. .2996
WEIGHT 7.0548g
DENSITY 13.3170
PELLET No. 5 LENGTH .4629"
O.D. .3000
WEIGHT 7.1670g
DENSITY 13.3663
PELLET No. 6 LENGTH .4631"
O.D. .3000
WEIGHT 7.1608g
DENSITY 13.3495
PELLET No. 7 LENGTH .4653"
O.D .2998
WEIGHT 7.1865g
DENSITY 13.3426
PELLET No. 8 LENGTH .4672"
O.D. .2998
WEIGHT 7.1867g
DENSITY 13.3432
LOWER INSULATOR MAT'L NAT.
LENGTH .4582"
O.D. .2994
WEIGHT 7.0587g
DENSITY 13.4482
LOWER DISC .298" DIA .060" THICKNESS
LOWER SPACER LENGTH 1.002"
WALL TK. .015"
TYPE SLOTTED
DWG NO 881D855
ENRICHED FUEL COLUMN
LENGTH 3.6955"
WEIGHT 56.9752g
INSPECTION INFO
TUBE No 2 FROM ITEM No 17
ON DWG No. 881D858
BOTTOM
IDENT No
(1)
(2)
(3)
(4)
(5)
(6)
(7)
(8)
(.341) O.D.
(.341) O.D.
(.311) O.D.
8.702 OVERALL LENGTH
FUEL PIN No. 1-4
FUEL TYPE U.C.
ENRICHMENT 6.8%
CLAD MATERIAL 348 S/S
CLAD WALL THICKNESS .020"
CLAD O.D. .342"
CLAD I.D. .302"
END PLUG TYPE B
DWG No. 881D859
DIAMETRAL GAP .002"
GAS IN GAP He
FUEL PIN WEIGHT 105.5832g
VOLUME 11 cc
POSITIONED IN CAPSULE No. 1
CAPSULE NO.
FUEL PIN & CAN NO. (NOTCHED) (CAPSULE POSITION No.)
TYPE OF FUEL
1 - 1-4
1 UO2
2 UO2
3 UO2
1-4 4 UC
PRE IRRADIATION FUEL PIN DATA OF PBRF IN PILE EXPERIMENT
R. SCHREIBER
4-18-63
SK No 50

Figure 10

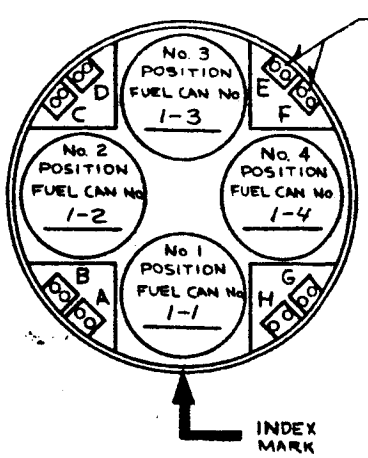

CAPSULE No. 1

ALUMINIUM BODY

CAPSULE TEST WIRE No.	MATERIAL	CONDITION
1-A-1	(L) 348	ANNEALED
1-A-2*		
1-B-1		
1-B-2*		
1-C-1		
1-C-2*		
1-D-1		
1-D-2*		
1-E-1	(U) 16-20	10% C.W.
1-E-2*		
1-F-1		
1-F-2*		
1-G-1		
1-G-2*		
1-H-1		
1-H-2*		
CAPSULE No. / CAPSULE POSITION & TEST WIRE No.		

* No. 2 WIRES ARE ½ INCH SHORTER THAN No. 1

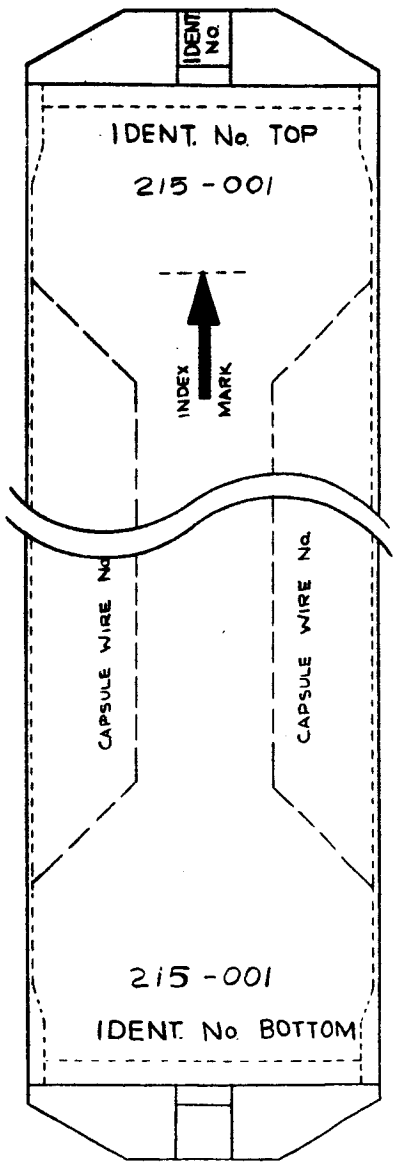

PRE-IRRADIATION CAPSULE DATA OF PBRF IN-PILE EXPERIMENT

[redacted] | 4-23-63 | SK No. 52

Figure 11

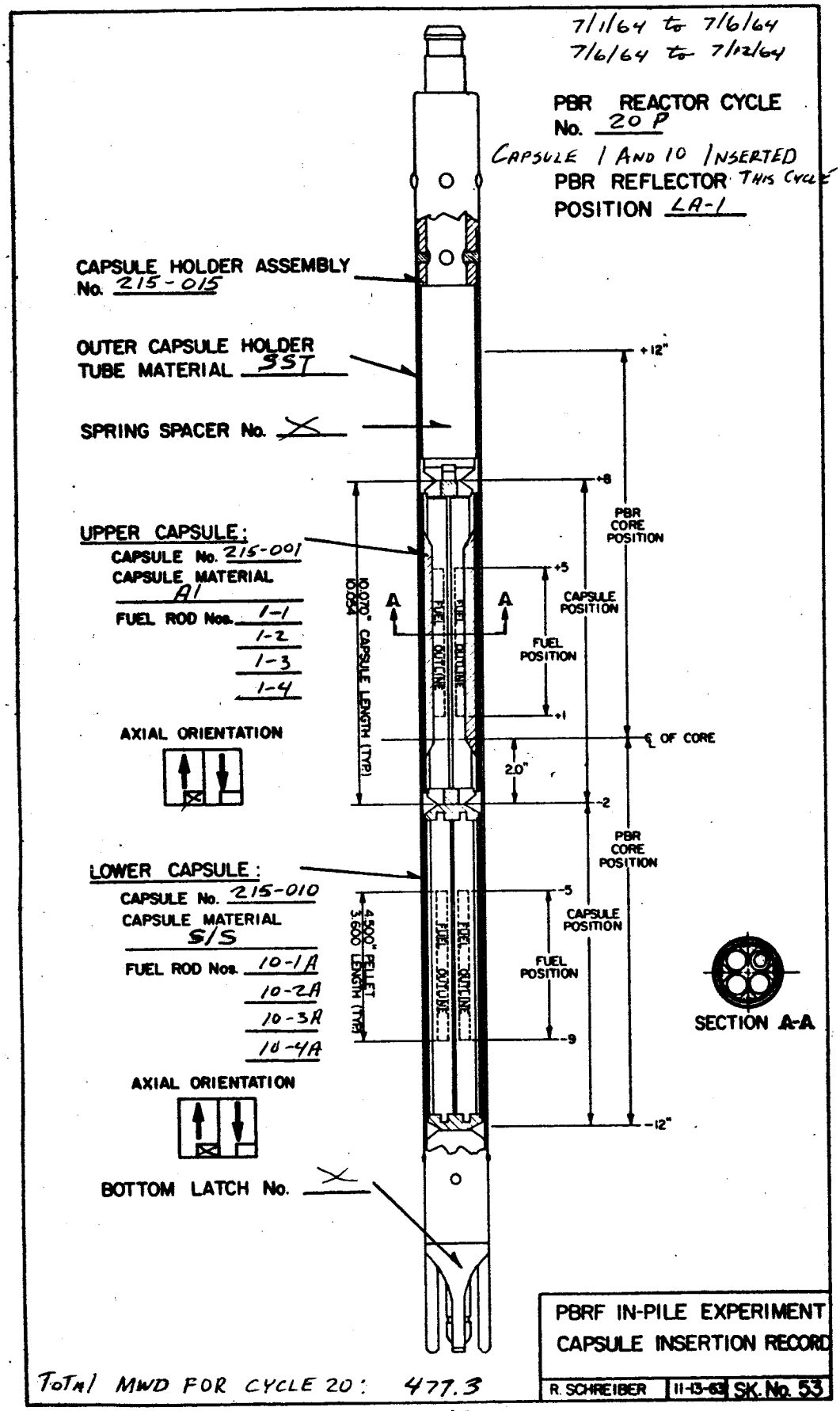
7/1/64 to 7/6/64
7/6/64 to 7/12/64
PBR REACTOR CYCLE No. 20 P
CAPSULE 1 AND 10 INSERTED
PBR REFLECTOR THIS CYCLE
POSITION LA-1
CAPSULE HOLDER ASSEMBLY No. 215-015
OUTER CAPSULE HOLDER TUBE MATERIAL SST
SPRING SPACER No. X
UPPER CAPSULE:
CAPSULE No. 215-001
CAPSULE MATERIAL Al
FUEL ROD Nos. 1-1
1-2
1-3
1-4
AXIAL ORIENTATION
LOWER CAPSULE:
CAPSULE No. 215-010
CAPSULE MATERIAL S/S
FUEL ROD Nos. 10-1A
10-2A
10-3A
10-4A
AXIAL ORIENTATION
BOTTOM LATCH No. X
+12"
+8
+5
+1
-2
-5
-9
-12"
PBR CORE POSITION
CAPSULE POSITION
FUEL POSITION
10.070" 10.054 CAPSULE LENGTH (TYP.)
4.800" PELLET 3.600 LENGTH (TYP.)
FUEL OUTLINE
℄ OF CORE
2.0"
A
A
SECTION A-A
TOTAL MWD FOR CYCLE 20: 477.3
PBRF IN-PILE EXPERIMENT
CAPSULE INSERTION RECORD
R. SCHREIBER
11-13-63
SK. No. 53

Figure 12

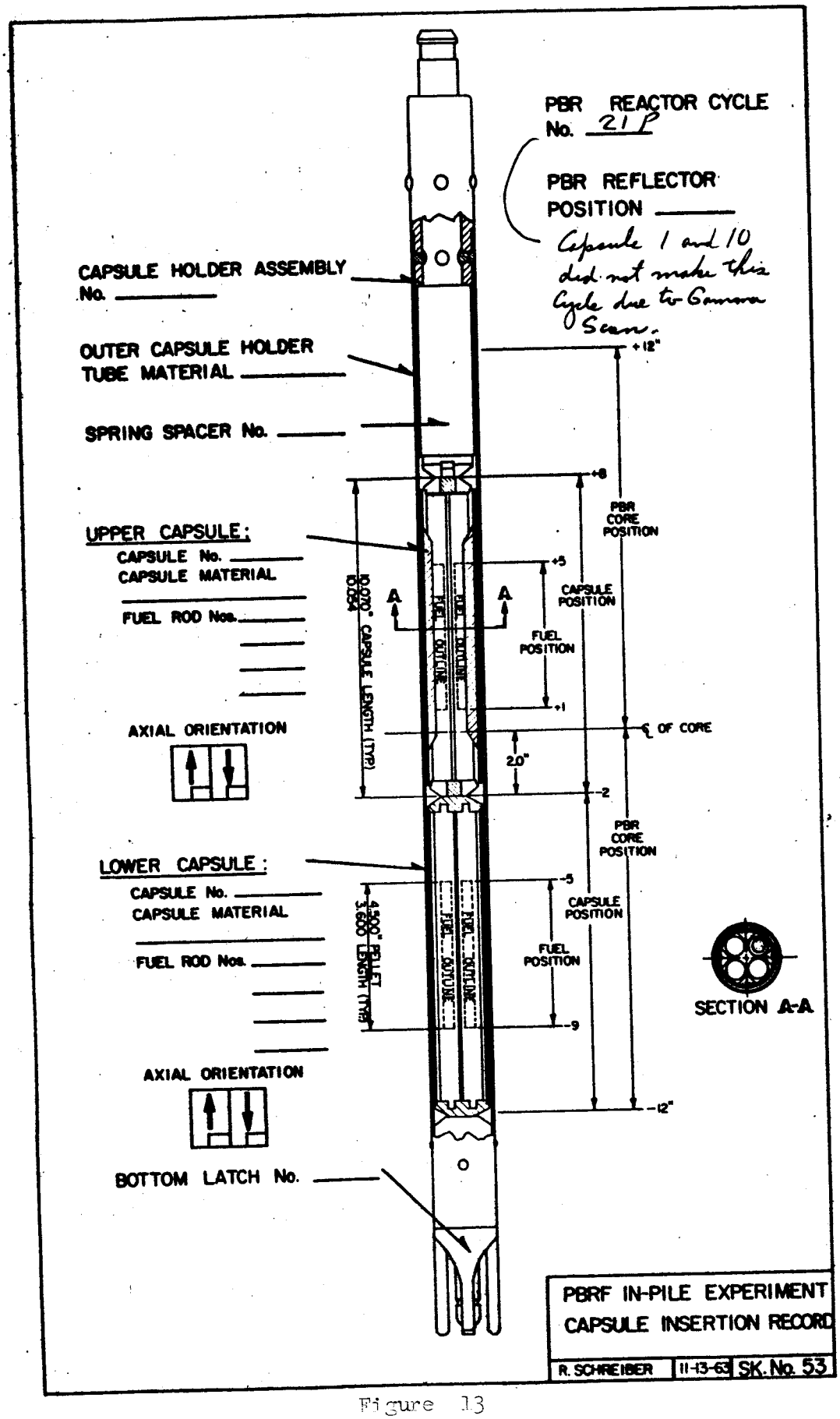
PBR REACTOR CYCLE No. 21P
PBR REFLECTOR POSITION
Capsule 1 and 10 did not make this Cycle due to Gamma Scan.
CAPSULE HOLDER ASSEMBLY No.
OUTER CAPSULE HOLDER TUBE MATERIAL
SPRING SPACER No.
UPPER CAPSULE:
CAPSULE No.
CAPSULE MATERIAL
FUEL ROD Nos.
AXIAL ORIENTATION
LOWER CAPSULE:
CAPSULE No.
CAPSULE MATERIAL
FUEL ROD Nos.
AXIAL ORIENTATION
BOTTOM LATCH No.
+12"
+8
+5
+1
-2
-5
-9
-12"
PBR CORE POSITION
CAPSULE POSITION
FUEL POSITION
℄ OF CORE
2.0"
A
A
SECTION A-A
PBRF IN-PILE EXPERIMENT
CAPSULE INSERTION RECORD
R. SCHREIBER
11-13-63
SK. No. 53

Figure 13

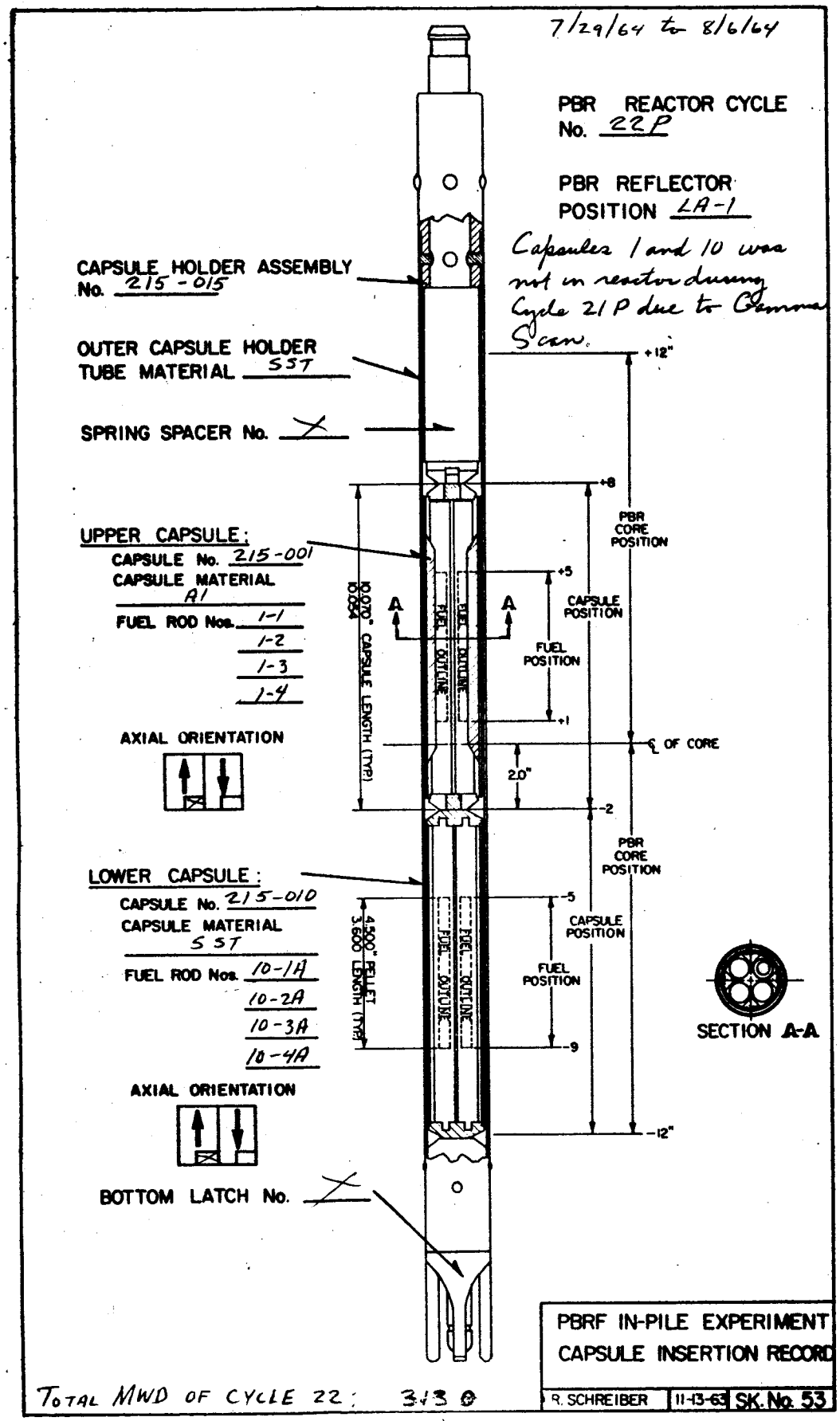
7/29/64 to 8/6/64
PBR REACTOR CYCLE No. 22P
PBR REFLECTOR POSITION 2A-1
Capsules 1 and 10 was not in reactor during Cycle 21P due to Gamma Scan.
CAPSULE HOLDER ASSEMBLY No. 215-015
OUTER CAPSULE HOLDER TUBE MATERIAL SST
SPRING SPACER No. X
UPPER CAPSULE:
CAPSULE No. 215-001
CAPSULE MATERIAL Al
FUEL ROD Nos. 1-1
1-2
1-3
1-4
AXIAL ORIENTATION
LOWER CAPSULE:
CAPSULE No. 215-010
CAPSULE MATERIAL SST
FUEL ROD Nos. 10-1A
10-2A
10-3A
10-4A
AXIAL ORIENTATION
BOTTOM LATCH No. X
10.000" CAPSULE LENGTH (TYP.)
4.500" PELLET 3.600 LENGTH (TYP.)
FUEL OUTLINE
A
A
+12"
+8
PBR CORE POSITION
+5
CAPSULE POSITION
FUEL POSITION
+1
℄ OF CORE
2.0"
-2
PBR CORE POSITION
-5
CAPSULE POSITION
FUEL POSITION
-9
-12"
SECTION A-A
PBRF IN-PILE EXPERIMENT
CAPSULE INSERTION RECORD
R. SCHREIBER
11-13-63
SK. No. 53
TOTAL MWD OF CYCLE 22: 313 0

Figure 14

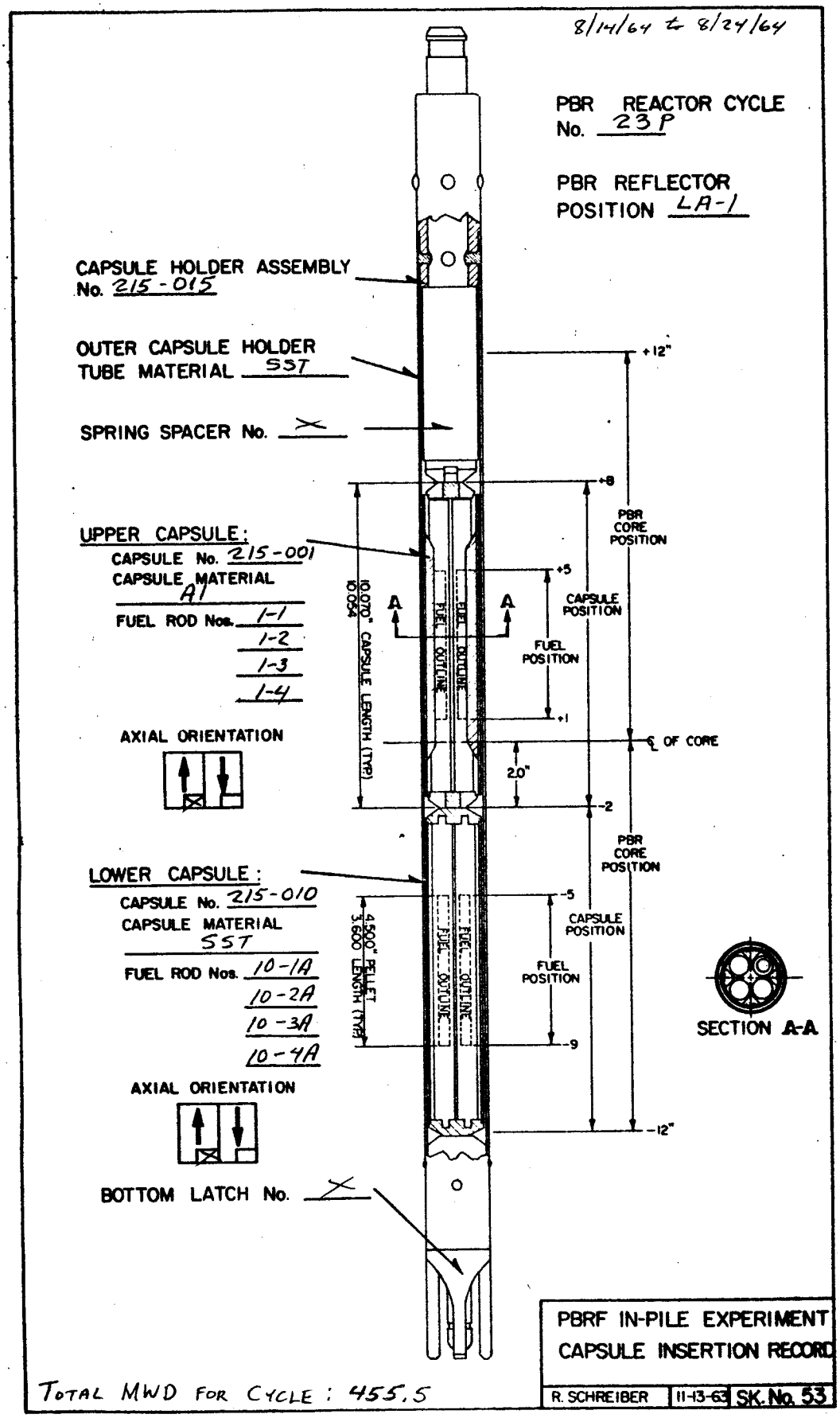
8/14/64 to 8/24/64
PBR REACTOR CYCLE No. 23P
PBR REFLECTOR POSITION LA-1
CAPSULE HOLDER ASSEMBLY No. 215-015
OUTER CAPSULE HOLDER TUBE MATERIAL SST
SPRING SPACER No. X
UPPER CAPSULE:
CAPSULE No. 215-001
CAPSULE MATERIAL Al
FUEL ROD Nos. 1-1
1-2
1-3
1-4
AXIAL ORIENTATION
LOWER CAPSULE:
CAPSULE No. 215-010
CAPSULE MATERIAL SST
FUEL ROD Nos. 10-1A
10-2A
10-3A
10-4A
AXIAL ORIENTATION
BOTTOM LATCH No. X
10.070" 10.054 CAPSULE LENGTH (TYP)
4.500" 3.600 PELLET LENGTH (TYP)
FUEL OUTLINE
+12"
+8
+5
+1
℄ OF CORE
-2
-5
-9
-12"
PBR CORE POSITION
CAPSULE POSITION
FUEL POSITION
2.0"
SECTION A-A
TOTAL MWD FOR CYCLE: 455.5
PBRF IN-PILE EXPERIMENT
CAPSULE INSERTION RECORD
R. SCHREIBER
11-13-63
SK. No. 53

Figure 15

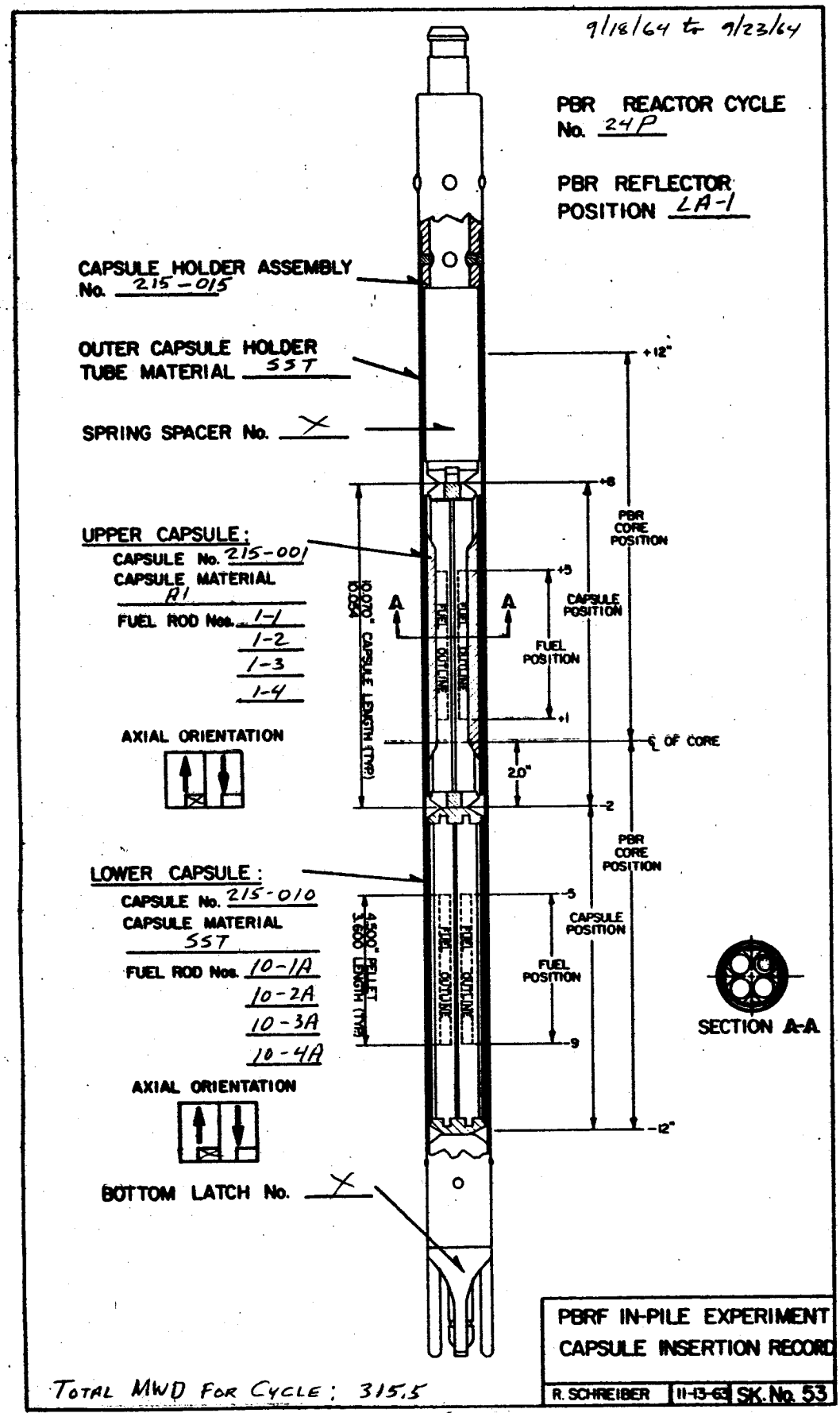
9/18/64 to 9/23/64
PBR REACTOR CYCLE No. 24P
PBR REFLECTOR POSITION 2A-1
CAPSULE HOLDER ASSEMBLY No. 215-015
OUTER CAPSULE HOLDER TUBE MATERIAL SST
SPRING SPACER No. X
UPPER CAPSULE:
CAPSULE No. 215-001
CAPSULE MATERIAL A1
FUEL ROD Nos. 1-1
1-2
1-3
1-4
AXIAL ORIENTATION
LOWER CAPSULE:
CAPSULE No. 215-010
CAPSULE MATERIAL SST
FUEL ROD Nos. 10-1A
10-2A
10-3A
10-4A
AXIAL ORIENTATION
BOTTOM LATCH No. X
10.000" CAPSULE LENGTH (TYP.)
4.500" PELLET STACK LENGTH (TYP.)
FUEL OUTLINE
FUEL OUTLINE
A
A
+12"
+8
+5
+1
℄ OF CORE
2.0"
-2
-5
-9
-12"
PBR CORE POSITION
CAPSULE POSITION
FUEL POSITION
PBR CORE POSITION
CAPSULE POSITION
FUEL POSITION
SECTION A-A
PBRF IN-PILE EXPERIMENT
CAPSULE INSERTION RECORD
R. SCHREIBER
11-13-63
SK. No. 53
TOTAL MWD FOR CYCLE: 315.5

Figure 16

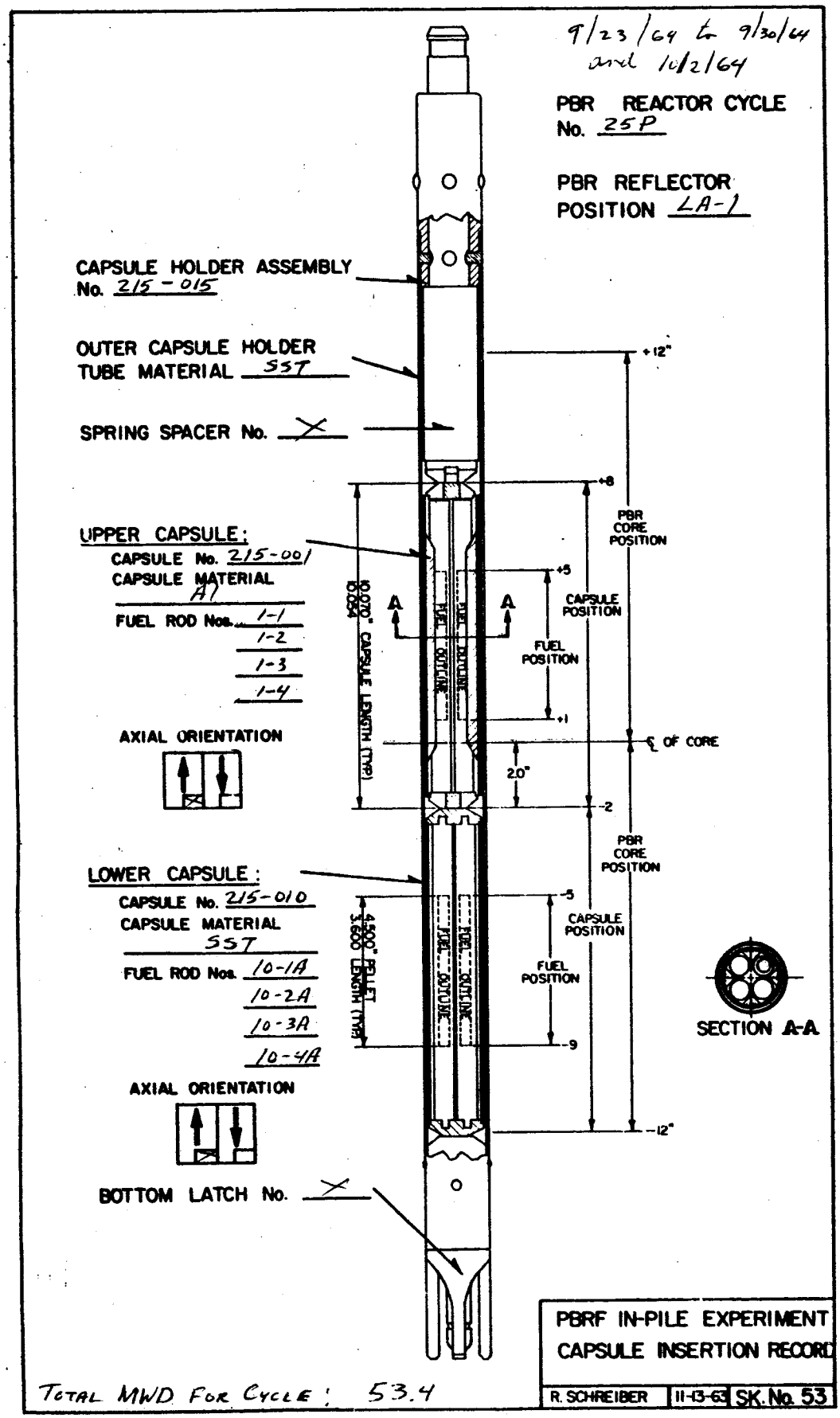
9/23/64 to 9/30/64
and 10/2/64
PBR REACTOR CYCLE
No. 25P
PBR REFLECTOR
POSITION LA-1
CAPSULE HOLDER ASSEMBLY
No. 215-015
OUTER CAPSULE HOLDER
TUBE MATERIAL SST
SPRING SPACER No. X
UPPER CAPSULE:
CAPSULE No. 215-001
CAPSULE MATERIAL
A1
FUEL ROD Nos. 1-1
1-2
1-3
1-4
AXIAL ORIENTATION
LOWER CAPSULE:
CAPSULE No. 215-010
CAPSULE MATERIAL
SST
FUEL ROD Nos. 10-1A
10-2A
10-3A
10-4A
AXIAL ORIENTATION
BOTTOM LATCH No. X
10.070" CAPSULE LENGTH (TYP.)
4.500" PELLET STACK LENGTH (TYP.)
FUEL OUTLINE
+12"
+8
+5
+1
-2
-5
-9
-12"
PBR CORE POSITION
CAPSULE POSITION
FUEL POSITION
℄ OF CORE
2.0"
A
A
SECTION A-A
TOTAL MWD FOR CYCLE: 53.4
PBRF IN-PILE EXPERIMENT
CAPSULE INSERTION RECORD
R. SCHREIBER
11-13-63
SK. No. 53

Figure 17

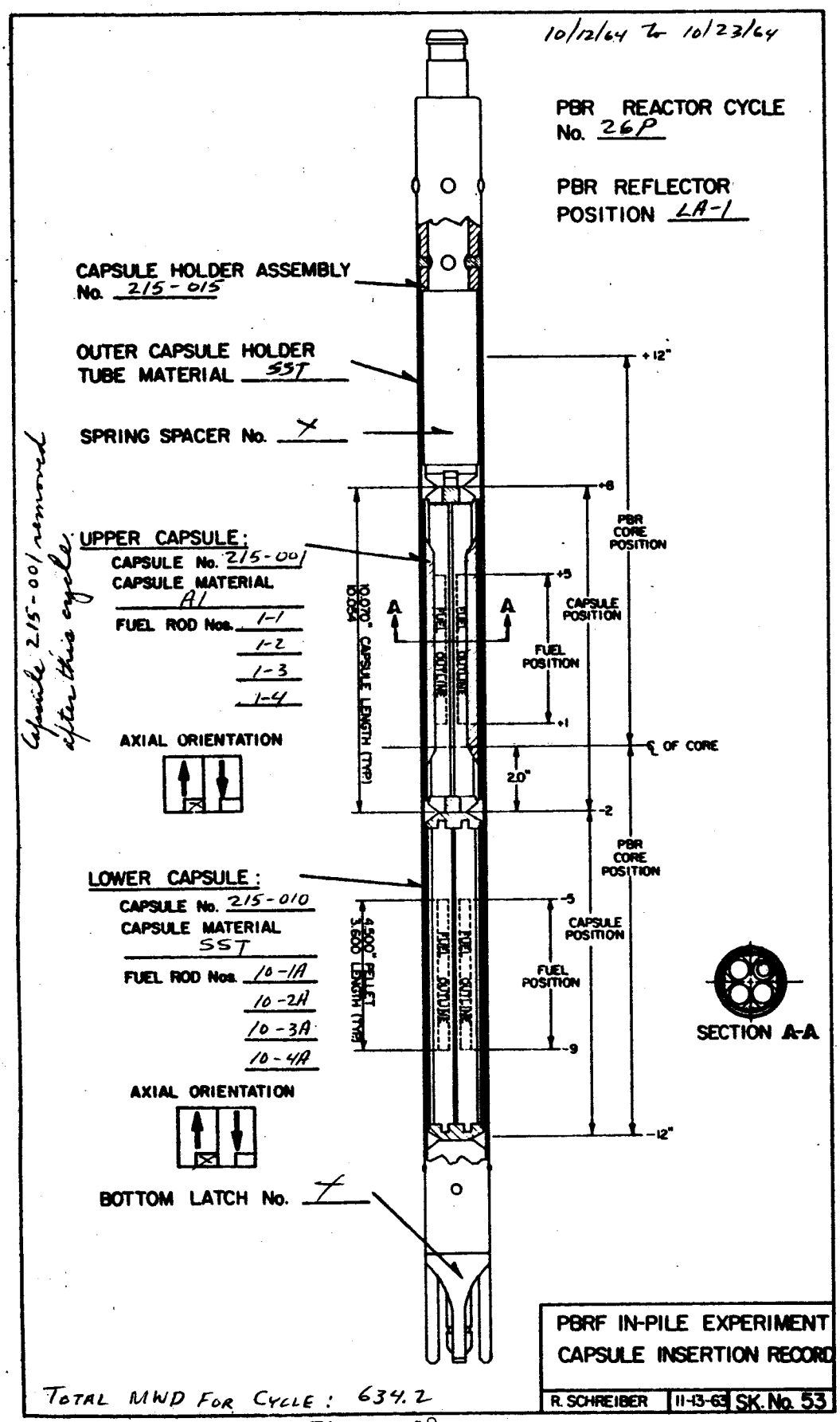
10/12/64 To 10/23/64
PBR REACTOR CYCLE No. 26P
PBR REFLECTOR POSITION LA-1
CAPSULE HOLDER ASSEMBLY No. 215-015
OUTER CAPSULE HOLDER TUBE MATERIAL SST
SPRING SPACER No. X
Capsule 215-001 removed after this cycle.
UPPER CAPSULE:
CAPSULE No. 215-001
CAPSULE MATERIAL Al
FUEL ROD Nos. 1-1 1-2 1-3 1-4
AXIAL ORIENTATION
LOWER CAPSULE:
CAPSULE No. 215-010
CAPSULE MATERIAL SST
FUEL ROD Nos. 10-1A 10-2A 10-3A 10-4A
AXIAL ORIENTATION
BOTTOM LATCH No. 1
10.000" CAPSULE LENGTH (TYP.)
4.500" PELLET STACK LENGTH (TYP.)
FUEL COLUMN
FUEL POSITION
CAPSULE POSITION
PBR CORE POSITION
+12"
+8
+5
+1
℄ OF CORE
20"
-2
-5
-9
-12"
A
SECTION A-A
TOTAL MWD FOR CYCLE: 634.2
PBRF IN-PILE EXPERIMENT
CAPSULE INSERTION RECORD
R. SCHREIBER 11-13-63 SK. No. 53

Figure 18

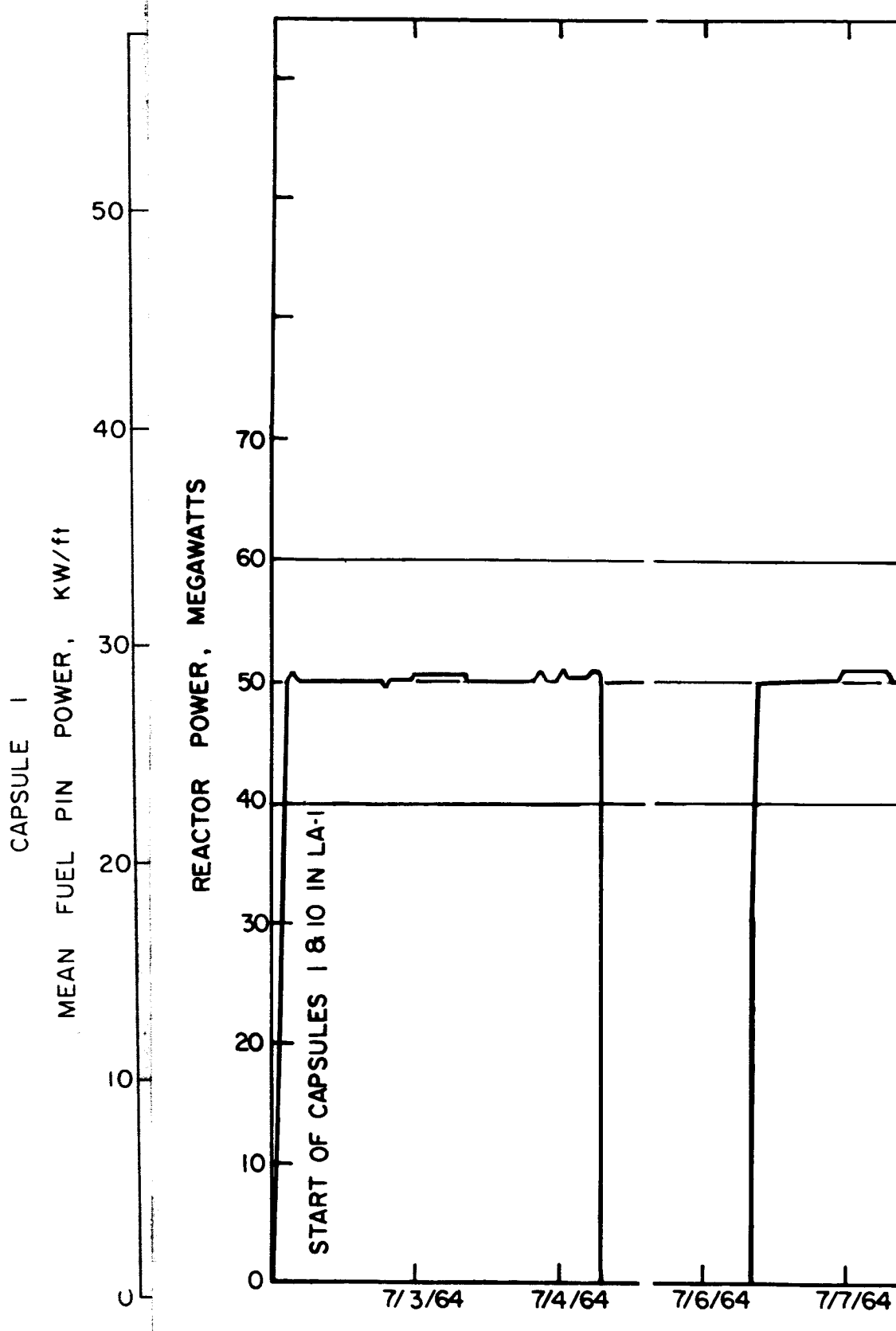
CAPSULE I
MEAN FUEL PIN POWER, KW/ft
0
10
20
30
40
50
REACTOR POWER, MEGAWATTS
0
10
20
30
40
50
60
70
START OF CAPSULES 1 & 10 IN LA-1
7/3/64
7/4/64
7/6/64
7/7/64

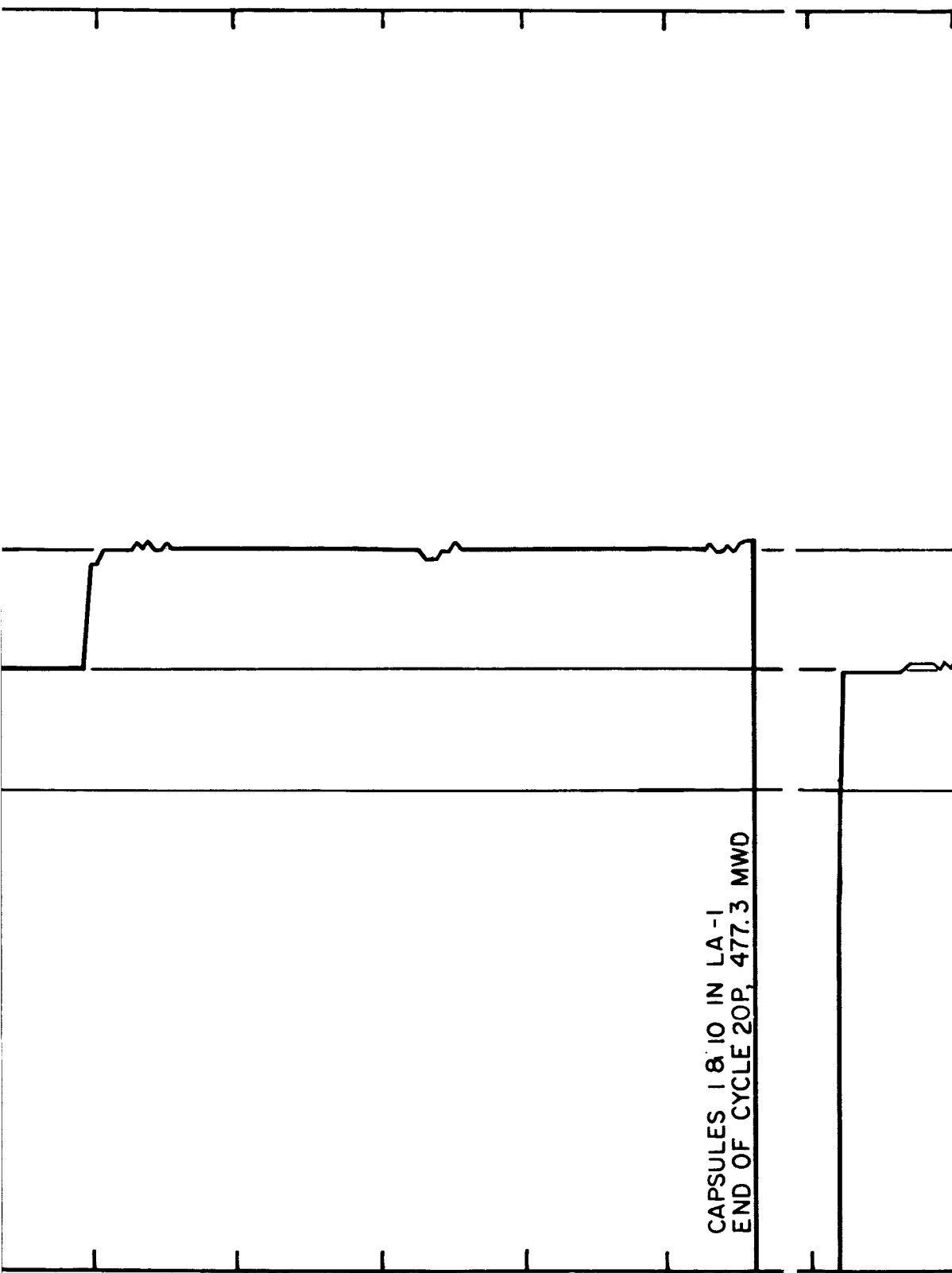
CAPSULES 1 & 10 IN LA-1
END OF CYCLE 20P, 477.3 MWD
7/8/64
7/9/64
7/10/64
7/11/64
7/12/64
8/1/64

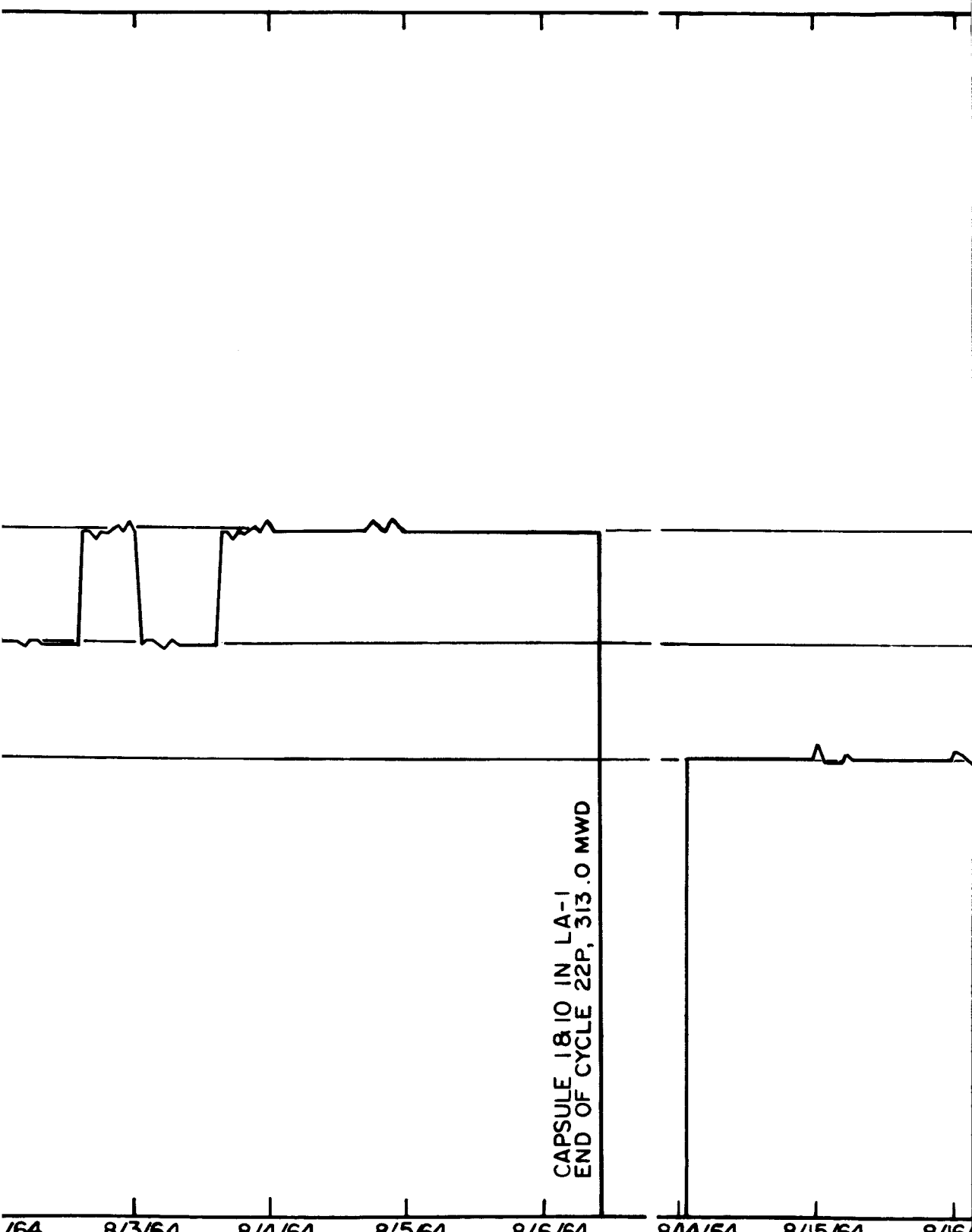

FIGURE 19 PLUMBROOK REACTOR PO

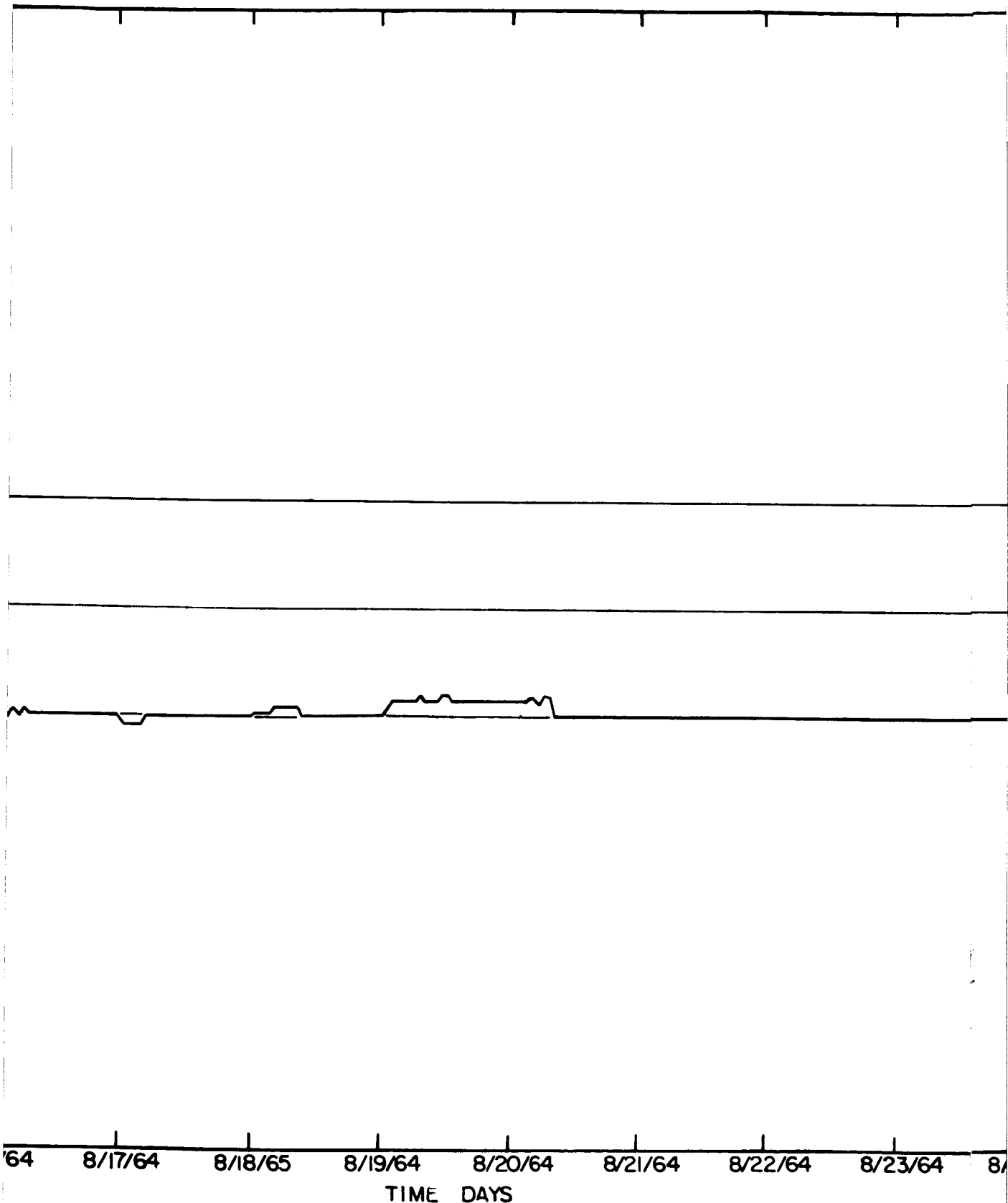

WER DURING IRRADIATION OF CAPSULE 215-001

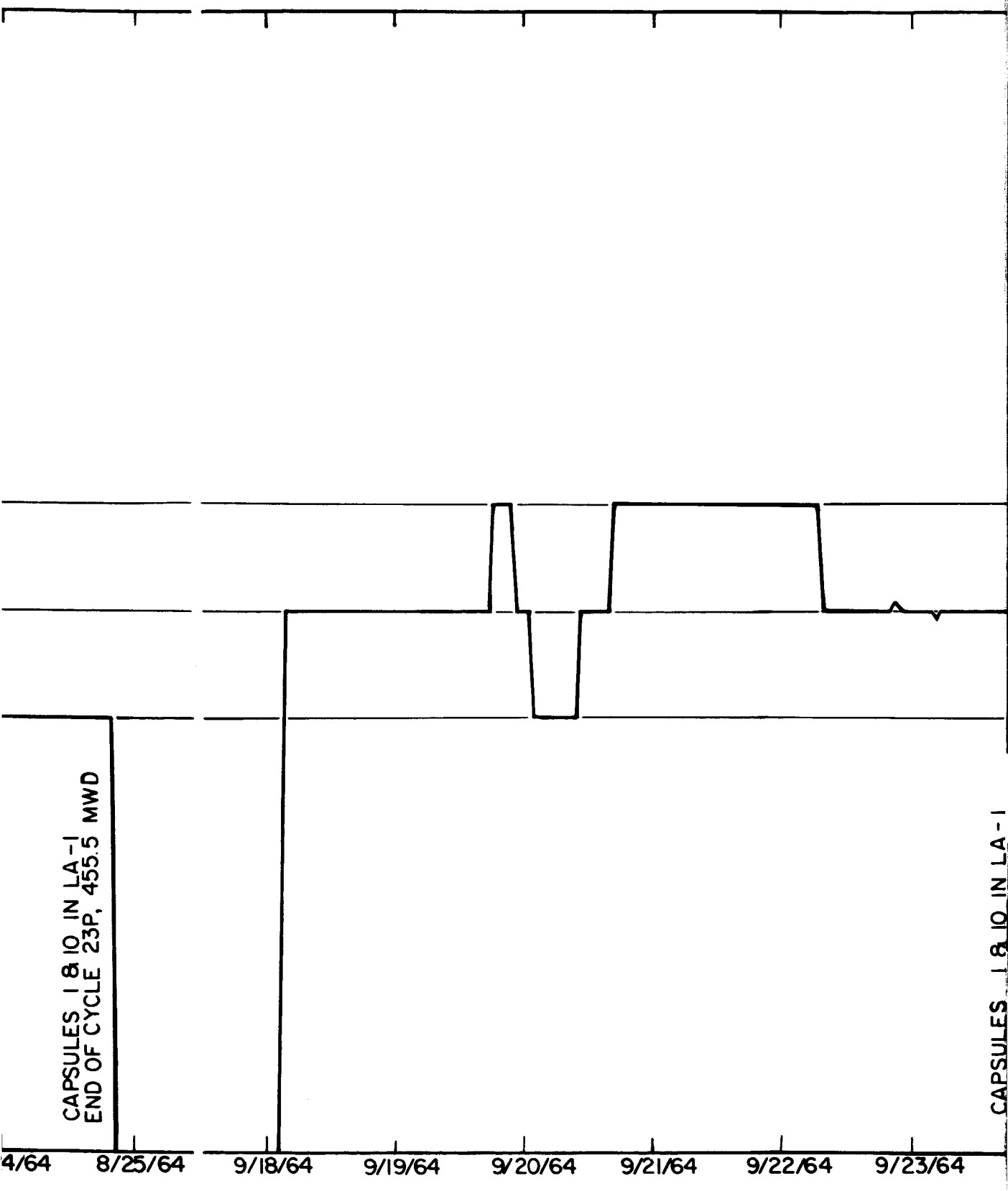
CAPSULES 1 & 10 IN LA-1
END OF CYCLE 23P, 455.5 MWD
4/64
8/25/64
9/18/64
9/19/64
9/20/64
9/21/64
9/22/64
9/23/64
CAPSULES 1 & 10 IN LA-1

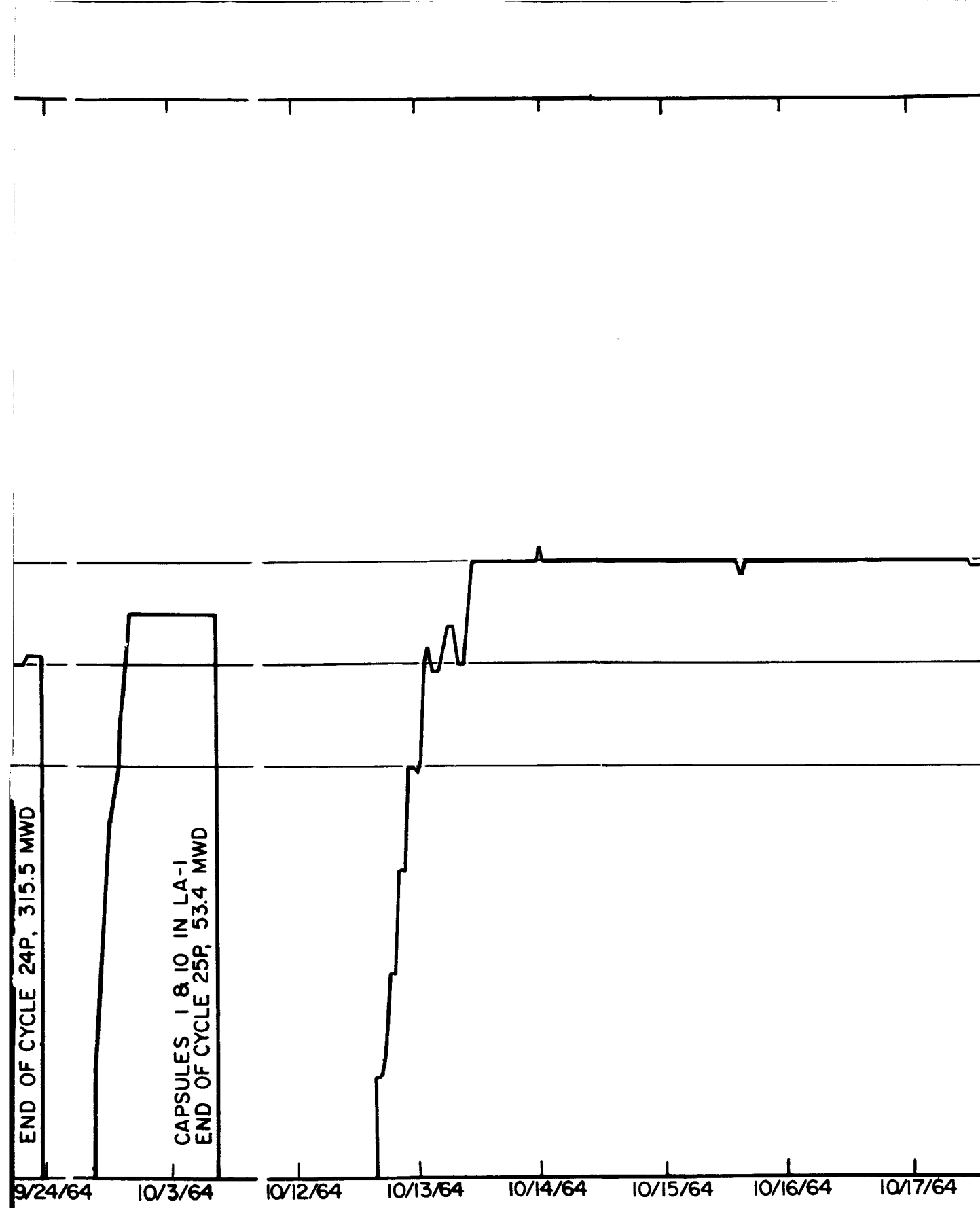
END OF CYCLE 24P, 315.5 MWD
CAPSULES 1 & 10 IN LA-1
END OF CYCLE 25P, 53.4 MWD
9/24/64
10/3/64
10/12/64
10/13/64
10/14/64
10/15/64
10/16/64
10/17/64

CAPSULE 1 & 10 IN LA-1
END OF CYCLE 26P, 634.2 MWD
CAPSULE 1 REMOVED AFTER THIS CYCLE. CAPSULE 10 WILL BE RE-INSERTED ALONG WITH CAPS. 11.
10/18/64
10/19/64
10/20/64
10/21/64
10/22/64
10/23/64
10/24/64

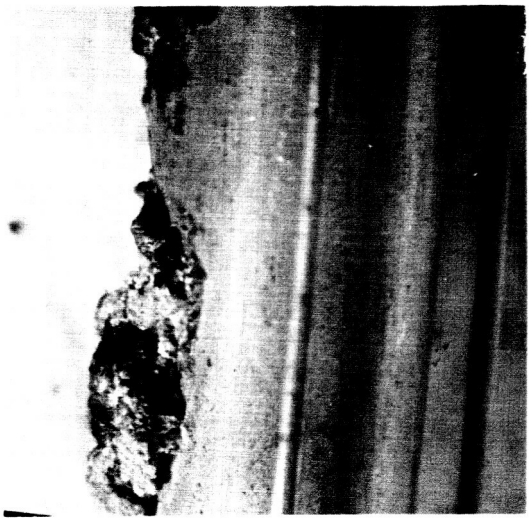

SIDE VIEW, END OF DEPOSIT.

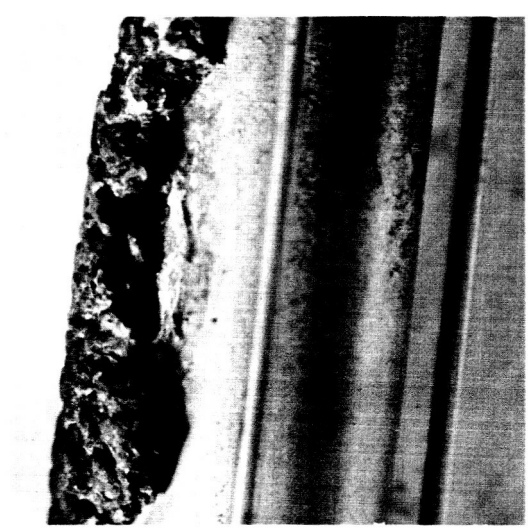

SIDE VIEW, CENTER OF DEPOSIT.

FRONT VIEW, DEPOSIT.

FUEL PIN 1-2

CLAD C

CLOSE UP VIE
LEFT TO RIG

FIGURE -1 RUPTURED FUEL PIN

TOP OF ENRICH-
ED FUEL COLUMN

FRONT VIEW, CLOSE-UP OF RUPTURE
NEAR END.

FRONT VIEW, CLOSE-UP OF RUPTURE
CENTER SECTION.

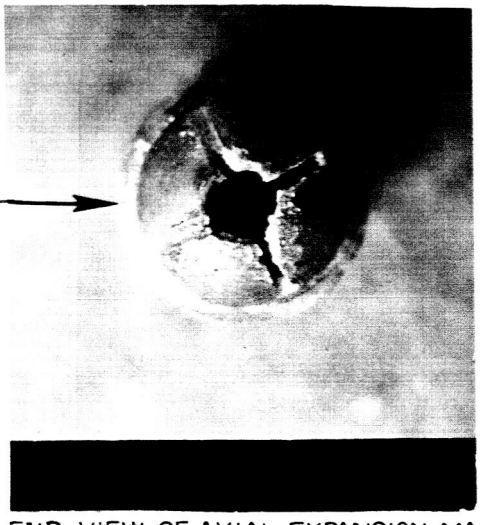

END VIEW OF AXIAL EXPANSION MARKER.
(PARALLEL EDGES INDICATES NO
AXIAL EXPANSION OF FUEL COLUMN)

.D. 0.344"

WS ARE REVERSED
HT.

N 1-2 FROM CAPSULE 215-001 . 20-2

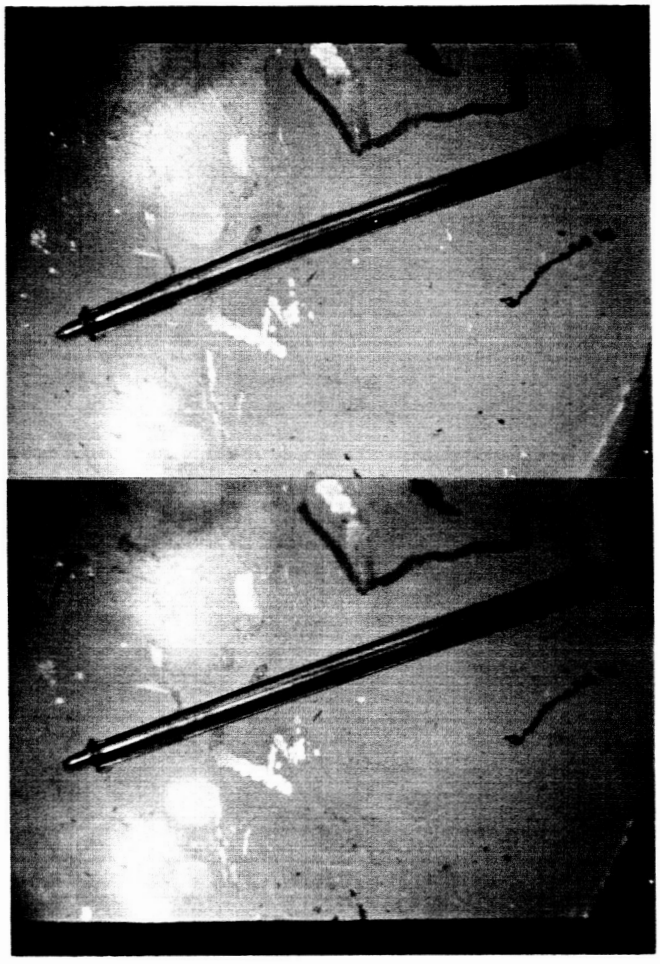

P65-0061

STEREO PHOTOGRAPH OF FUEL PIN I-I
AFTER IRRADIATION.

P65-01185

PELLET 1-1-1, TOP

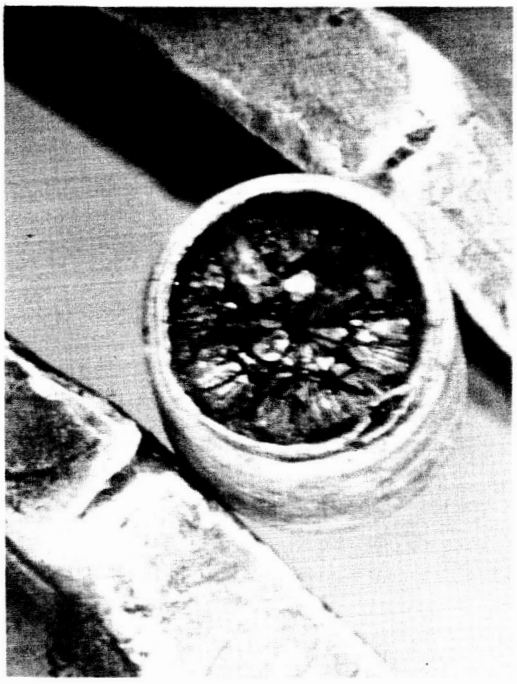

P65-01187

PELLET 1-1-2, TOP

P65-01186

PELLET 1-1-1, BOTTOM

P65-01183

PELLET 1-1-2, BOTTOM

P65-0189

NOT TAKEN

PELLET 1-1-3, TOP

PELLET 1-1-4, TOP

P65-0190

NOT TAKEN

PELLET 1-1-3, BOTTOM

PELLET 1-1-4, BOTTOM

FIGURE 21 3 MACROPHOTOGRAPHS OF FUEL PIN

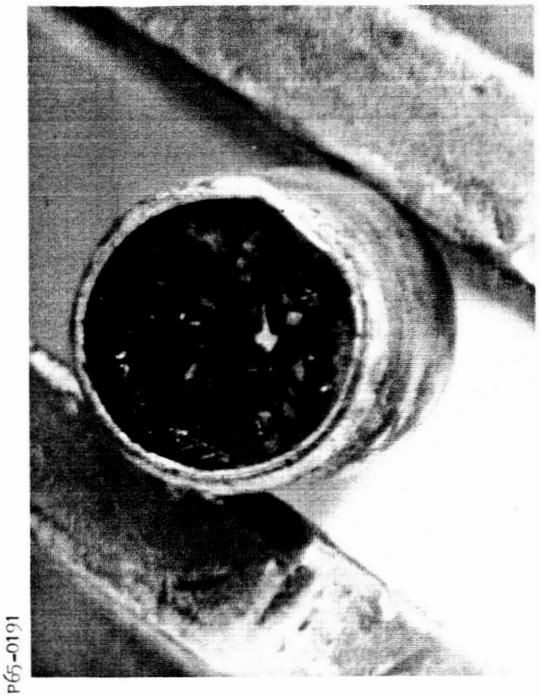

P65-0191

PELLET 1-1-5, TOP

P65-0193

PELLET 1-1-6, TOP

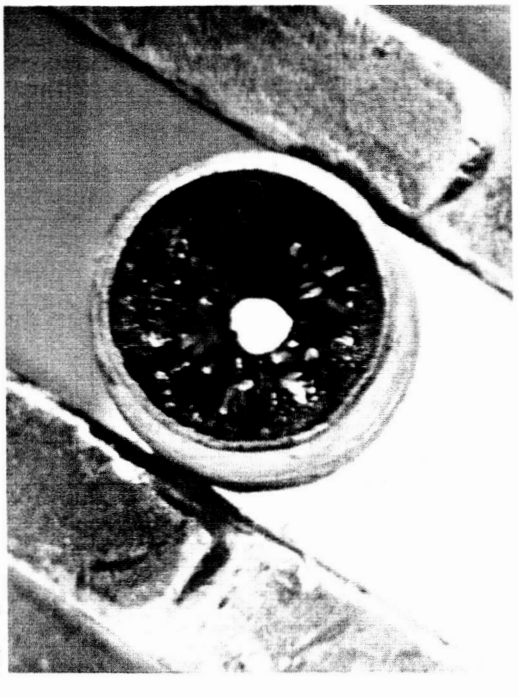

P65-0192

PELLET 1-1-5, BOTTOM

P65-0194

PELLET 1-1-6, BOTTOM

-1 FROM CAPSULE 215-001. (UO_2, .010" CLAD).

P65-0195

PELLET 1-1-7, TOP

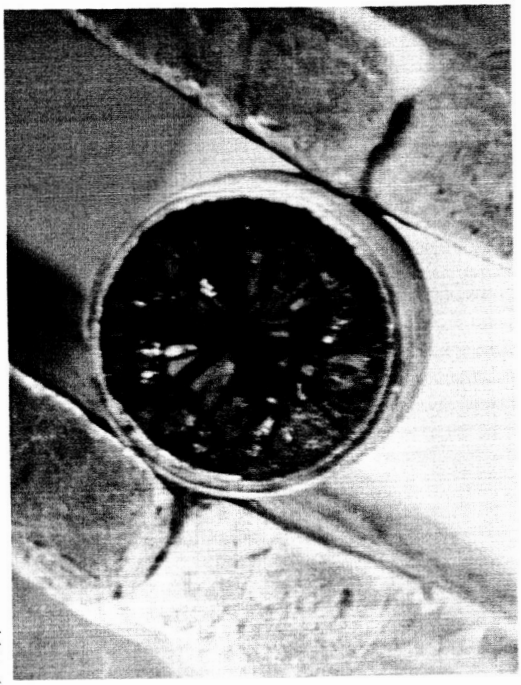

P65-0197

PELLET 1-1-8, TOP

P65-0196

PELLET 1-1-7, BOTTOM

P65-0198

PELLET 1-1-8, BOTTOM

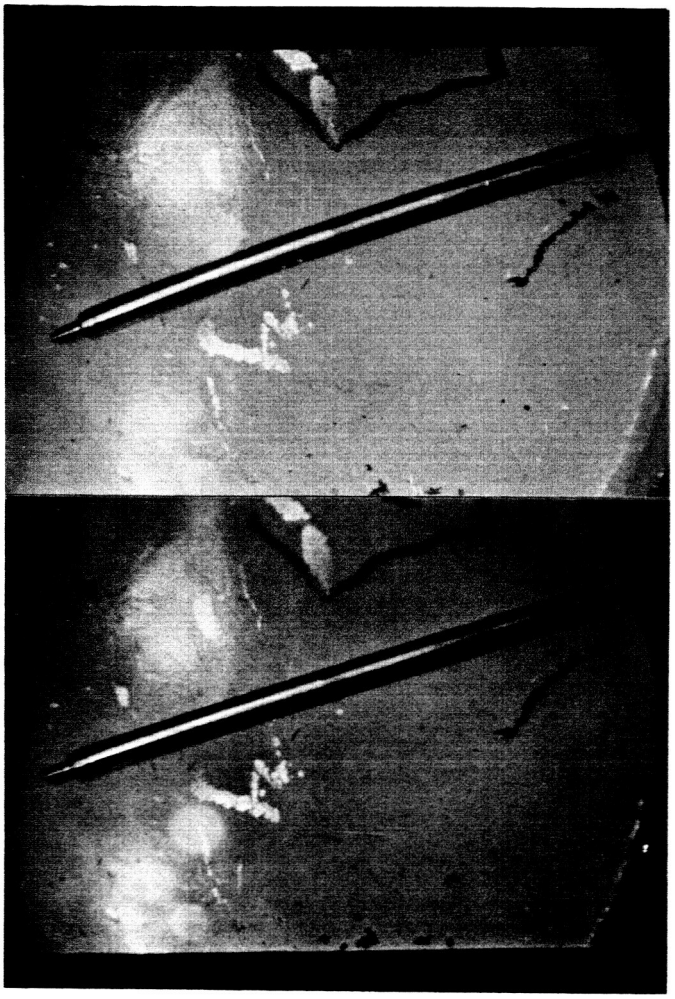

P65-0062

STEREO PHOTOGRAPH OF FUEL PIN 1-3
AFTER IRRADIATION.

P65-0199

PELLET 1-3-1, TOP

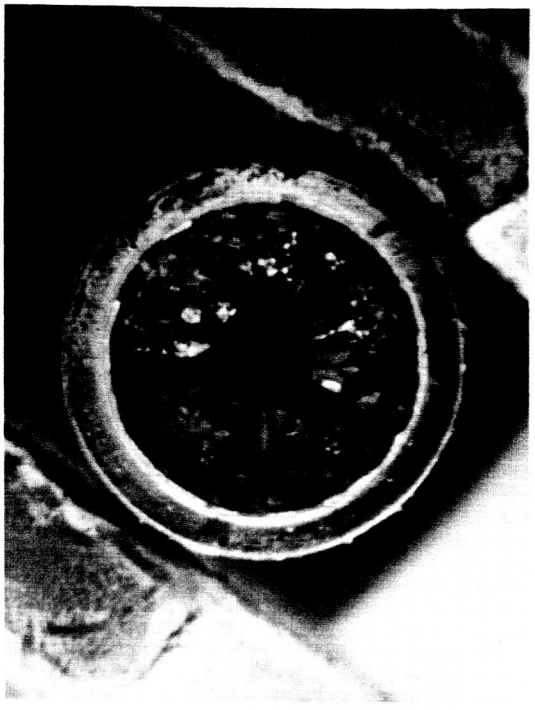

P65-0201

PELLET 1-3-2, TOP

P65-0200

PELLET 1-3-1, BOTTOM

P65-0202

PELLET 1-3-2, BOTTOM

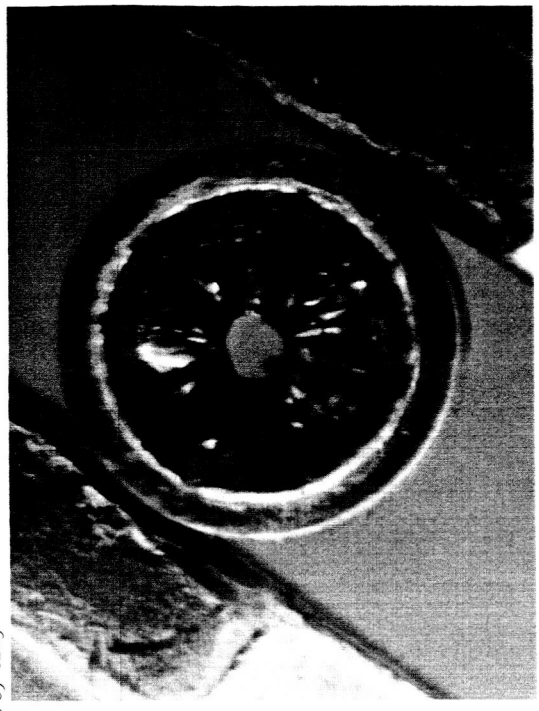

P65-0203

PELLET 1-3-3, TOP

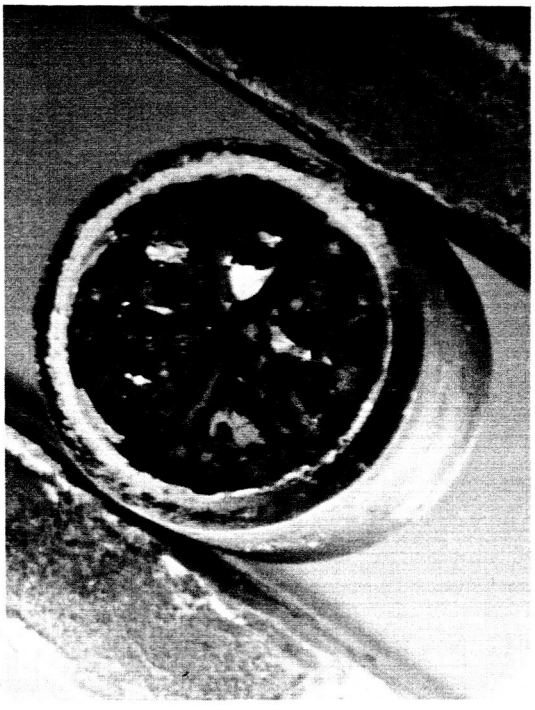

P65-0205

PELLET 1-3-4, TOP

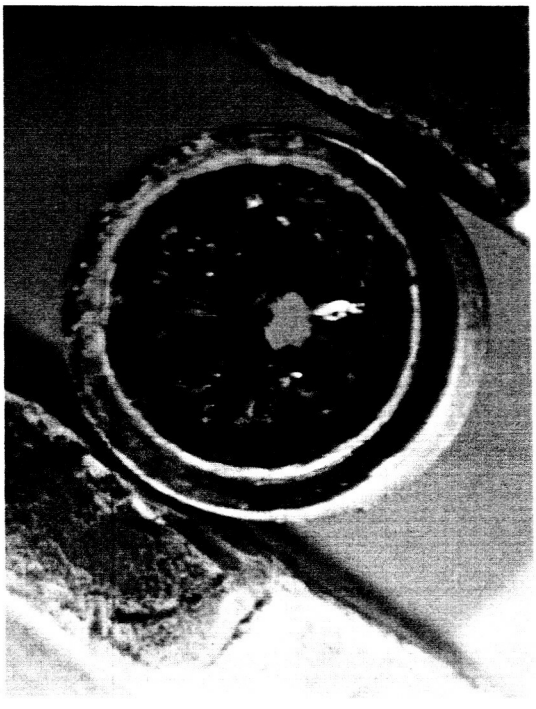

P65-0204

PELLET 1-3-3, BOTTOM

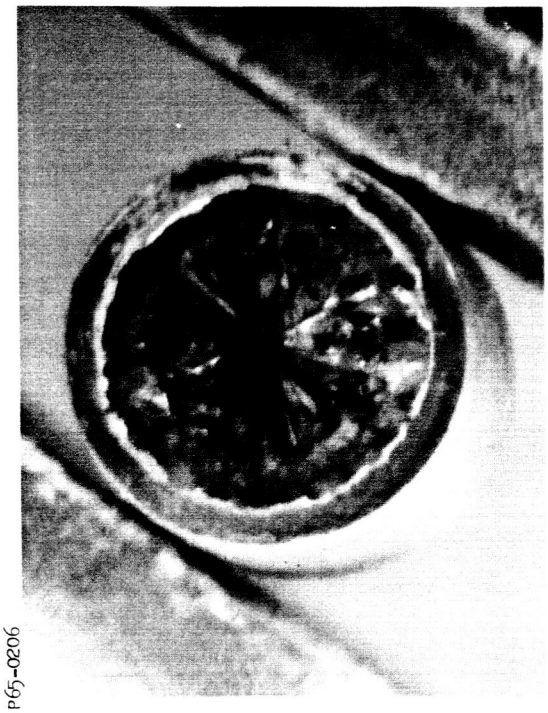

P65-0206

PELLET 1-3-4, BOTTOM

FIGURE -3 MACROPHOTOGRAPHS OF FUEL PIN 1-3 FRO

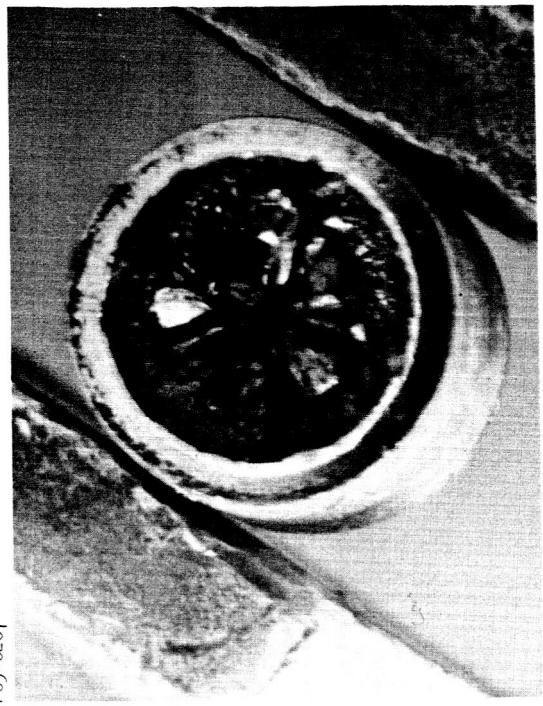

P65-0207

PELLET 1-3-5, TOP

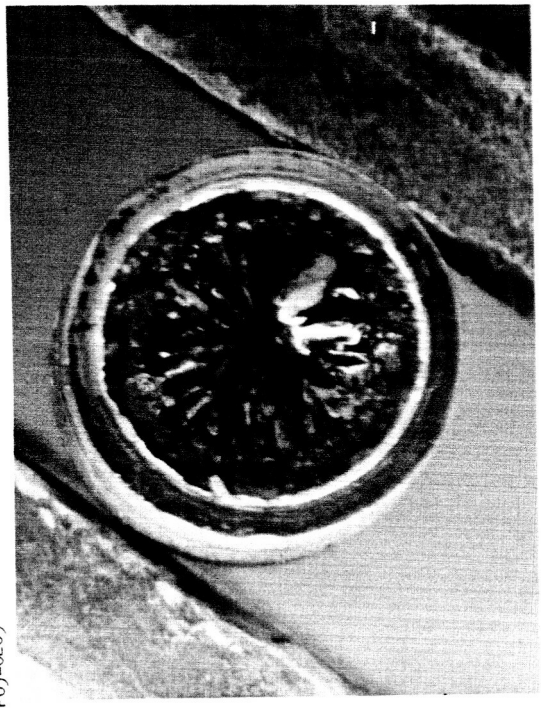

P65-0209

PELLET 1-3-6, TOP

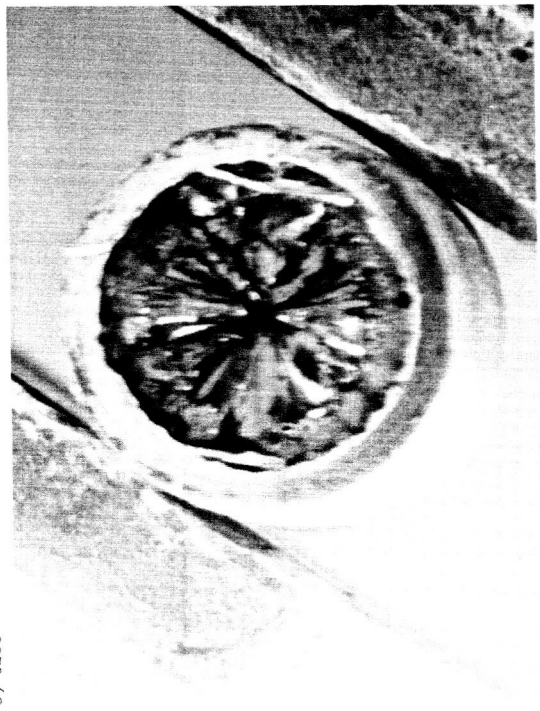

P65-0208

PELLET 1-3-5, BOTTOM

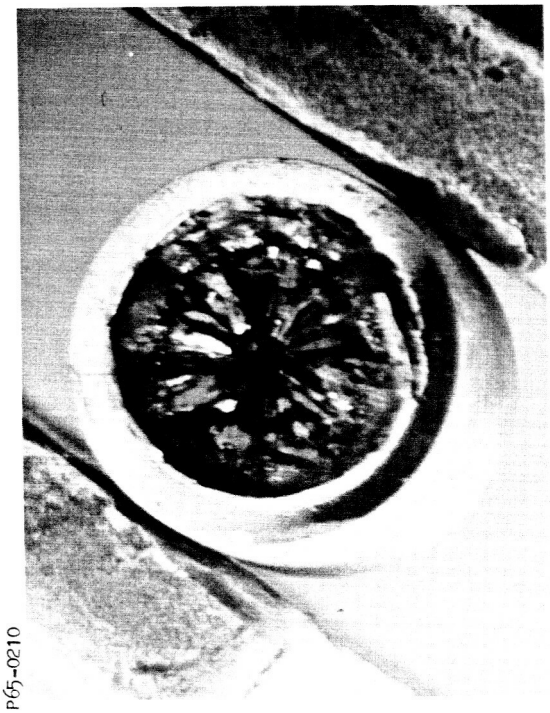

P65-0210

PELLET 1-3-6, BOTTOM

M CAPSULE 215-001. (UO_2, .030" CLAD).

22-4

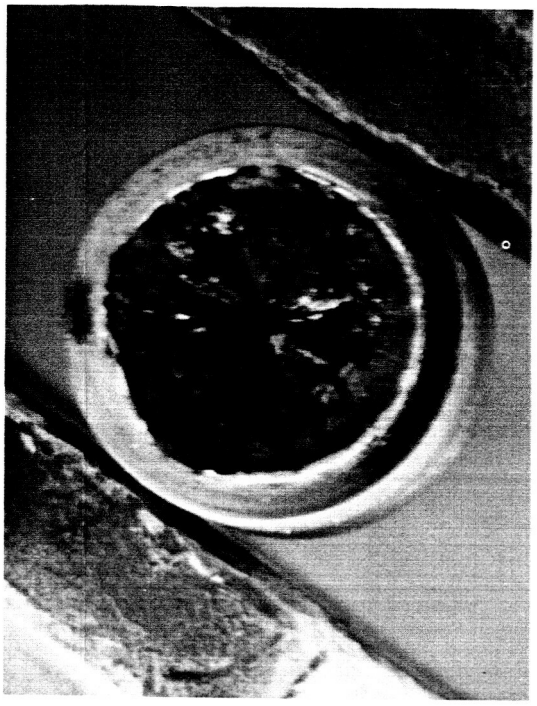

P65-0211

PELLET 1-3-7, TOP

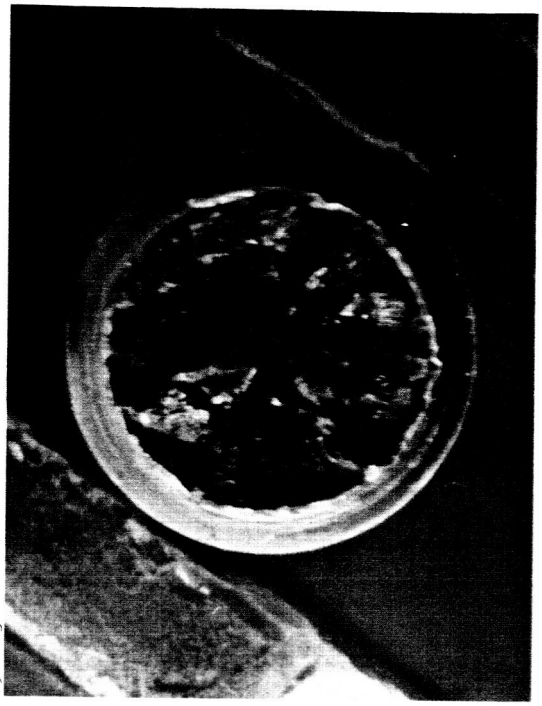

P65-0213

PELLET 1-3-8, TOP

P65-0212

PELLET 1-3-7, BOTTOM

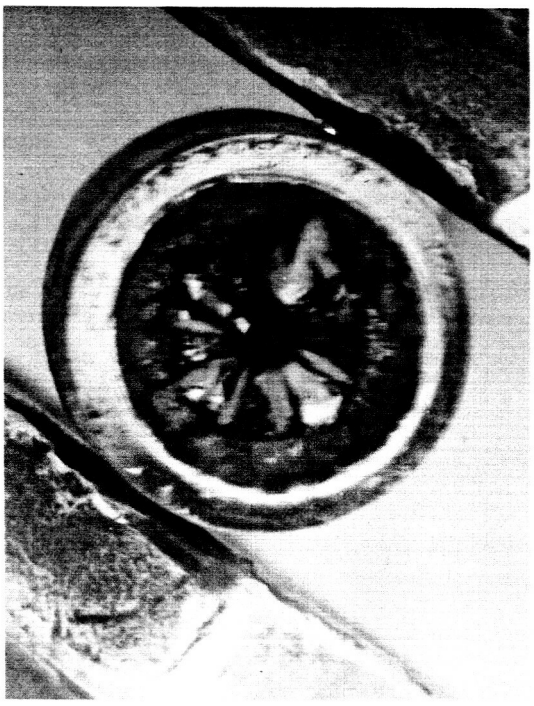

P65-0214

PELLET 1-3-8, BOTTOM

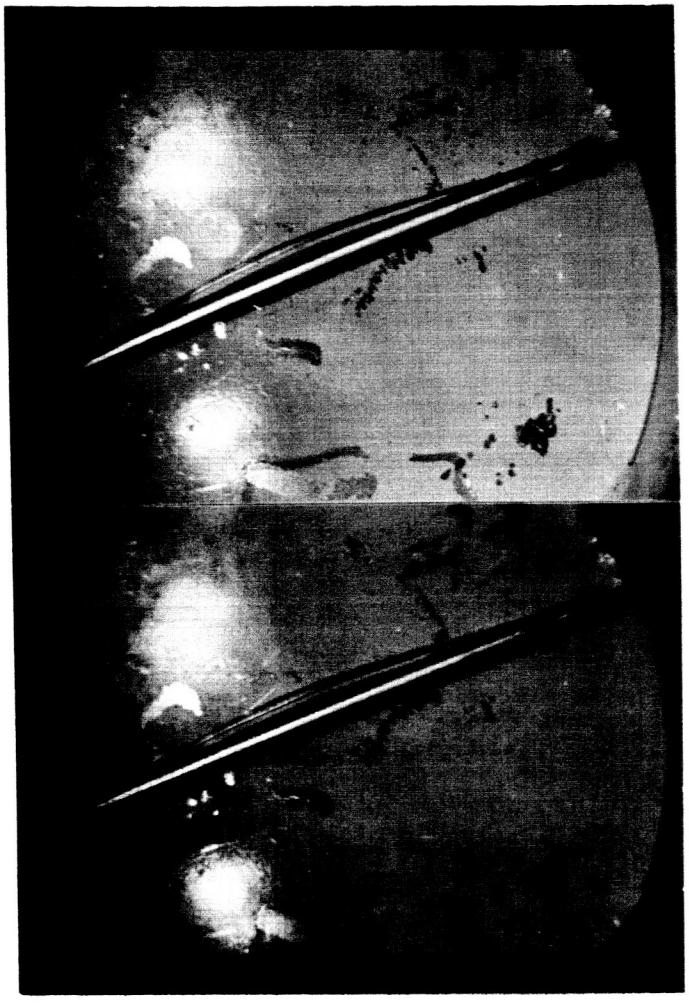

P65-0063

STEREO PHOTOGRAPH OF FUEL PIN 1-4
AFTER IRRADIATION.

P65-0215

PELLET 1-4-1, TOP

P65-0217

PELLET 1-4-2, TOP

P65-0216

PELLET 1-4-1, BOTTOM

P65-0218

PELLET 1-4-2, BOTTOM

P65-0219

PELLET 1-4-3, TOP

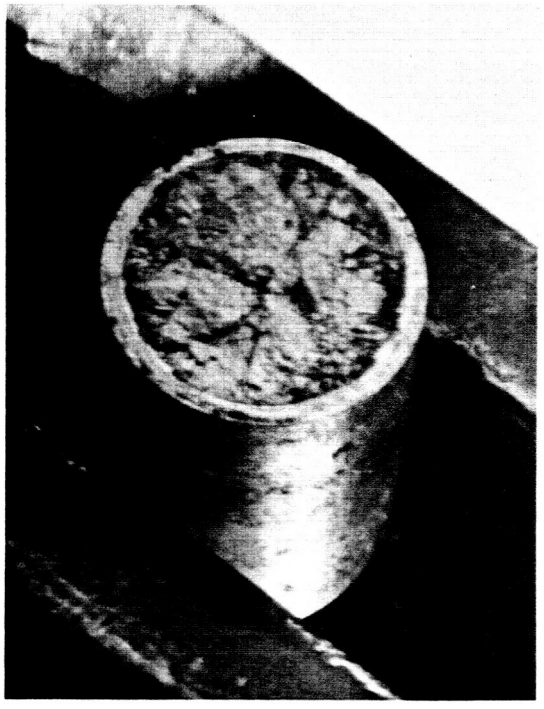

P65-0221

PELLET 1-4-4, TOP

P65-0220

PELLET 1-4-3, BOTTOM

P65-0222

PELLET 1-4-4, BOTTOM

FIGURE 23 MACROPHOTOGRAPHS OF FUEL PIN 1-4 FROM

P65-0223

PELLET 1-4-5, TOP

P65-0225

PELLET 1-4-6, TOP

P65-0224

PELLET 1-4-5, BOTTOM

P65-0226

PELLET 1-4-6, BOTTOM

1 CAPSULE 215-001. (UC, .020" CLAD).

23-4

P65-0227

PELLET 1-4-7, TOP

NOT TAKEN

PELLET 1-4-8, TOP

P65-0228

PELLET 1-4-7, BOTTOM

P65-0230

PELLET 1-4-8, BOTTOM

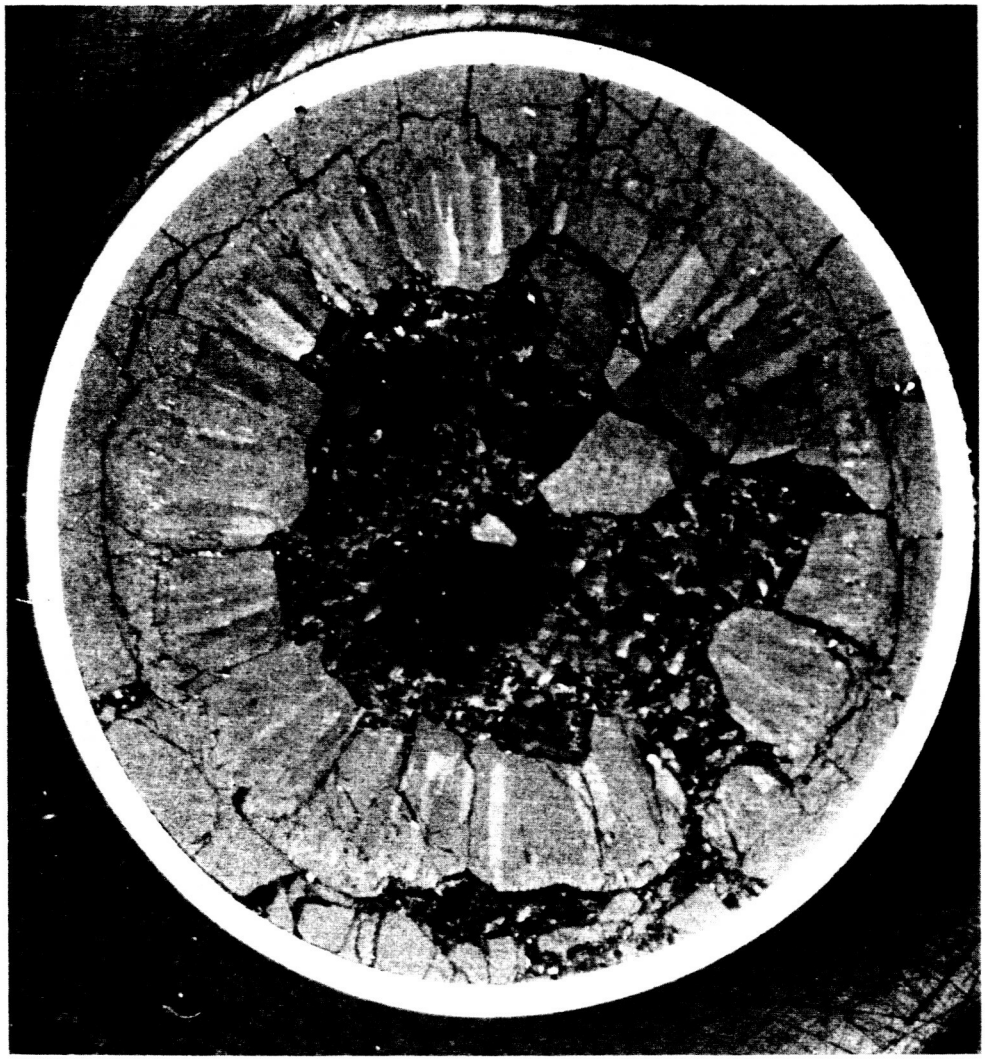

Photo 2837

Fig. 24 PELLET 1-1-2

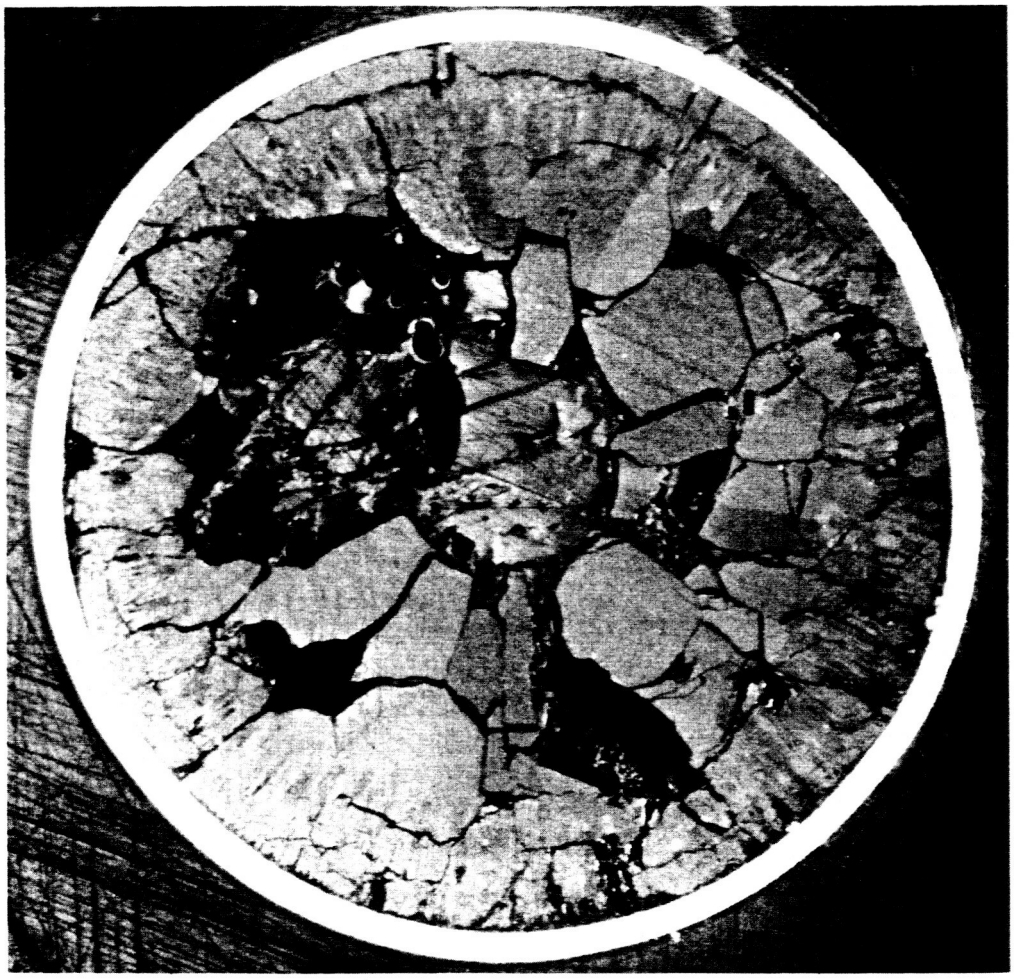

Photo 2842

Fig. 25 PELLET 1-1-5

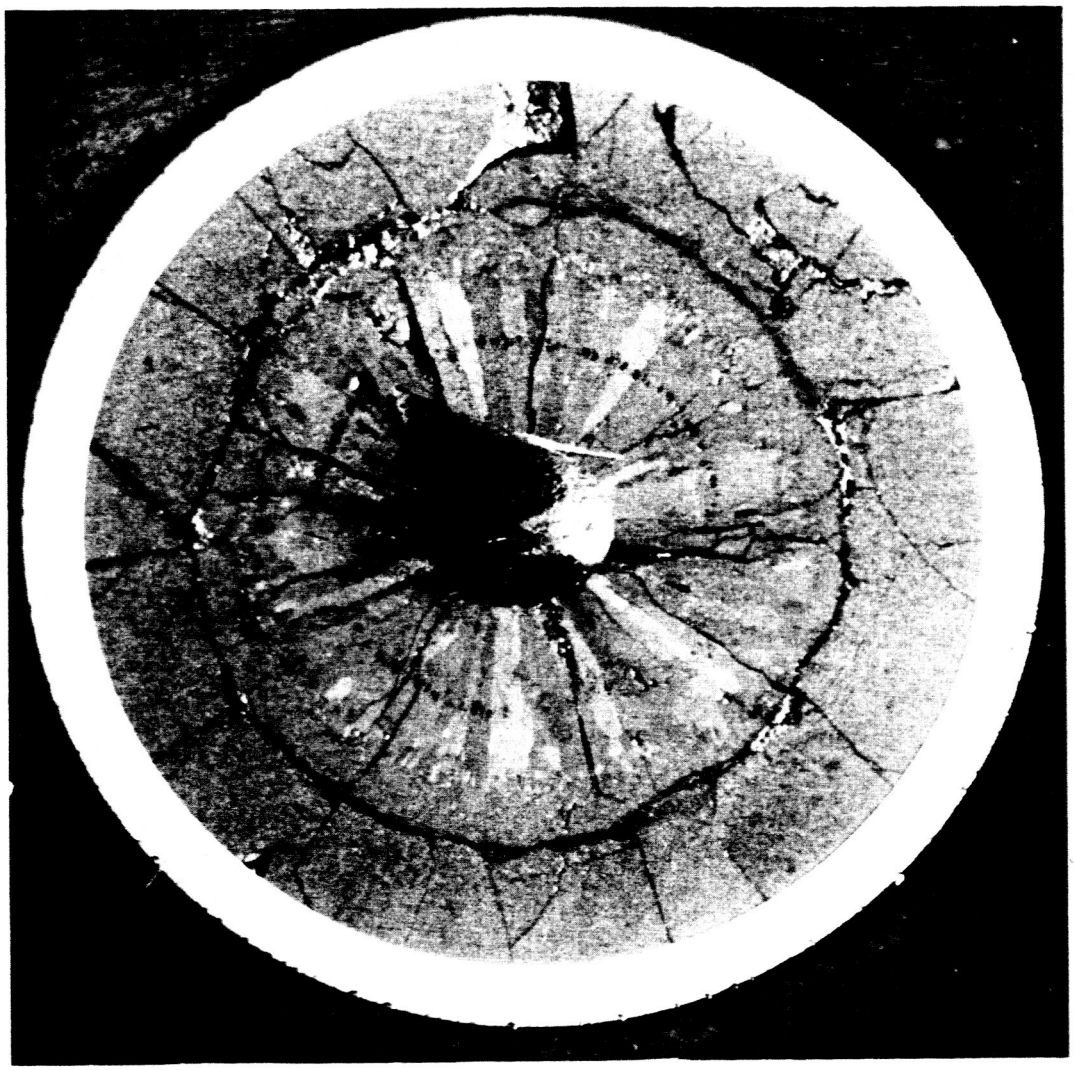

Photo 2814

Fig. 26 TOP GUARD PELLET, 2-3/8" From Top, Bottom Surface, Pin 1-2

Photo 2813

Fig. 27 PELLET 1-2-1, 2-5/8" From Top, Bottom Surface

Photo 2808

Fig. 28 PELLET 1-2-2, 2-5/8" From Top

Photo 2809

Fig. 29 PELLET 1-2-3, 3-1/16" From Top

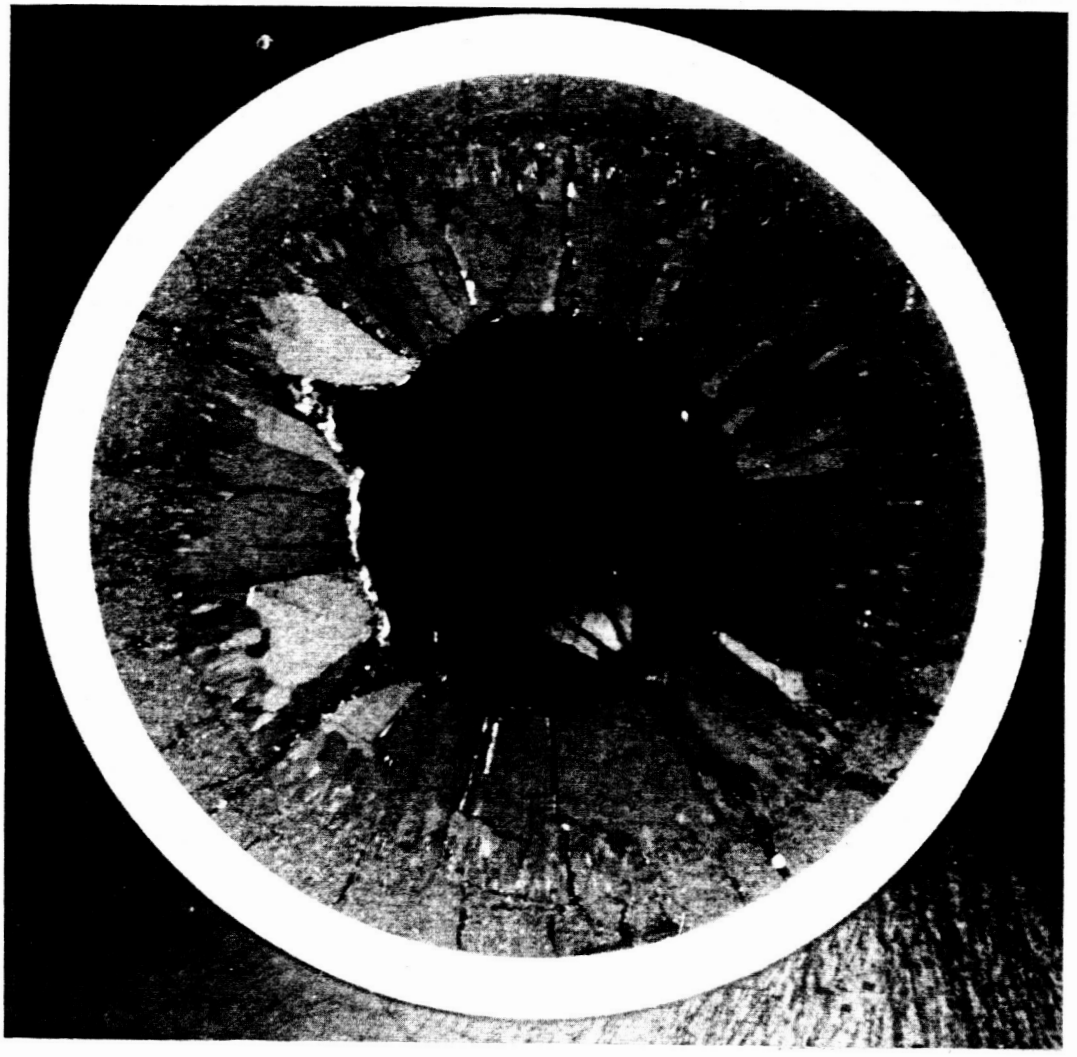

Photo 2810

Fig. 30 PELLET 1-2-4, 3-7/16" From Top

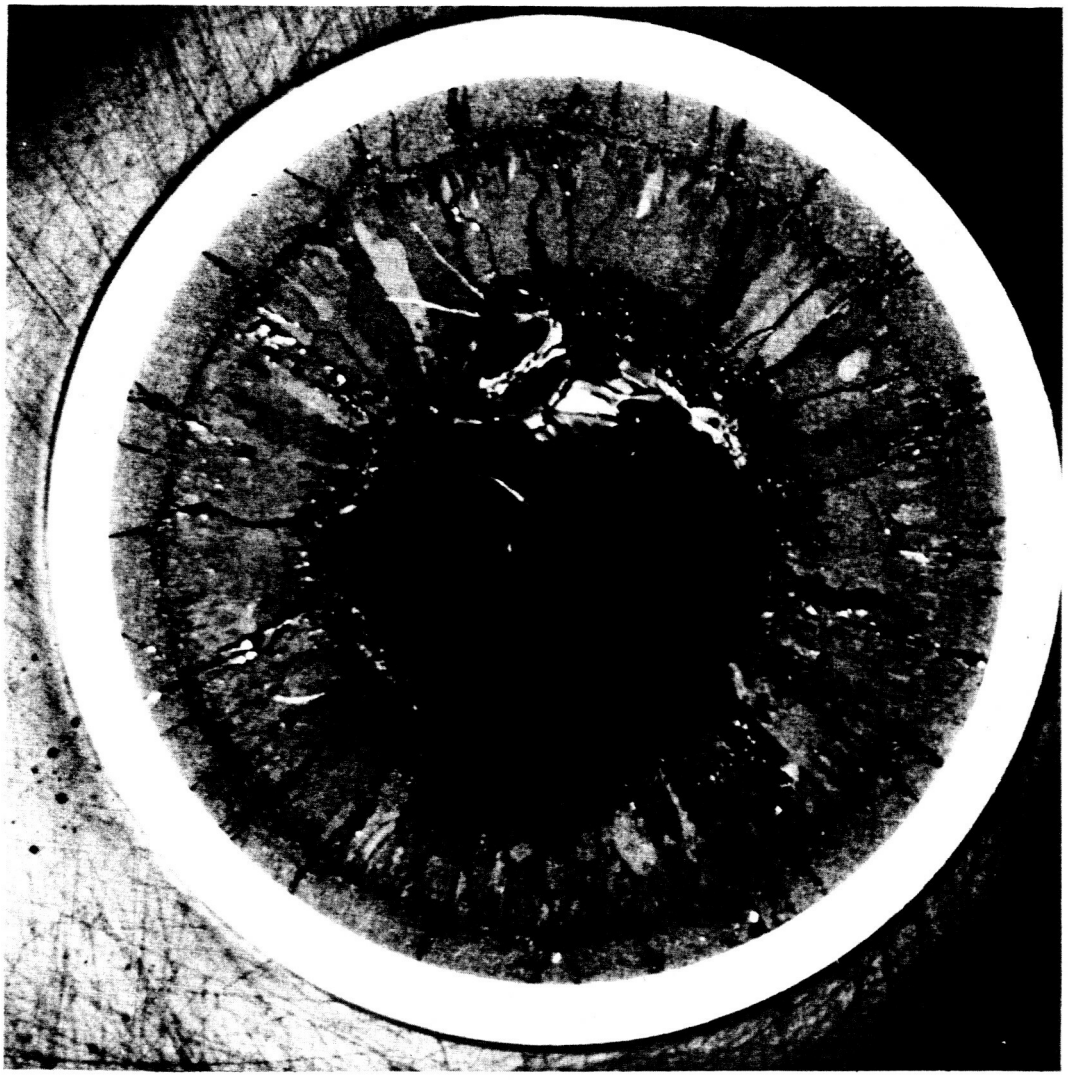

Photo 2811

Fig. 31 PELLET 1-2-5, 3-7/8" From Top

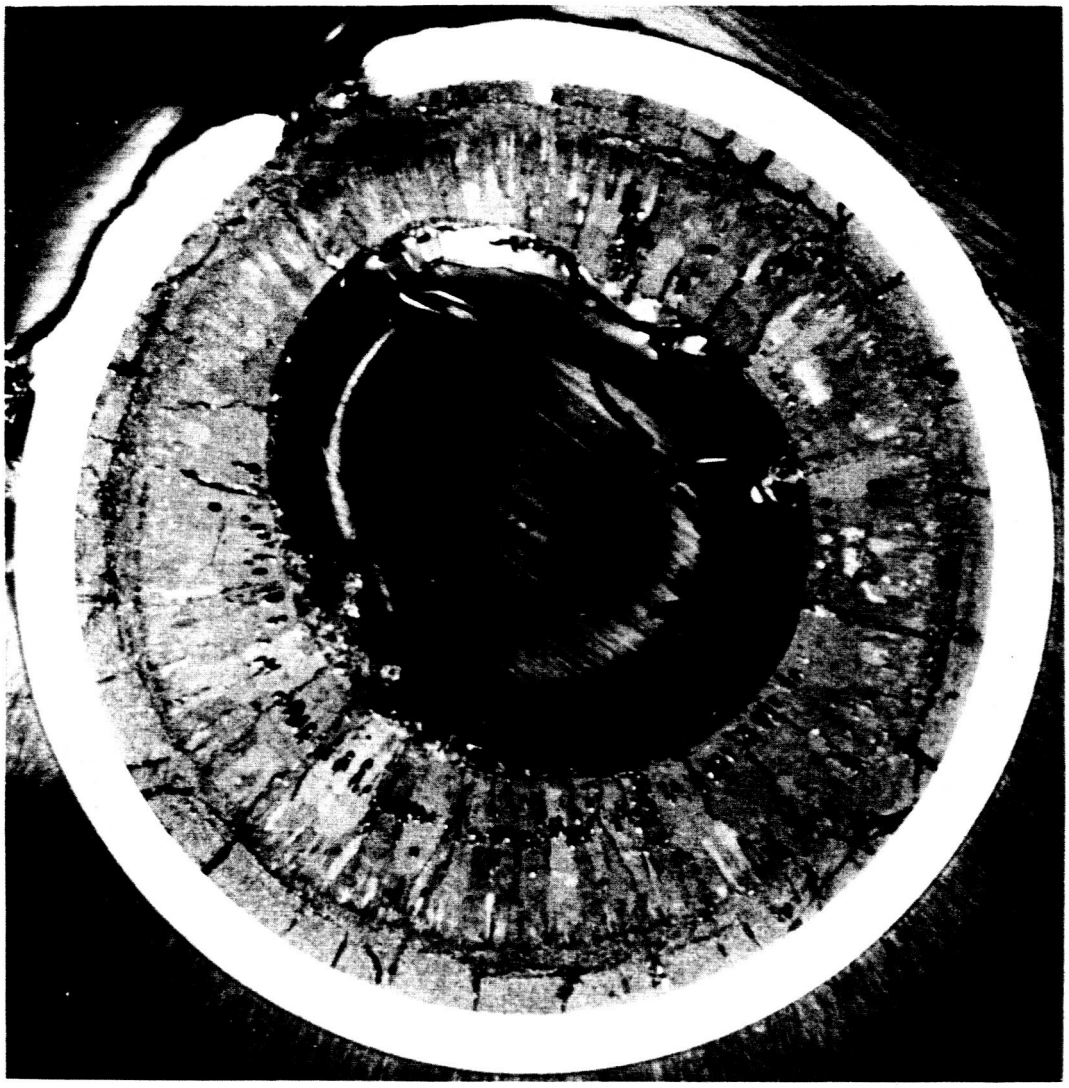

Photo 2812

Fig. 32 PELLET 1-2-6, 4-5/16" From Top

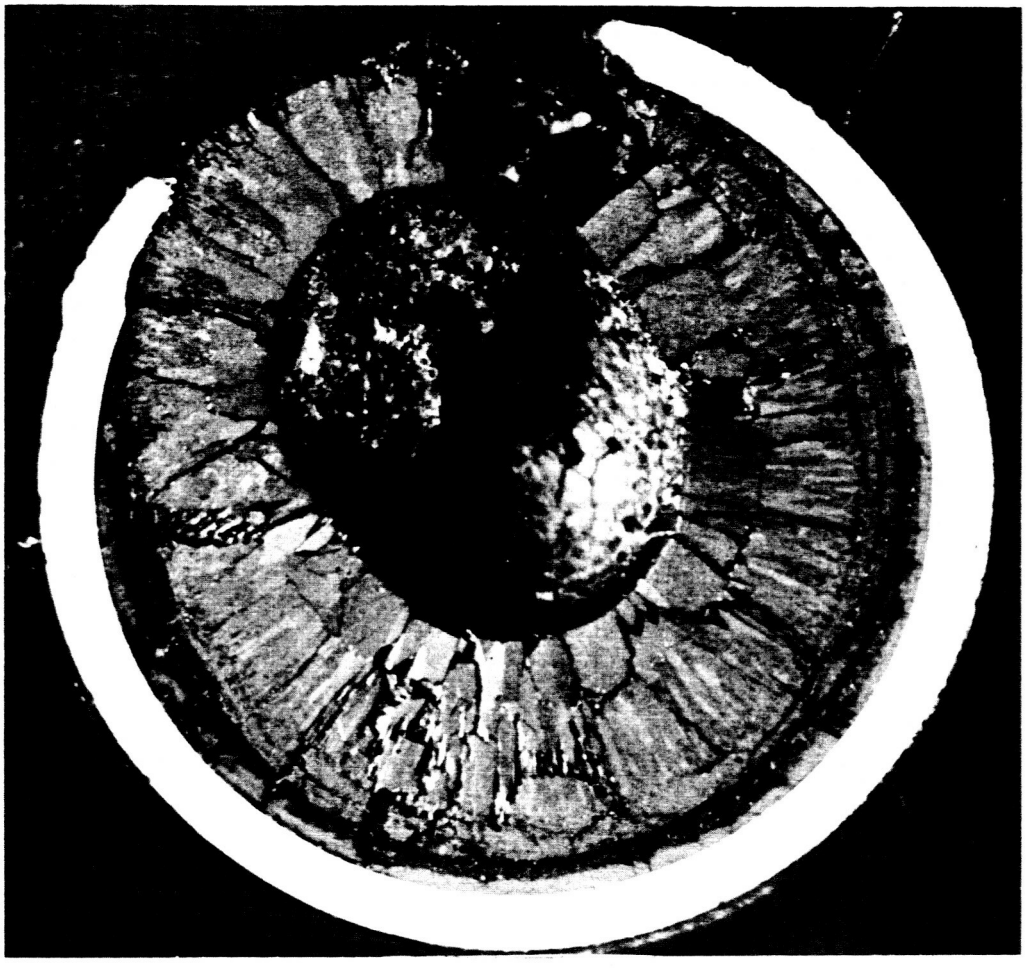

Photo 2833

Fig. 33 PELLET 1-2-8, ~ 5-7/8" From Top

Photo 2818

Fig. 34 LOWER GUARD PELLET, 6-3/8" From Top, Top Surface, Pin 1-2

Photo 2839

Fig. 35 PELLET 1-3-2

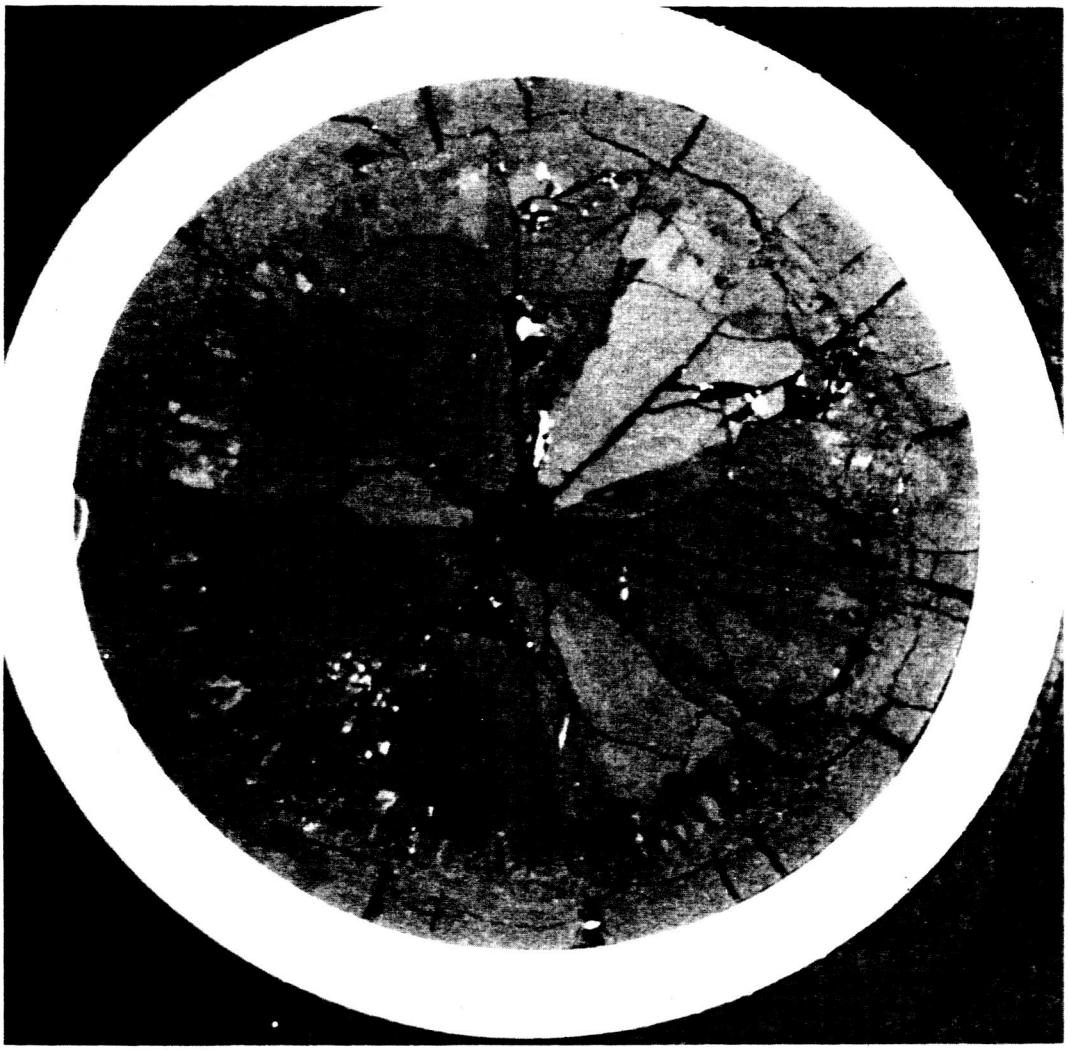

Photo 2840

Fig. 36 PELLET 1-3-5

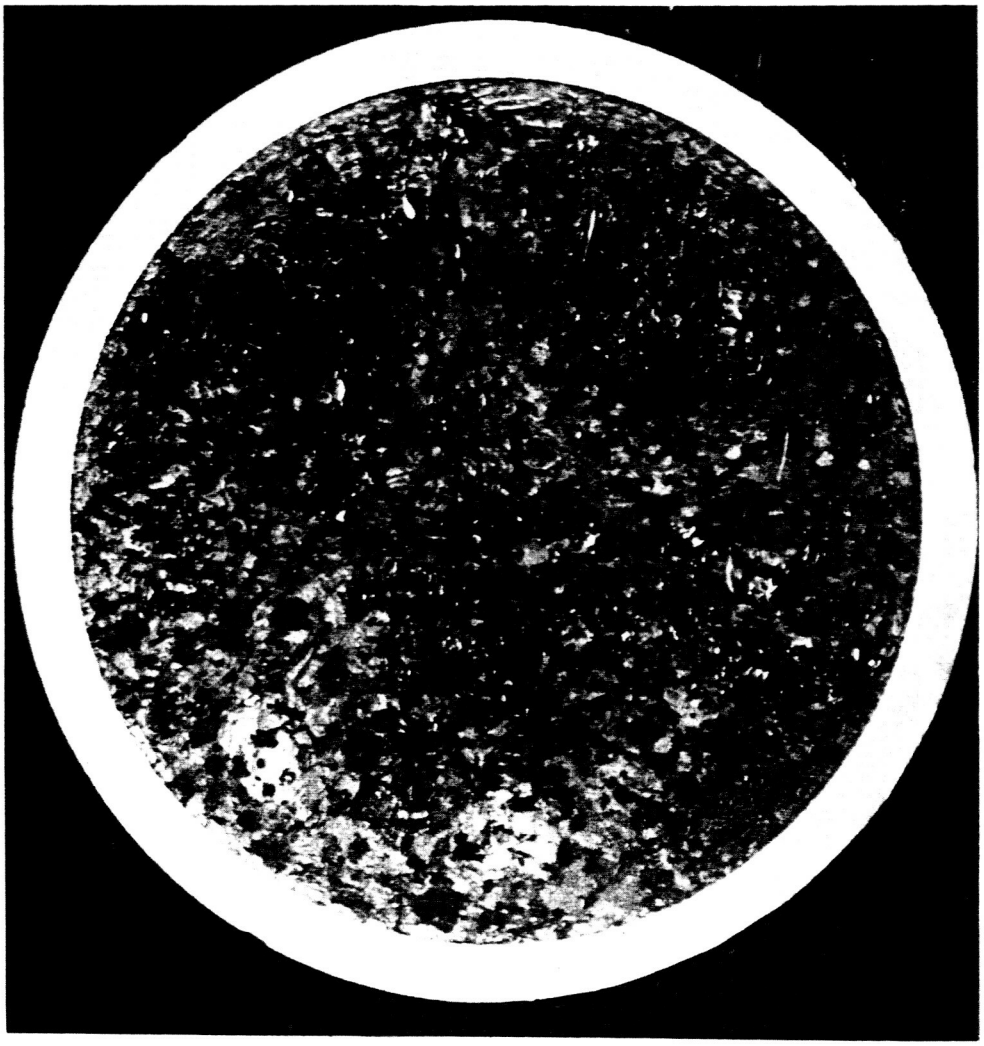

Photo 2834

Fig. 37 PELLET 1-4-2

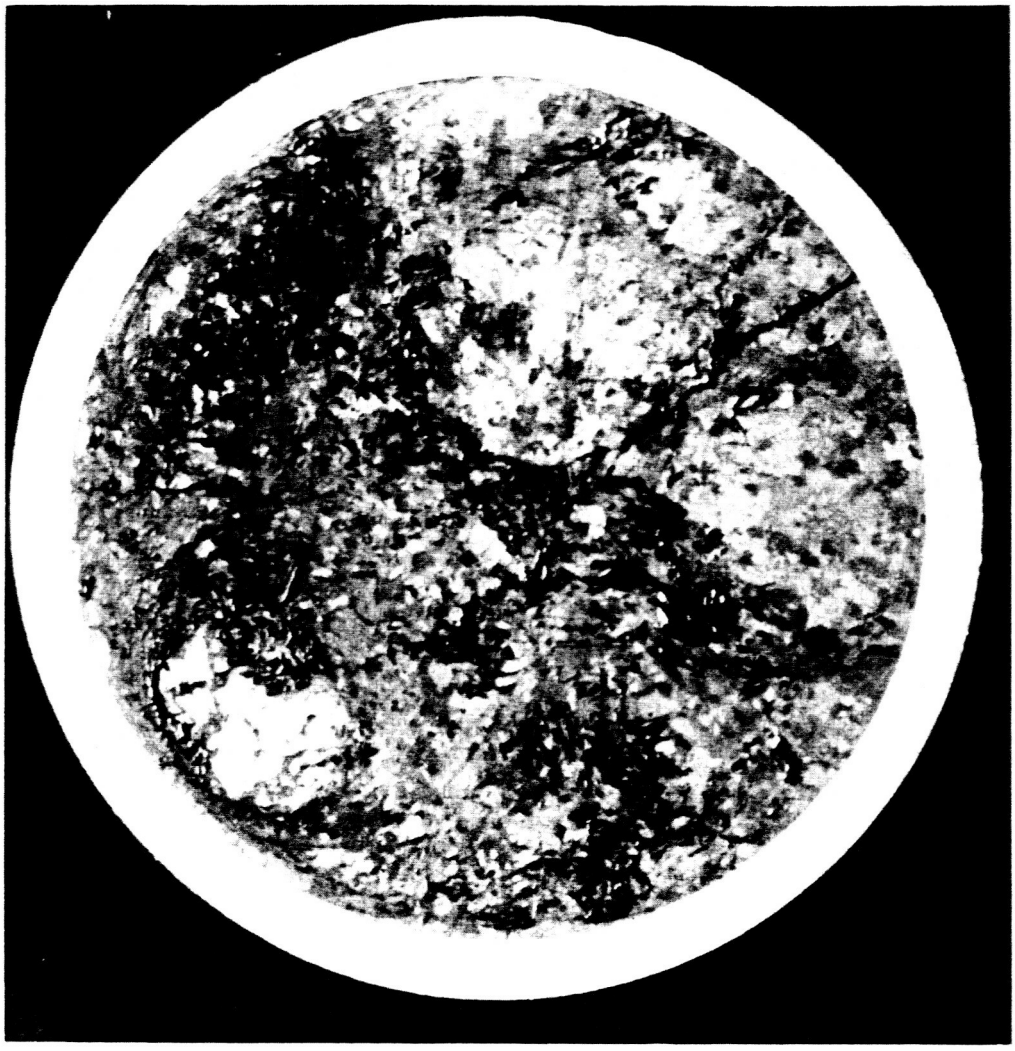

Photo 2844

Fig. 38 PELLET 1-4-5

Photo 462 A

Fig. 39 PELLET 1-4-5, NEAR CENTER, ~ 500X